The Use of Crosslinked Polyethylene for the Manufacturing of Membranes

ALBERTUS MARITZ VAN WYK
B. Sc., B. Ing. (PU vir CHO)

Dissertation submitted in the School for Chemical and Minerals Engineering of the *Potchefstroomse Universiteit vir Christelike Hoër Onderwys* in partial fulfillment of the requirements for the degree

Magister Ingenieurswese

Supervisor:	Prof. R.C. Everson
Assistant-supervisors:	Dr. T.A. du Plessis
	Mr. L.R. Koekemoer

Potchefstroom
1999

To Francis...

"There are many fine woman in the world.

But you are the best of them all!"

Proverbs 31: 29

DECLARATION

I, ALBERTUS MARITZ VAN WYK, declare that the dissertation with the title: THE USE OF CROSSLINKED POLYETHYLENE FOR THE MANUFACTURING OF MEMBRANES as partial fulfillment of the degree *Magister Ingenieurswese*, is my own work. This dissertation has not been submitted before at any university.

Signed at SECUNDA

on the ..... day of ..... 1999.

.....

Signature

ACKNOWLEDGEMENTS

I would like to thank the following people who assisted me, directly or indirectly, in this investigation.

Mr. Leon Koekemoer (PU vir CHO) for his guidance as assistant supervisor for the duration of the research.

Prof. Johan Smit (PU vir CHO) for initiating and co-ordinating the project.

Prof. Ray Everson (PU vir CHO) for his valuable input during this investigation.

Dr. Andrè du Plessis (Gammatron) for his continued motivation and for introducing me to the world of irradiation.

Ms. Maryna Heidstra (Iso-Ster) for the irradiation of the polyethylene samples.

Mr. Rob Patmore (Plastomark) for supplying polymer materials for the testwork.

Mr. Manie Prinsloo (Safripol) for assistance during the DSC measurements.

Mr. Ron Thomas (Mintek) for assisting with the experimental setup and testwork.

Ms. Marie Vlok for the philological revision of the dissertation.

A very special thanks to my wife Francis, for her love and support.

My parents, for their education, support and guidance over the years.

Finally, and most importantly, I would like to thank God, for giving me the talents to make this possible.

ABSTRACT

Key words: Irradiation-induced crosslinking, polyethylene, supported liquid membranes (SLM).

Increasing environmental awareness over the past decade as well as stringent environmental laws forced all factories to invest in water treatment processes for effluent treatment before discharge or re-use. Most of these effluent treatment processes utilize membranes as the physical barrier for separation. The membranes used in water applications are expensive and alternative materials and production techniques will increase the viability of membrane separation processes.

Experiments conducted on irradiated polyethylene showed that some of its properties were enhanced while others deteriorated. However, the enhanced properties make the polyethylene, in particular ultra-high molecular weight polyethylene, an ideal membrane material. The manufactured membranes were tested in extraction experiments, and satisfactory results were obtained. Permeation studies on the membranes compared favourably with similar studies done on commercially available membranes. An extraction rate of 1.08 g/(m^2h) nickel was achieved. A preliminary cost evaluation showed that these membranes can be manufactured at a low cost (R13.45/m^2), and can be applied as supported liquid membranes. Future research should focus on methods to decrease the brittleness and stiffness of the membranes.

OPSOMMING

Sleutelwoorde: Geïnduseerde kruisbinding, poliëtileen, ondersteunende vloeistof membrane (OVM).

Die strenger wetgewing rakende die omgewing en 'n toename in omgewingsbewustheid gedurende die afgelope dekade, het fabrieke genoodsaak om water behandelingsprosesse te gebruik om hulle uitvloeisels te behandel voor dit in die omgewing gestort of hersirkuleer word. Membraanprosesse is wêreldwyd besig om die gewildste metode van waterbehandeling te word. Dit kan toegeskryf word aan die gehalte van water wat gelewer word. Die membrane wat vir waterbehandeling gebruik word, is egter duur en alternatiewe materiale en produksiemetodes kan die proses ekonomies vatbaar maak.

Eksperimente wat op bestraalde poliëtileen uitgevoer is, het getoon dat sommige van sy eienskappe verbeter en sommige verswak het. Die eienskappe wat verbeter het, maak die poliëtileen, en in besonder ultra hoë digtheid poliëtileen, 'n ideale vervaardigingsmateriaal vir membrane. Die vervaardigde membrane is getoets in ekstraksie eksperimente, en bevredigende resultate is verkry. Permeasie eksperimente het getoon dat die vervaardigde membrane vergelykbaar met die kommersiële membrane is. 'n Ekstraksietempo van 1.08 g/(m^2h) nikkel is behaal. 'n Voorlopige ekonomiese evaluasie het getoon dat die membrane teen 'n lae koste vervaardig kan word (R13.45/m^2), en mededingend op die gebied van mikrofiltrasie en OVM ekstraksie kan wees. Verdere navorsing is egter nodig om metodes te ondersoek om die brosheid van die membrane te verminder.

CONTENTS

LIST OF TABLES

LIST OF FIGURES

Nomenclature

a	activity	
c	coefficient	
d	diameter	[m]
g	osmotic coefficient	
m	mass	[g]
n	number	
r	radius	[m]
t	time	[s]
x	distance	[m]
z	valence	
A	area	[m^2]
C	molecular concentration	[mol/m^3]
D	diffusion coefficient	[m^2/s]
F	force	[N]
J	flux	[$g/(m^2 \cdot s)$]
P	pressure	[Pa]
R	gas constant	[J/(mol·K)
T	temperature	[K]
V	molar volume	[m^3/mol]

Greek letters

Π	osmotic pressure	[Pa]
δ	thickness	[m]
η	viscosity	[P]
μ	chemical potential	[J/mol]
ψ	electric potential	[V]
θ	contact angle	[°]
σ	surface tension	[N]

Subscript

1,2,...,i	species
a	apparent
g	glass transition
m	membrane
p	pore
par	particle

Abbreviations

CA	Cellulose acetate
CTFE	Chlorotrifluoroethylene
DSC	Differential scanning calorimetry
HDPE	High density polyethylene
HMWC	High molecular weight cut-off
LDPE	Low density polyethylene
LMWC	Low molecular weight cut-off
MF	Microfiltration
NF	Nanofiltration
PAN	Polyacrylonitrile
PP	Polypropylene
PSO	Polysulphone
PVDF	Polyvinylidenedifluoride
RO	Reverse osmosis
SEM	Scanning electron microscope
SLM	Supported liquid membrane
UF	Ultrafiltration
UHMWPE	Ultra high molecular weight polyethylene
DEHPA	Di-(ethylhexyl) phosphoric acid
DHN	Decahydronaphthalene

Glossary

Alkyl radical: $-\left(CH_2-\dot{C}H-CH_2\right)-$

Allyl radical: $-CH-\dot{C}H=CH-$

Amorphous polymers: Polymers with sufficient steric irregularities at the molecular or segmental levels as to prohibit more often than permit intermolecular or intramolecular association of polymer chains.

Crosslinking: The formation of C-C bonds between molecules of neighbouring chains.

Crystalline melting temperature: The temperature at which the transition between the rubbery and liquid state takes place.

Gel: The network structure of a polymer that is insoluble in a solvent.

Gel point: The minimum degree of crosslinking at which the insoluble network first begins to form.

Gelling dose: The dose corresponding to the gel point.

Glass transition temperature: The temperature at which the transition from the rigid solid (glass) to the flexible rubber state takes place.

Gray (Gy): The unit in which radiation is measured. When a kilogram of matter absorbs the energy of one joule, this matter is said to have received a dose of one gray.

Softening point: The temperature at which softening of a polymer occurs.

Sol:	The fraction of the polymer that is soluble in a solvent.
Anisotropic membranes:	These membranes consist of a thin top layer (skin) supported by a thicker, more porous sublayer.
Asymmetric membranes:	These are anisotropic membranes manufactured from the same material.
Composite membranes:	The top layer and sublayer of these anisotropic membranes are manufactured from different materials.
Dialysis:	Dialysis refers to operations in which the driving force is a transmembrane concentration difference.
Electrodialysis:	Electrodialysis is an operation by which ions are driven through ion-selective membranes under the influence of an electrical potential.
Electrodialysis reversal:	An electrodialysis process in which the polarity of the electrodes is reversed on prescribed intervals thus reversing the direction of ion movement in a membrane stack.
Gas diffusion:	A gas/gas membrane separation process in which the activity difference is maintained through a pressure difference across a porous membrane.
Gas permeation:	A gas/gas membrane separation process in which the activity difference is maintained through a pressure difference across a dense membrane.
Ion-exchange membranes:	Ion-exchange membranes are a specific type of nonporous membrane, consisting of highly swollen gels carrying fixed positive or negative charges.

Microfiltration:	Microfiltration is a particulate removal (clarification) process.
Nanofiltration:	Nanofiltration is a separation process designed for the removal of multivalent ions in softening operations.
Nonporous membranes:	These membranes can be considered as dense media. Diffusion of species takes place in the free volume present between the macromolecular chains of the membrane material.
Pervaporation:	Pervaporation is a liquid/vapor separation process where a liquid is partially vaporized through a dense membrane.
Porous membranes:	Porous membranes are membranes with fixed pores.
Reverse osmosis:	Reverse osmosis is a pressure-driven process in which the solvent of the solution is forced through a dense membrane that retains salt and low molecular weight solutes.
Sintering:	Sintering refers to any change in shape undergone by a small particle or a cluster of particles of uniform composition when held at an elevated temperature.
Tensile strength:	The maximum nominal stress that a specimen can support before fracture.
Ultrafiltration:	Ultrafiltration is defined as a clarification and disinfection membrane process. Particles as well as pathogens will be removed with these membranes.
Yield strength:	The stress at which appreciable plastic deformation begins.

CHAPTER 1 INTRODUCTION

"Research is the process of going up alleys to see if they are blind."
- Marston Bates -

1.1 Introduction and motivation

151. (1) No person may -

(i) unlawfully and intentionally or negligently commit any act or omission which pollutes or is likely to pollute a water resource or coastal marine waters;

(j) unlawfully and intentionally or negligently commit any act or omission which detrimentally affects or is likely to affect a water resource or coastal marine waters;

(2) Any person who contravenes any provision of subsection (1) is guilty of an offence and liable, on the first conviction, to a fine or imprisonment for a period not exceeding five years, or to both a fine and such imprisonment and, in the case of a second or subsequent conviction, to a fine or imprisonment for a period not exceeding ten years or to both a fine and such imprisonment.

This citation from the National Water Act (1998) emphasizes the South African government's intention to apprehend polluters. This is in line with the worldwide trend to pass more strict environmental laws to protect the environment.

Modern factories are striving to find ways to maximize the output of saleable products and minimize the effluents that may be detrimental to the environment. As effluent clean-up operations are usually expensive, an efficient though inexpensive process will find wide application in this field. The current slump in the chemical markets worldwide, and the fact that water treatment is not a money generating exercise, underline the importance to implement inexpensive yet effective water treatment programs.

Since the development of synthetic membranes in 1960, a steady growth of interest in membrane processes for water and wastewater treatment was experienced. This recent global increase in the use of membranes in environmental engineering applications is attributed to at least three factors:

1. Increased regulatory pressure to provide better treatment for potable and wastewater.
2. Increased demand for water requiring exploitation of water resources of lower quality than those utilized before.
3. Market forces surrounding the development and commercialization of membrane technologies as well as the waste water industries themselves.

The worldwide sales of synthetic membranes during 1990 were in excess of US $2000 million. The fact that in most industrial applications, membranes account for about 40% of the total investment costs for a complete membrane plant, emphasizes the need to find durable yet inexpensive membranes (Mallevialle *et. al*, 1996:1.5).

1.2 Objectives

The objectives for the investigation can be summarized as follows:

1. The production of water treatment membranes from irradiated polyethylene.
2. The identification of possible applications for the membranes produced in the testwork.

1.3 Scope of the investigation

In order to meet the objectives of the investigation, the scope was set as follows:

1. Polyethylene samples of different densities are irradiated under different dose for property enhancement.
2. The polyethylene samples are used as raw material to produce membranes under different manufacturing parameters (temperature and pressure).
3. The characteristics of the membranes are evaluated to choose the best polyethylene material.
4. The manufacturing parameters are changed according to an experimental design to find the optimum membrane characteristics.
5. The extraction of nickel through the manufactured membrane is compared with the extraction through a commercial membrane.
6. In a preliminary evaluation, the economical feasibility of the final polyethylene membrane is compared with that of conventional membranes.

Although there are unique characteristics for membranes used in specific applications, the literature survey showed that porosity and mean pore size are the

most common characteristics used to discriminate between water treatment membranes.

CHAPTER 2 LITERATURE SURVEY, THEORY AND PRACTICE

"The only way to discover the limits of the possible is to go beyond them into the impossible."
- Arthur C. Clarke -

The past decade showed a marked increase in research focused on decreasing the impact of human expansion on the environment. This chapter deals with the raw material polyethylene, how it is made and where it is applied. It also gives background information on irradiation and the different membranes currently available.

2.1 Polyethylene

2.1.1 Background

Polyethylene was first produced at the ICI Ltd. laboratories (Winnington, United Kingdom) in 1933. The researchers subjected ethylene and benzaldehyde to a temperature of 170°C and a pressure of 190 MPa to produce a substance with unique properties. This discovery led to the first patent in 1936 and small-scale production in 1939. The polyethylene made by utilizing high pressures, became known as low-density polyethylene (LDPE) with typical densities of 915-925 kg/m^3.

During the early 1950s, three research teams working independantly from each other, discovered three different catalysts, which allowed the production of essentially linear polyethylene at low pressures and temperatures. The density of these polymers was in the region of 960 kg/m^3 and therefore named high-density polyethylene (HDPE). Of the three discoveries at Standard Oil (Indiana), Phillips Petroleum and by Karl Ziegler at the Max Planck Institute in Germany, only the latter two have been commercialized. Ultra high molecular weight polyethylene (UHMWPE) was commercialized shortly after HDPE and is characterized by an extremely high molecular mass and a narrow molecular mass distribution. The introduced coordination catalysts allowed for the first time the copolymerization of ethylene with other olefins such as butene, which by introducing side branches reduces the crystallinity and allows a low-density polyethylene to be produced at comparatively low pressures. Du Pont of Canada introduced such a process in 1960, but only small volumes were produced worldwide until 1978, when Union Carbide

announced their Unipol process. The product from this process was coined linear low-density polyethylene (LLDPE) and is produced worldwide in large volumes (Whiteley, 1992:488-489).

2.1.2 Production of polyethylene

Modern polyethylene production processes make it possible to produce more than one type of polyethylene using the same reactor. Table 2.1 lists the various types of polyethylene and the most common processes utilized for their manufacture.

Table 2.1 The technical applicability of processes for polyethylene manufacture*

Process	Installed worldwide capacity, 10^6 t/a	LDPE	LLDPE	HDPE	UHMWPE
High-pressure autoclave	9.08	+	+	0	-
High-pressure tubular	6.52	+	+	-	-
Gas-phase fluidized bed	6.69	-	+	+	0
Slurry phase autoclave/loop	9.15	-	0	+	+
Solution autoclave	2.35	-	+	+	-

* + = suitable; 0 = technically feasible with some limitations; - = unsuitable or not possible.

2.1.2.1 High-pressure process

The high-pressure production process may utilize two type of reactors: a stirred-autoclave or a jacketed tube. The reaction pressure is in the range 150-250 MPa for the autoclave reactors and 200-350 MPa for the tubular reactors. Apart from the different reactors, the rest of the process is essentially identical.

The tubular reaction vessel can be up to 2 km long, and is thick-walled with an internal diameter of up to 6.4 cm. Ethylene gas under high pressure, initiater and chain-transfer agent is fed into one end of the tube. At the other end, a mixture of polyethylene and ethylene is discharged through a pulsating valve to much lower pressures.

When a stirred-autoclave is used, ethylene, initiaters and chain-transfer agents are injected into the autoclave, usually at the top. The polyethylene is recovered by controlled discharge of the polyethylene/ethylene mixture at the bottom of the autoclave. The molecular weight distribution of the resin produced in autoclaves is overall broader, with the central portion of the molecular weight distribution curve being more narrow and peaked than tubular resins. Figure 2.1 is a schematic presentation of the following steps.

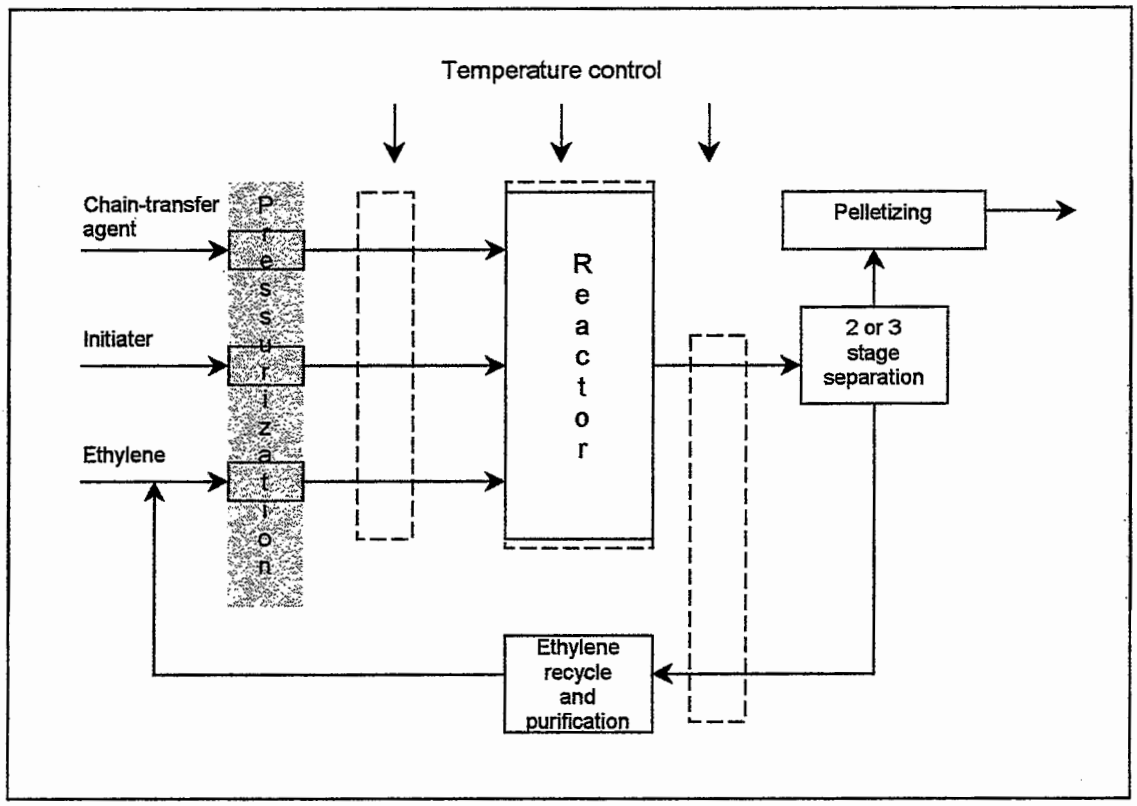

Figure 2.1 High-pressure process for polyethylene production

The ethylene feed stream is pressurized from below 10 MPa to 150-350 MPa before being fed to the reactor. Pressurized free-radical initiaters such as oxygen or peroxides are fed to the reactor, resulting in a free-radical polymerization reaction involving free-radical initiation, polymer-chain propagation and chain-transfer. Chain-transfer agents are also pressurized and added to terminate chain growth and control molecular weight. The overall molecular weight and molecular weight distribution is controlled by the type and ratios of initiator and chain-transfer agents. The temperature is controlled by heating the inlet streams to the reactor and cooling the outlet streams from the reactor. The polimerisation reaction is exothermic, and therefore the temperature control is crucial. To prevent decomposition, the reaction temperature is not allowed to increase over 300°C. Conversion of ethylene to

polyethylene is 15-40%, and the remaining ethylene in the product stream is separated from the polyethylene by flash devolatilization and recirculated to the input (Boysen, 1981:412-413).

2.1.2.2 Suspension (slurry) process

The early Ziegler plants had to include a catalyst residue removal stage that added to cost and complexity. Developments in the 1960s made it possible to eliminate this step. Variations in the plants are based on the selection of diluents. High-boiling diluents require more energy to remove all traces from the polymer, and steam-stripping is commonly applied. Low-boiling diluents such as hexane require more care in the design and operation of the plant, but this seems to be preferred in modern plants.

The suspension polymerization process has been used extensively for HDPE production, while the Phillips process is better suited for making lower density polyethylene. The Phillips Particle Form process is shown in Figure 2.2.

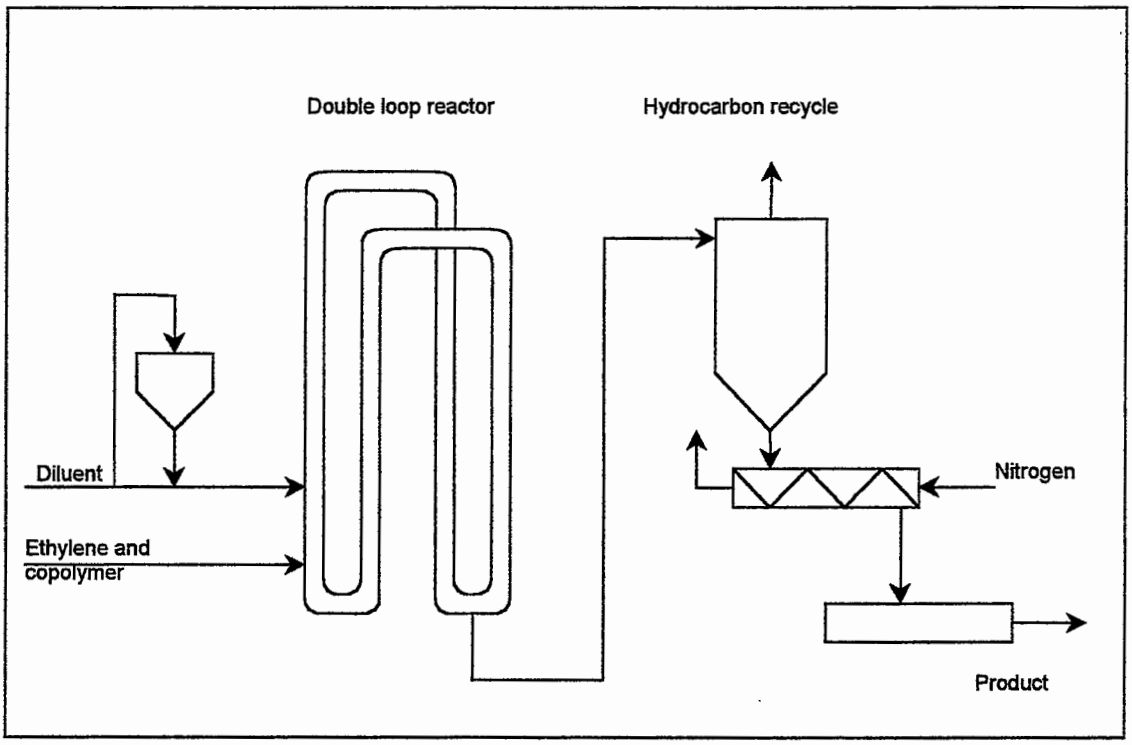

Figure 2.2 Flowsheet of the Phillips Particle Form process

2.1.3 Uses of polyethylene

LDPE and LLDPE are sold into the same market and are used predominantly for films, not all of which is for packaging. LDPE retains its position as the preferred packaging material because of its transparency, toughness, limp feel and its ability to take on the shape of the contents of the bag. The consumption of LDPE is shown in Figure 2.3.

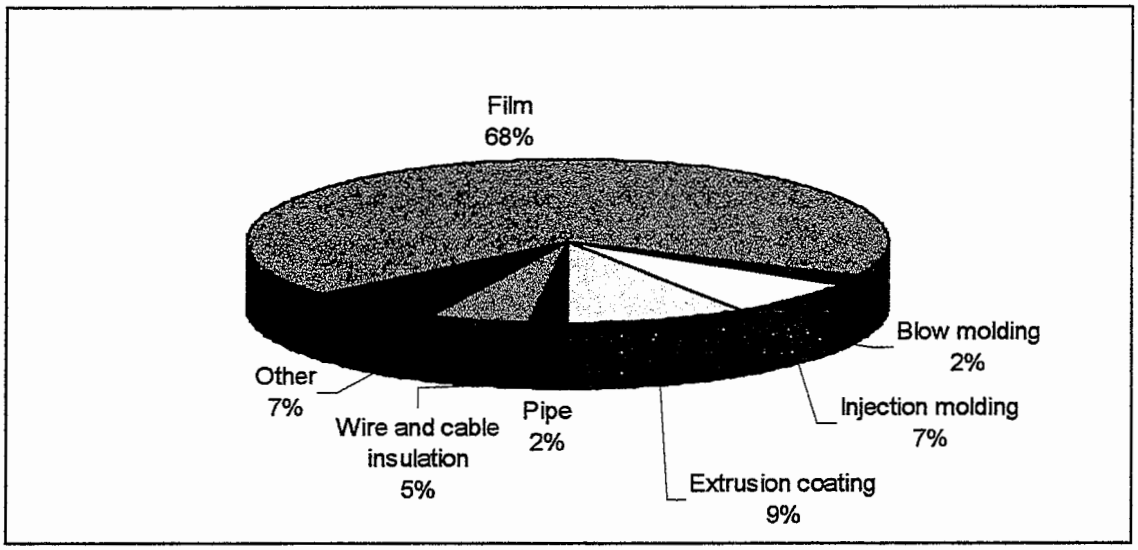

Figure 2.3 Wordwide consumption of LDPE

HDPE is used in more structural applications because of its greater rigidity and better creep properties. It also has important applications in the packaging of aggressive liquids such as bleach, detergents and hydrocarbons. The consumption of HDPE is presented in Figure 2.4.

2.1.4 Properties of polyethylene

Polyethylene is a thermoplastic polymer, which softens or deforms readily on heating and recovers rigidity on cooling. It is tasteless and generally odorless. It has a slight waxy feel, is warm to the touch and is not well wetted by water (hydrophobic). Solid polyethylene (at temperatures lower than the crystalline melting point) has good toughness and pliability over a wide temperature range. The plastics can also be machined, cut, welded and heat-sealed in the solid state. However, the low crystalline melting point (approximately 115°C) limits the temperature range of good mechanical properties. Polyethylene is also an excellent electrical insulator.

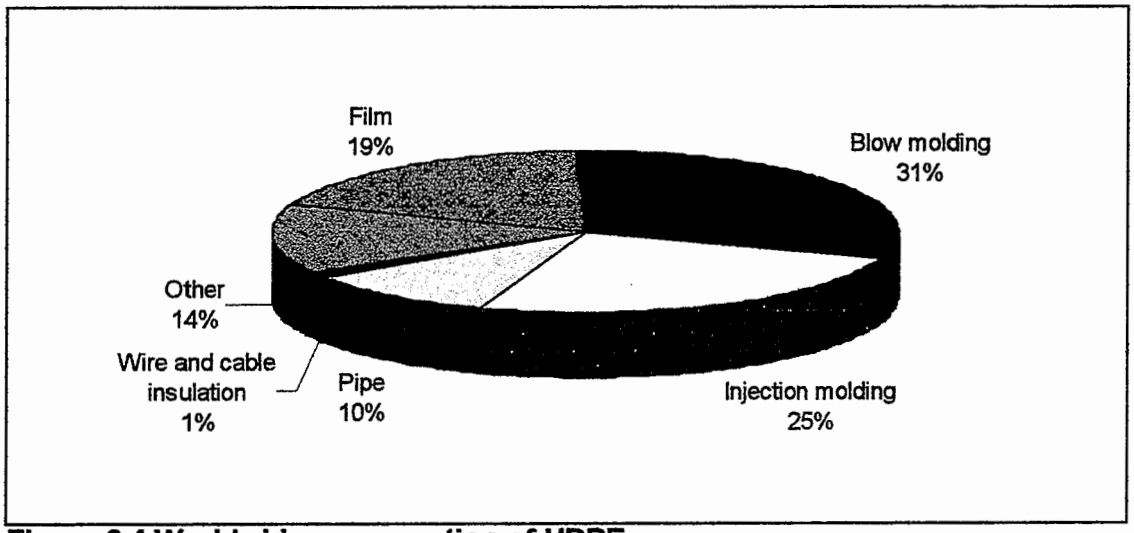

Figure 2.4 Worldwide consumption of HDPE

Chemically, polyethylene is extremely stable and inert to most reagents. Although soluble in many solvents at temperatures above 100°C, no solvents exist at room temperature. This chemical resistance is a function of the degree of polymerization; polymers of the highest density and molecular weight are most resistant and least soluble. Polyethylene introduced to heat will result in the breakage of molecular chains at random points leading to a decrease in the molecular weight of the polymer. When heated or worked at elevated temperatures, the material also undergoes crosslinking. On exposure to ultraviolet light and ionizing radiation, crosslinks will also form. Polyethylene ages on exposure to light and oxygen, resulting in loss of strength, elongation and tear resistance. Although stabilizers (hindered phenols, amines and phosphites) retard the deterioration, few are sufficiently compatible with the polymer to be effective. Polyisobutylene is one of only a few plasticizers compatible with polyethylene in concentrations higher than 1%.

The physical properties of polyethylene are influenced by three independant variables: degree of short-chain branching, molecular weight and molecular weight distribution. The fewer the number of short-chain branch points per molecule, the greater the crystallinity and density of polyethylene will be. An increase in density will increase properties such as stiffness, tear strength, chemical resistance, hardness, softening temperature and yield point. The toughness and flex life of polyethylene, as well as the permeability of liquids and gases, will decrease with an increase in molecular weight. Some of the properties of low-density and high-density polyethylene are given in Table 2.2 (Bobyn & Spector, 1986:3649-3653).

Table 2.2 Properties of LDPE and HDPE

Property	LDPE	HDPE
Density range, kg/m^3	910-940	940-970
Approximate crystallinity, %	60-70	80-95
Short branches	15-30	1-5
Crystalline melting point, °C	110-120	130-136
Hardness, Shore D	41-46	60-70
Impact strength, J/m notch	No break	80-600
Flexural strength, MPa	No break	15-20
Flexural modulus, MPa	60-410	680-1780
Tensile strength, MPa	7-17	20-40
Tensile modulus, MPa	100-260	410-1230
Elongation at break, %	≤ 650	≤ 800

UHMWPE has a remarkable combination of chemical inertness, abrasion resistance, low friction, toughness, abrasion resistance and acceptability in contact with foodstuffs. Some properties are listed in Table 2.3. Although the polymer is unbranched, the density is only 940 kg/m^3 because the extremely high viscosity hinders crystallization (Whiteley, 1992:494).

Table 2.3 Properties of UHMWPE

Property	Value
Density, kg/m^3	940
Molecular mass	4.5 x 10^6
Reduced specific viscosity, cm^3/g	2300
Crystalline melting range, °C	135-138
Tensile yield strength, MPa	22
Tensile rupture strength, MPa	44
Elongation at rupture, %	> 350
Impact energy, notched, kJ/m^2	210
Volume resistivity, $\Omega \cdot \mu$	> 10^{13}

2.1.5 Irradiation of polyethylene

2.1.5.1 Background

The history of the effects of ionizing radiation on polymers started in 1928 when Fromandi found that natural rubber and polyisoprene solutions exposed to electrical

discharges resulted in a decrease of viscosity, iodine number, molecular weight and softening point. Hock and Leber reported in 1940 that when air was excluded from the system, radiation led to an increase in the viscosity and molecular weight of the rubber, and eventually to gelation. Extensive studies of the physical properties of plastics exposed to nuclear reactor pile radiation were carried out during and following World War II. However, the first comprehensive publications in the open literature came from Charlesby in 1952, who discussed effects of pile radiation on polyethylene (Bovey, 1958:49).

South Africa has been a pioneer in many polymer radiation processes. Gammatron (Pretoria, South Africa) is using the Raprex® process to investigate the following applications (Du Plessis, 1997:1):

- Heat-shrink film for general packaging and timber pole protection.
- Film for protective coatings and binders.
- Under-rail shock absorbing pads with superior cold-flow properties.
- High-density polyethylene pipes.
- Insulation for electrical cables and wire.
- Plasticized PVC for footwear.
- Radiation crosslinking of natural gums.
- Case-hardening of orthopedic prostheses.

Gamma radiation is generated when atomic nuclei disintegrate. These electromagnetic radiations travel with the same velocity as ordinary light and are usually described in terms of their wavelengths. These wavelengths are given in Figure 2.5 (Halliday & Resnick, 1988:393).

2.1.5.2 Crosslinking and degradation

One of the most important observations made in the study of radiation effects in linear polymers is the fact that polymers either crosslink or degrade depending on their chemical structure. These observations were first reported by Charlesby and Lawton. Although there is no definite explanation why some polymers crosslink and

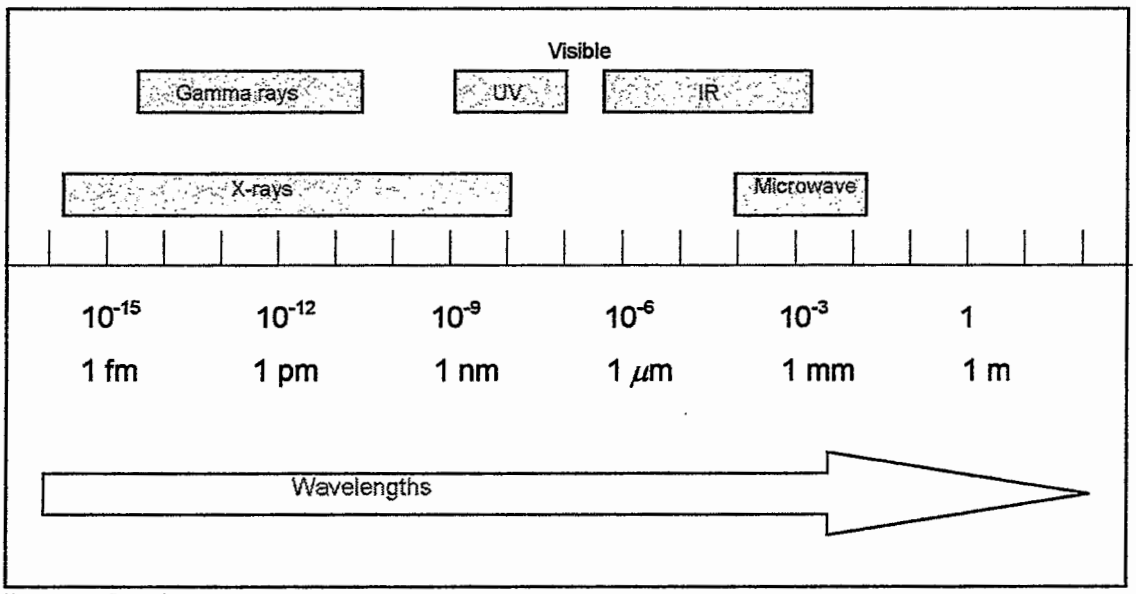

Figure 2.5 The electromagnetic spectrum

others degrade; a general empirical rule can be derived when examining the structure of polymers. Most vinyl polymers, which have the structure

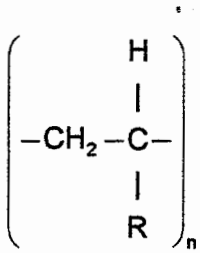

(2.1)

all undergo crosslinking, whereas polymers of the structure

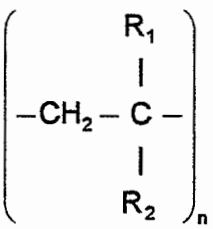

(2.2)

all degrade. It follows that when the structure of a vinyl polymer is such that each carbon of the main chain carries at least one hydrogen atom, the polymer crosslinks, and if a tertiary carbon is present in the monomer unit, the polymer degrades. Table 2.4 shows the classification of polymers into the two groups (Chapiro, 1962:352).

Table 2.4 Irradiated polymers: crosslinking versus degradation

Crosslinking polymers	Degrading polymers
Polyacrolene	Cellulose and derivatives
Polyacrylamide	Polyisobutylene
Polyacrylates	Polymethacrylamide
Polyamides	Polymethacrylates
Polyesters	Poly (α-methylstyrene)
Polyethylene	Polytetrafluoroethylene (PTFE)
Polypropylene	Polytrifluorochloroethylene
Polysiloxanes	
Polystyrene	
Polyvinyl alcohol	
Polyvinyl chloride (PVC)	
Polyvinyl pyrrolidene	
Rubbers	

2.1.5.3 Mechanism of crosslinking

The occurrence of crosslinking is usually attributed to the formation of polymer radicals at adjacent sites on neighboring chains. Close pairs would not occur often enough to account for the observed degree of crosslinking if the radicals were produced at random sites. It therefore seems probable that the initially ejected hydrogen atom may remove a neighbouring hydrogen atom, forming molecular hydrogen. Schultz has listed the possible reactions that may occur during the irradiation of polyethylene and the subsequent chemical relaxations (Schultz, 1974:106). These reactions are:

$$-CH_2CH_2CH_2- \gg\gg -CH_2\dot{C}HCH_2- + H^{\bullet} \qquad (2.3)$$

$$-CH_2CH_2- \gg\gg -CH=CH- + H_2 \qquad (2.4)$$

$$H^{\bullet} + -CH_2- \rightarrow -\dot{C}H- + H_2 \qquad (2.5)$$

$$H^{\bullet} + CH=CH \rightarrow \text{a radical} \qquad (2.6)$$

$$2H^{\bullet} \rightarrow H_2 \qquad (2.7)$$

$$2-\left(\dot{C}H\right)-\rightarrow \begin{matrix} -\ CH\ - \\ |\qquad\quad \\ -\ CH\ - \end{matrix} \quad \text{(a crosslink)} \qquad (2.8)$$

$$-CH_2\dot{C}HCH_2-+-CH_2CH=CH-\rightarrow -CH_2CH_2CH_2-+-\dot{C}HCH=CH- \qquad (2.9)$$

$$-CH_2\dot{C}HCH_2-+-\dot{C}H-CH=CH-\rightarrow \begin{matrix} -CH_2-CH-CH_2- \\ |\qquad\qquad\quad \\ -CH-CH=CH- \end{matrix} \quad \text{(a crosslink)} \qquad (2.10)$$

The symbol ⋗⋗⋗ denotes high-energy knock-on. Equations 2.8 and 2.10 are the only reactions that result in crosslinking and involve the destruction of alkyl radicals. The alkyl groups can be formed at very low temperatures, and will remain intact until the polymer is heated. When the polymer is subsequently heated to room temperature, the primary reaction products combine to form the allyl radical and/or crosslink.

2.1.5.4 Radiation effects in polyethylene

Irradiated polyethylene shows a number of physical, chemical and electrical changes similar to irradiated low molecular paraffins. The following major effects are observed after irradiation (Charlesby, 1960:201):

1. The evolution of low molecular weight hydrocarbons and hydrogen.
2. Crosslinking occurs. The newly formed bonds convert the polymer into one that is partly insoluble and infusible.
3. An increase in unsaturation. At low irradiation doses, the degree of unsaturation is proportional to the dose but eventually tends to a maximum value.
4. Destruction of crystallinity. The percentage of material present in the crystalline form at room temperature decreases and eventually disappears with increasing dose.
5. Colour changes. Polyethylene acquires a yellow tinge on irradiation.
6. Oxidative reactions take place near the surface of the polymer sample, when the irradiation is carried out in the presence of oxygen or stored in air without the prior annealing thereof in an inert atmosphere.

2.1.5.4.1 Crosslinking and solubility changes

Crosslinking is the predominant reaction on irradiation of polyethylene. The crosslinking is accompanied by the formation of an insoluble gel fraction representing the crosslinked network, and ultimately by the insolubility of the entire irradiated specimen (Billmeyer, 1971:373).

The new network of linked chains resulting from irradiation manifests itself in the solution behaviour of the system. This giant interlinked molecule is insoluble in solvents for unirradiated polyethylene, and forms a gel. At a lower radiation dose, both a sol and a gel can be present. The approximate criterion for the formation of gel is that the number of crosslinks be equal to the number of the chain molecules, if the crosslinks form at random locations. If these crosslinks do not form at random locations, this rule may not be obeyed (Schultz, 1974:106).

2.1.5.4.2 Effect of crosslinking agents

Polymers are very seldom used in their pure polymeric form and usually contain plasticizers, antioxidants and stabilizers to facilitate the processing of these materials. These additives can greatly influence the stability of the polymer towards ionizing radiation, as no additive can be considered to be inert with regard to radiation. Some additives have a protective influence on the polymer, while others assist in radiation degradation. It is often observed that oxygen can lead to an accelerated degradation even months after the irradiation of the polymer because of long-lived polymeric radicals that may form during irradiation (Du Plessis, 1978:19).

Grobbelaar *et al.* (1978:371) showed that the presence of acetylene or an equimolar mixture of acetylene and chlorotrifluoroethylene (CTFE) resulted in higher radiation crosslinking of HDPE films when compared with the polymer irradiated in nitrogen as an inert atmosphere. Their results are shown in Figure 2.6. Acetylene starts to polymerize when irradiated to form a polymer called alprene. When polyethylene is irradiated in the presence of acetylene, graft copolymers are formed. Furthermore, they found that polyethylene taken from within a bulky HDPE sample did not undergo an enhanced crosslinking in the presence of acetylene. This is due to the limited diffusion of the crosslinking agent into the sample. Therefore, crosslinking agents compounded into the polymer before irradiation are employed in the accelerated crosslinking of bulky HDPE samples.

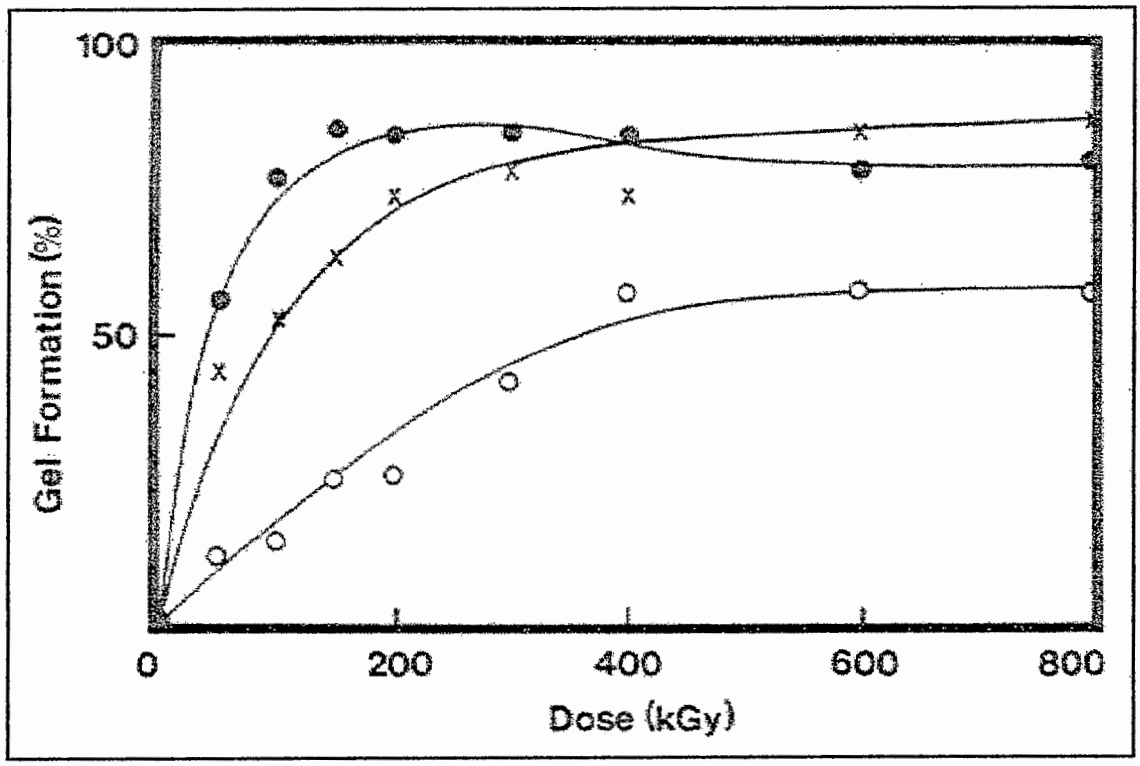

Figure 2.6 The percentage gel formation as a function of the irradiation dose for HDPE samples, taken from the surface of the sample, in the presence of crosslinking agents and nitrogen. o, nitrogen; x, acetylene; •, acetylene and CTFE

2.1.5.4.3 Changes in crystallinity

Thermoplastics form either a noncrystalline or a partly crystalline solid when solidified from the liquid state. Polyethylene is an example of a thermoplastic that solidifies to form a partly crystalline structure. When polyethylene solidifies and cools, its specific volume suddenly decreases, as indicated by the line *BE* in Figure 2.7. The high-efficient packing of the polymer chains into crystalline regions causes this decrease in specific volume. The polyethylene at *E* will have the structure of crystalline regions in a supercooled liquid (viscous solid), noncrystalline matrix. Further cooling results in the glass transition area, as indicated by the slope change between *E* and *F*. As cooling is continued, the supercooled liquid matrix transforms to the glassy state, and thus the structure of polyethylene at *F* consists of crystalline regions in a glassy noncrystalline matrix (Smith, 1990:340).

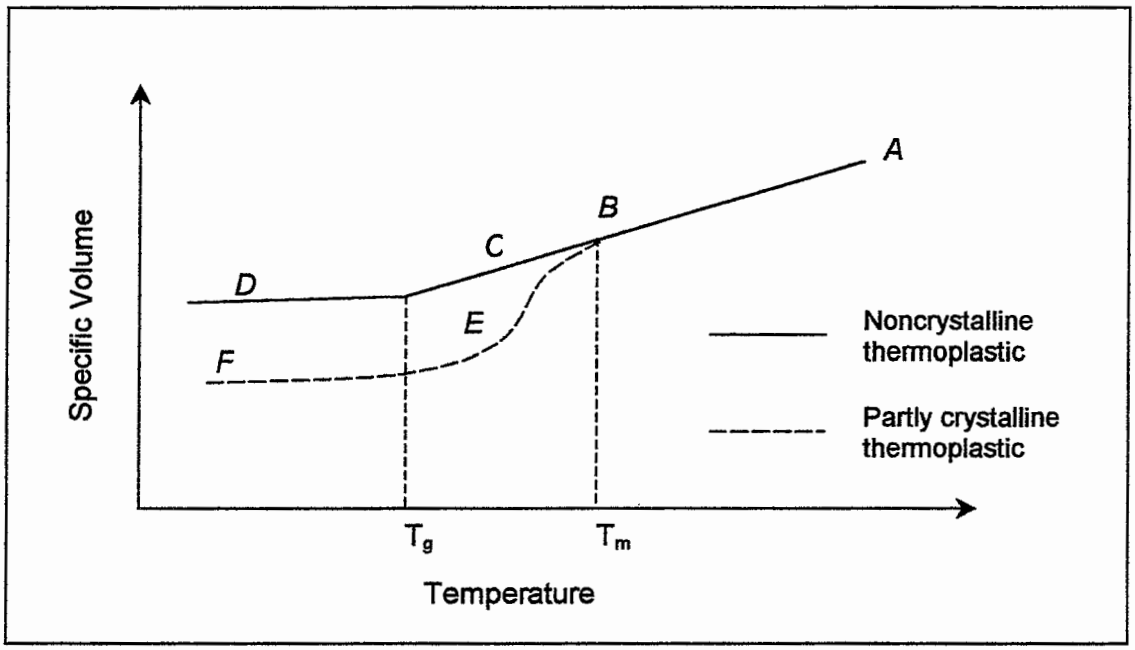

Figure 2.7 Solidification and cooling of noncrystalline and partly crystalline thermoplastics

Irradiation causes important modifications of the structure of the polyethylene molecule (branching and unsaturation), resulting in alterations in the geometry of the molecule which prevents to some extent the orientation of the chains to form regular molecular arrangements. The crystalline regions of the polymer are greatly affected by irradiation, which causes a gradual decrease in crystallinity with increased dose (Chapiro, 1962:389).

2.1.5.4.4 Chemical changes

Chapiro (1962:405-423) noted different chemical changes in polyethylene when samples were irradiated:

Gas evolution: When polyethylene was irradiated in the absence of air, appreciable amounts of gases were evolved in the process, leading to a measurable loss of weight of the polymer sample. The evolved gas was found to be composed of 98% hydrogen and smaller amounts of methane, ethane, propane and butane.

Change in unsaturation: Chemical methods and infrared analysis were used to study the change in the degree of unsaturation produced by irradiation. It was further reported that the vinylidene-type double bonds, which are originally present in the polymer, rapidly disappeared under irradiation. Trans-vinylene-type bonds accumulated under irradiation. Subsequent work further demonstrated that vinyl unsaturation also disappeared very rapidly at an early stage of the process.

Influence of oxygen: Irradiation of polyethylene in the presence of air leads to marked oxidation of the polymer. The weight of the polyethylene samples increased after irradiation in the presence of air, while gas evolution caused a decrease in the weight if irradiation occurred in vacuum.

2.1.5.4.5 Mechanical and electrical properties

Grobbelaar *et al.* (1978:371-373) investigated the effect of irradiation on the physical properties of polyethylene in the presence of nitrogen and crosslinking agents:

Softening point: The softening point of polyethylene increased with increased dose. Above a dose of 200 kGy, no further increase was observed. When crosslinking agents were used, the softening point increased even more with increased dose.
Tensile strength: Tests were carried out on the crosslinked polyethylene at both low and high speeds and showed a slight increase in strength with increasing dose.
Surface hardness: The experiments done on irradiated polyethylene indicated that the surface hardness of the treated polymer increased remarkably with an increase in radiation dose, with the crosslinking agents producing the best hardness.
Impact strength: The impact strength of the crosslinked polyethylene decreased drastically with increased radiation dose, almost independant of the presence of a crosslinking agent. Radiation dose higher than 150 kGy should therefore be prevented if high impact strengths are required.
Abrasion resistance: The crosslinked polyethylene showed a substantial improvement in abrasion resistance compared to unirradiated controls.
Conductivity: Charlesby (1960:513) found that, although many polymers (polyethylene, etc.) are good insulators, their conductivity is greatly increased by exposure to high-energy radiation. This increase was observed even at very low intensities, insufficient to cause appreciable chemical changes. However, this effect was not permanent; if the radiation on the specimen was stopped, the current decreased again.

2.2 Membranes

A membrane is defined as a thin film separating two phases, acting as a selective barrier to the transport of matter. This definition is illustrated in Figure 2.8.

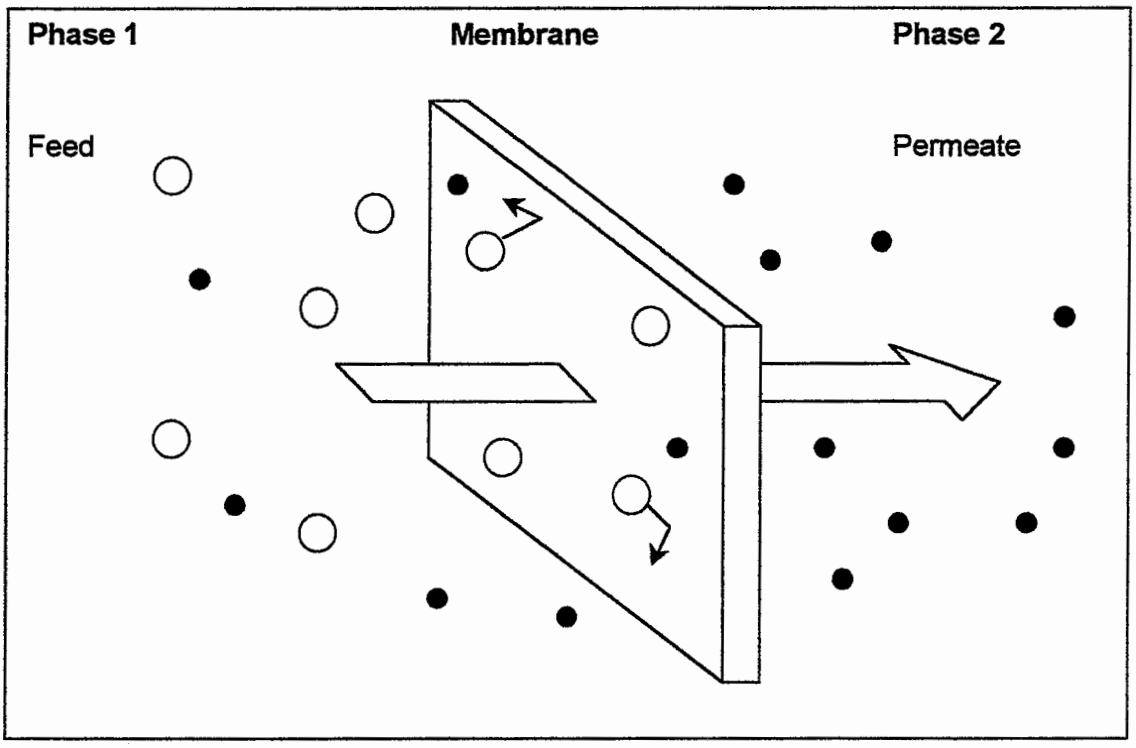

Figure 2.8 Schematic definition of a membrane

2.2.1 Background

The history of synthetic polymeric membranes began after the invention of the first synthetic polymer, cellulose nitrate, by Schönbein in 1846. The history of polymeric membranes was concerned largely, but not exclusively, with cellulosic types throughout the first century of their existence. Fick already utilized cellulose nitrate membranes to perform his classical studies on diffusion. In the same year Lhermite was the first person to state that permeation occurs as a result of the interaction of permeant species with the membrane. He also stated that solution and capillary theories were not mutually exclusive but merged without any abrupt change into another.

The first tubular cellulose nitrate membranes were developed by Schumacher in 1860; a configuration which were to remain popular into the present century. In 1872, Baranetzky developed the first flat-sheet membranes. Bechhold varied the cellulose nitrate concentration resulting in the first series of microfiltration membranes of graded pore size in 1906. He also defined the relationship between the bubble point, surface tension and pore radius. Karplus developed the concept of pore size distribution by combining the bubble point and Hagen-Poiseuille permeability techniques.

The focus on membrane development then shifted to the structural interpretation of the synthetic polymers. In the 1920s Staudinger determined that polymers were high molecular weight compounds. Meyer and Mark made use of X-ray diffraction to establish the existence of long-range order (crystallinity) in dense polymer structures. The most convenient technique for the study of molecular weight distribution, gel permeation chromatography, was developed by Benoit *et al.* in 1966.

The study on macromolecular architecture was done more recently. Branched polyethylene was developed by Swallow in 1935 and linear stereospecific polyethylene by Ziegler in 1953. Random, block and graft copolymers and the effects of their primary, secondary and tertiary structures upon film and membrane structure and performance have been studied since 1960.

The early manufacturers had problems in reproducing membranes consistently. Zsigismondy *et al.* and Elford developed two practical series of graded cellulose nitrate membranes, while Brown was the first to employ cellulose acetate as a membrane material.

The development of ion-exchange membranes was postponed because of the difficulty of making ion-exchangers in the shape of thin films. The general accepted model for ion-exchange membranes was already developed in 1935 by Teorell and 1936 by Meyer and Sievers. However, it was not until 1949 that Juda and McRae developed practical ion-exchange membranes. The first commercial microfiltration membranes were produced in Germany in 1927, but it was not until the 1950s that commercial production began in America.

The golden age of membranology (1960-1980) began in 1960 with the invention by Loeb and Sourirajan of the first integrally-skinned cellulose acetate reverse osmosis membrane. Their development stimulated both commercial and academic interest, first in desalination by reverse osmosis and then in other membrane applications.

During those 20 years, significant progress was made in virtually all the phases of membranology: applications, research tools, membrane formation processes, chemical structures, physical structures, configurations and packaging. However, even though the basic principles and methodology have already been established, optimization of membranes for a growing number of specific applications has only just begun and should continue well into the next century (Kesting, 1985:2-10).

2.2.2 Membrane separation processes

The transmembrane flux for each chemical species is generalized by the following equation:

$$\text{Flux} = \text{force} \times \text{concentration} \times \text{mobility} \tag{2.11}$$

The concentration will vary with distance through the membrane and through the boundary layers at the two interfaces of the membrane fluid. Therefore, equation 2.11 can be treated as a local equation where the local forces are the gradients of chemical potentials $d\mu/dx$ of every chemical species that can be transported. The variation of the chemical potential of species *i* can be expressed as:

$$d\mu_i = RTd\ \ln a_i + V_i dP + z_i F d\psi \tag{2.12}$$

The operator can control both the pressure *P* and electrical potential ψ to improve the separation between the mobile components. An applied pressure acts on every component in proportion to its molar volume V_i, while an electric field acts on every ionic species according to its valence z_i, without effecting non-ionic species. Membrane operations can be divided into:

- Concentration-driven membrane operations.
- Electrical potential-driven operations.
- Pressure-driven operations (Aptel & Buckley, 1996:2.4-2.6).

2.2.2.1 Concentration-driven processes

Diffusion refers to the migration of a substance across a concentration gradient and plays a vital role in concentration-driven processes. Fick's first law of diffusion describes the mass transport or flux, J, through a membrane in terms of the concentration gradient of the solute:

$$J = -D\frac{\partial C}{\partial x} \tag{2.13}$$

where the proportionality factor D is called the diffusion coefficient (Bird *et al.* 1960:502).

2.2.2.1.1 Diffusion dialysis

Diffusion dialysis (Figure 2.9) is a membrane separation process that is utilized to recover acids (e.g. hydrochloric, nitric, sulfuric, and hydrofluoric) or bases from effluent streams that have been contaminated with metal ions such as iron, chromium and nickel. Diffusion dialysis is based on the natural diffusion of ions across a semipermeable membrane from a region of high concentration to a region of low concentration. The process is capable of recovering 80 to 95% of the initial acid and 60 to 95% of the contaminant metal.

2.2.2.1.2 Supported liquid membranes (SLMs)

Danesi (1985:857) described a supported liquid membrane as a thin layer of organic solution consisting of solvent extraction reagents, immobilized on microporous inert supports interposed between two aqueous solutions for the selective removal of metal ions from a mixture. The organic extractant extracts the metal species present in the first aqueous solution (referred to as the feed solution), while the second aqueous solution is necessary to strip the metal species from the organic phase present in the membrane (referred to as the strip solution).

The organic extractant, also known as the metal carrier, is usually diluted in a water immiscible organic diluent before being absorbed into a microporous polymeric film, which acts as the solid support for the liquid membrane. The thickness of this polymeric membrane, made from polypropylene, is typically between 25 and 30 μm and has pore sizes ranging from 0.02 to 5 μm.

The traditional extraction methods used for the selective removal and concentration of metal ions from solutions, are ion-exchange techniques and liquid-liquid extraction. SLMs represent an attractive alternative to these conventional techniques. Some of the advantages displayed by SLMs, are:

- Small volumes of organic extractants are needed. The extractants are constantly regenerated which makes it economically feasible to utilize some of the more exotic and expensive extractants available.
- The permeation of metal species through SLMs can be described as the simultaneous extraction and stripping operation combined in a single stage, and hence eliminates some process steps that would be required by conventional solvent extraction.

- SLMs can operate in unclarified feed solutions eliminating the need of a filter.
- The only waste generated by a SLM is the exhausted membrane after a period when regeneration is no longer effective. This represents a far smaller volume to be disposed of compared to the volume of the spent solvents used in a liquid-liquid extraction unit.
- The equipment required, is simple and has very low energy consumption.

Researchers took up the challenge to develop and manufacture a low-cost SLM, resulting in a high number of publications on the subject. The literature survey on SLM did not provide any proof of existing SLM plants on industrial scale. This may be due to the instability of the membranes (Tulasi 1997). However, a developer of SLM technology, Commodore Separation Technologies, has recently won its first contract with the American state of Baltimore for the clean-up of chromium (VI) using its SLM technology (Anon., 1998:4).

It was reported that the use of SLM extraction to recover copper for reuse has already undergone extensive pilot testing by researchers at the Katholieke Industriele Hogeschool (Gent, Belgium). The pilot plant incorporates a membrane with 19 m^2 of surface area, with a copper extraction rate of 50 g/hr, making it one of the largest SLM pilot plants presently available (Anon., 1998:31).

2.2.2.2 Electromembrane processes

Salts and electrolytes are composed of cations and anions that dissociate in water. If a direct electric current is passed through this solution, the cations and anions will conduct the current and move in opposite directions. The speed and direction of flow of these ions will depend on the current potential and current density, as well as upon the resistance of both solutions and membranes and the characteristics of individual ions, such as charge classification and valence. The only commercially significant electromembrane process is electrodialysis. It is utilized to deplete aqueous solutions containing low formula weight ionic solutes (Kesting, 1985:38).

2.2.2.2.1 Electrodialysis

Many variations of electrodialysis are used, but the most widely encountered form is the transport of ions through selective cation and anion exchange membranes as a result of the passage of an electrical current. Electrodialysis can be used for the separation of electrolytes from nonelectrolytes, the fractionation of electrolytes,

depletion or concentration of electrolytes, ion replacement, metathesis reactions and the separation of electrolysis products (Bunga, 1995).

Electrodialysis, similar to evaporation or reverse osmosis, can recover pure water from a salt solution or concentrate the total dissolved solids in a waste stream. Electrodialysis acts to remove unwanted salt (TDS) which builds up in process solutions (Peavy *et al.* 1985:194).

2.2.2.3 Pressure-driven processes

Pressure-driven membrane separations are processes designed to separate suspended or dissolved particles of different sizes by utilization of membranes containing appropriately sized pores. A summary of the differences between the processes and the membranes that they utilize is found in Table 2.5 (Wagner, 1996:9).

2.2.2.3.1 Microfiltration (MF)

Microfiltration is the oldest of the pressure-driven processes and ideally rejects only suspended solids, while even proteins pass the membrane freely (Wagner, 1996:9). Because of the large pores of MF membranes, there is relatively little resistance to flow and low pressures suffice as driving force. Another reason why low pressures are utilized, is the high porosity of MF membranes, since they are subject to distension under pressure. Several types of microfiltration membranes are commercially available (Kesting, 1985:44-46):

1. Phase inversion membranes consist of porous open-celled matrices whose structures in depth are either isotropic or anisotropic.
2. Crystalline or semicrystalline films into which pores have been introduced and maintained via stretching and annealing, respectively.

2.2.2.3.2 Ultrafiltration (UF)

The modern definition of ultrafiltration is different from the definition used in the early days of the technology. UF was then defined as the filtrative separation of particles in the colloid-size range, which we now know include both MF and UF. In UF the solute passes through the membrane less readily than the solvent for one of several reasons:

Table 2.5 Summary of pressure-driven separation processes and membranes

Property	Pressure-driven process			
	Microfiltration	**Ultrafiltration**	**Nanofiltration**	**Reverse Osmosis**
Membrane	Symmetrical Asymmetrical	Asymmetrical	Asymmetrical	Asymmetrical
Thickness Film	10-150 μm	150-250 μm 1 μm	150 μm 1 μm	150 μm 1 μm
Porosity	< 50%	< 40%	< 25%	< 15%
Pore Size	4-0.02 μm	0.2-0.02 μm	< 0.002 μm	< 0.002 μm
Rejecting	Particles, clay, bacteria	Macro molecules, proteins, polysaccha-rides	HMWC, mono-, saccharides, di-saccharides, oligosaccha-rides and poly-valent anions	HMWC, LMWC, sodium chloride, glucose, amino acids
Membrane materials	Ceramic, PP, PSO, PVDF	Ceramic, PSO, PVDF, CA Thin film	CA Thin film	CA Thin film
Membrane module	Tubular, hollow fiber	Tubular, hollow fiber, spiral wound, plate-and-frame	Tubular, spiral wound, plate-and-frame	Tubular, spiral wound, plate-and-frame
Operating pressure	< 2 bar	1-10 bar	5-35 bar	15-150 bar

- It is absorbed in the surface of the filter and its pores (primary adsorption).
- It is either retained within the pores or excluded therefrom (blocking).
- It is mechanically retained on top of the filter (sieving).

The desired effect of UF is sieving and therefore primary adsorption and blocking must be eliminated as completely as possible. The membranes used in UF are usually asymmetric polymers used in plate-and-frame, tubular, spiral wound or

hollow-fiber configurations. The primary applications of UF are and will probably remain in the purification of macromolecular solutions and colloidal suspensions by the selective permeation of microsolutes. It is also used for the filtration of water to remove colloidal foulants prior to demineralization by ion-exchange or reverse osmosis (Schutte, 1997:34-42).

2.2.2.3.3 Nanofiltration (NF)

Nanofiltration is also called low-pressure reverse osmosis or membrane softening. NF is used extensively for the separation of monovalent and multivalent ions in water treatment. The osmotic backpressure experienced in NF is therefore much lower than RO and consequently, the operating pressure for NF is much lower than RO. More recently, NF has also been employed for organics control (Aptel & Buckley, 1996:2.7).

2.2.2.3.4 Reverse osmosis (RO)

Reverse osmosis lies at the tight-end of the pressure-driven membrane separation process spectrum. Therefore, membrane pore size is smaller, porosity lower and pore density higher than for UF and MF membranes. These properties make it possible for RO membranes to retain microsolutes with sizes less than 10 Å. According to van't Hoff, the osmotic pressure of a dilute solution can be described with an equation, analogous to the ideal gas equation:

$$\Pi V = nRT \tag{2.14}$$

where Π is the osmotic pressure, V is the solvent volume, n is the number of moles of the solute, R is the gas constant and T is the absolute temperature. After manipulation, this equation can be rewritten as:

$$\Pi = gRTC \tag{2.15}$$

where g is the osmotic coefficient used to correct for certain effects such as solute-solute interaction and C the molecular concentration of solute. In other words, at a given temperature, Π is proportional to the molar concentration of solute (Kesting, 1985:44-46).

2.2.3 Polymeric membrane materials

When looking at the selections of membranes offered by the various suppliers, it may appear to be confusing. Although it may seem that many materials are used to make membranes under an array of trade names, in reality only few materials are used in quantity.

2.2.3.1 Integral membranes

Integral membranes are membranes consisting of a single layer manufactured from a single material.

2.2.3.1.1 Cellulose acetate (CA)

Cellulose acetate is the original membrane material. CA membranes are utilized in RO, NF and UF. This material has a number of limitations, mostly with respect to pH and temperature. The main advantage of CA is its low price and the fact that it is hydrophilic, which makes it less prone to fouling. Although there are other membrane materials available, there exist many membrane users who insist on buying the same membrane as last time and who simply stay with CA membranes because they work for them. An inherent weakness of CA is that it can be consumed by microorganisms.

2.2.3.1.2 Polysulphone (PSO)

Polysulphone in a number of varieties has been used for MF and UF membranes since 1975. The main advantages of PSO are exceedingly good temperature and pH resistance. PSO is practically the only membrane material used for a number of high quality food and dairy applications. These membranes do not tolerate oil, grease, fat or polar solvents.

2.2.3.1.3 Polyvinylidenedifluoride (PVDF)

Polyvinylidenedifluoride is a traditional membrane material. However, it is not used much as a membrane material because it is difficult to make membranes with good and consistent separation characteristics. Its main advantage is high resistance to hydrocarbons and oxidizing environments (Wagner, 1996:11).

2.2.3.2 Composite membranes

Composite membranes are also called thin film composite membranes and appear under various acronyms such as TFC and TFM. These membranes were produced to replace CA reverse osmosis membranes and are made in two-layer and three-layer designs; the precise composition remaining a secret. They have excellent

temperature and pH resistance, but do not tolerate oxidizing environments. Their main advantage is the combination of relatively high flux and very high salt rejection; greater than a 99.5% NaCl rejection is common for composite membranes. Generally speaking, a thin film composite membrane consists of a PSO membrane as support for the very thin skin-layer, which is polymerized *in situ* on the UF membrane. The three-layer design has two thin film membranes on top of the PSO support membrane. Around 1980, FilmTec marketed the two-layer design that immediately became the industry standard for water desalination, and has dominated the water desalination market ever since. Although the membrane has been improved over the years, the basic design remained unchanged and several companies are producing this type of membrane. In the mid 1980s DESAL started manufacturing membranes with the three-layer design. These membranes had difficulties in competing with the two-layer membranes in water desalination, but proved to work better on industrial process streams where they are more stable and less prone to fouling. This design is available for RO and NF and is still the best design for treating difficult process streams.

2.2.4 Membrane selection and characterization

2.2.4.1 Introduction

The selection of a membrane process and ultimately the membrane for a given separation task, can be a very unrewarding task. If the task is not fulfilled, the membrane will be blamed for the failure, but if the process runs smoothly, the credit is usually attributed to the separation process as a whole. Although it is unfair to blame only a part of the separation process (the membrane), there is a certain element of truth in the statement, as membrane selection can be such a critical factor.

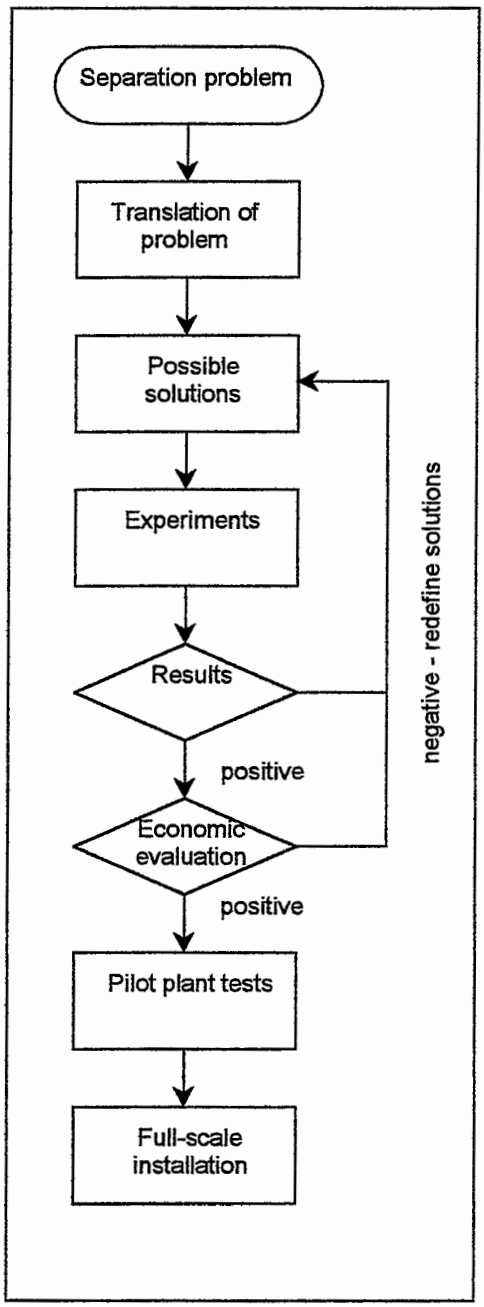

Figure 2.9 Selection scheme

The scheme proposed by Franken (1998:7) and presented in Figure 2.9 is used to select a membrane process and the appropriate membrane for a given application. This scheme includes all stages from the definition of the membrane process until the realization of a full-scale system. The actual membrane selection takes part during the phase 'translation of problem'. During this phase, all aspects of the separation problem are translated into an idea of full-scale installation.

There is a wide range of membranes available today. Membrane suppliers use the characteristics of the membranes to discriminate between them. These characteristics will also determine the application in which the membranes can be used. Some of the properties used to characterize membranes are included in the Hagen-Poiseuille relationship:

$$J = \frac{n\pi r_p^4 A_m P t}{8\eta\delta_m} \qquad (2.16)$$

where J = effluent flux,
n = number of pores per cm^2,
r_p = pore radius,
A_m = surface area of membrane,
P = pressure,
t = time,
η = viscosity of flowing fluid, and
δ_m = membrane thickness.

The following membrane properties are used to characterize membranes (Cheryan, 1986: 53):

- Porosity, and
- pore size and pore size distribution.

These two characteristics are relevant only to truly porous membranes (Kesting, 1985:50).

2.2.4.2 Porosity

Porosity (void volume) is the fraction of the membrane volume that is not occupied by the polymer substrate. If all these void volumes are interconnected and the membrane is completely wetted by an imbibed liquid such as water, the porosity can be calculated both from the density of the void-free polymer and from the difference between the wet and dry weights of the membrane. However, closed voids occur in real membranes, and their volume can not be determined easily. Porosity is expressed as a fraction or percentage void volume and is estimated with the equation:

$$V = n\pi r_p^2 \qquad (2.17)$$

with V = porosity, and
n = number of pores per square centimeter.

2.2.4.3 Pore size and pore size distribution

The pore size distribution can be measured or determined using several techniques:

1. *The bubble point technique*. Pore size was first evaluated by Bechhold who measured the pressure necessary to blow air through a water-filled membrane. He made use of Cantor's relationship:

$$r = \frac{2\sigma}{P} \tag{2.18}$$

with r = radius of the capillary,
σ = the surface tension (water/air), and
P = the pressure.

This technique is utilized in practice by placing a filter apparatus upside down so that air can impinge on the membrane from beneath. Bubbles of air are then observed as they penetrate the membrane into an overlaying layer of water. This method tends to yield high values, since the larger holes open at lower pressures. However, this is an advantage in estimating the pore size distribution. If the number of pores permeable to air increases substantially with but a small increase in pressure, a narrow pore size distribution is indicated. Conversely, a gradual increase in the number of air-permeable pores is indicative of a broad pore size distribution. The bubble point method is strictly valid when the imbibed medium completely wets the membrane and when the ratio of the pore diameter to that of the permeant species is large. A weakness of the bubble point technique is that the values obtained vary with the rate of pressure increase.

2. *The mercury-intrusion method.* This method is a variation of the bubble point technique. Discrepancies between actual pore size and pore size calculated using Canton's equation, come from non-zero contact angles. This equation was modified to take into account the contact angle θ:

$$r = \frac{-2\sigma\cos\theta}{P} \tag{2.19}$$

with θ = the contact angle between the mercury and the membrane.

A membrane is placed in a porosimeter chamber and pressure is applied, forcing mercury into the membrane. It is assumed that all the void spaces in the membrane are filled with mercury at the highest pressure (usually 75 atm). This assumption is valued only for cases where the voids are of the open-cell variety. The weights of the membranes at the lowest and highest pressures are used to obtain bulk densities. These bulk densities are then used to obtain the porosity by difference (Kesting, 1985:48-49).

3. *Direct microscopic observation*. Both scanning electron microscopy (SEM) and transmission electron microscopy (TEM) are employed to provide pore statistics.
4. *The solute passage technique*. This method constitutes the most reliable way of evaluating pore size distribution. The membranes to be tested are exposed to solutions of well-defined compounds whose molecular weights are known. These compounds are usually polysaccharides (dextrins, dextrans), aminoacids or proteins.

2.2.4.4 Membrane thickness

The membrane thickness is an important property of the membrane. Equation 2.16 shows that flux is inversely proportional to membrane thickness. Direct microscopic techniques are usually employed to determine membrane thickness.

2.2.5 Membrane manufacturing processes

The manufacturing of membranes can be divided into two processes: the manufacturing of dense polymeric films and the process of phase-inversion (Wagner, 1996:15).

2.2.5.1 Polymeric films

Dense polymeric membranes form the high-density extreme of the spectrum of variously swollen structures, which includes porous membranes and is bounded at the other end by liquid membranes. Dense polymeric films can be prepared by solution, melt and polymerization methods.

2.2.5.1.1 Solvent-cast films

Polymeric films are prepared from polymer solutions by dissolving a polymer substrate in a solvent medium, followed by the application of a liquid film onto a suitable substrate and complete evaporation of the solvent to form a dense film. The morphology of the resulting film is determined by the nature of both polymer and solvent.

2.2.5.1.2 Melt-extruded films

Thermoplastic polymers can be heated and extruded through a die to produce molten structures. During the heating process, energy is added to the system, which enables first groups and eventually smaller and larger chain segments to move. As the incipient membrane emerges from the die, it solidifies in a manner depending on the crystallization conditions. A thermoplastic forms either a noncrystalline or a partly crystalline solid.

2.2.5.1.3 Polymerization

If polymerization is attended by simultaneous crosslinking and consequent intractability of the resultant polymer, membranes of such polymers must necessarily be formed during polymerization. The homogeneous ion-exchange membrane is the most important class that fits into this category.

2.2.5.2 Phase-inversion membranes

Phase-inversion refers to the process by which a polymer solution inverts into a swollen three-dimensional macromolecular gel. The process either begins with a homogeneous single-phase solution (Sol 1) which undergoes a transition into a heterogeneous solution of molecular aggregates consisting of two interdispersed liquid phases (Sol 2) prior to gelation, or it begins directly with Sol 2. This can be summarized as follows:

1. Sol 1 → Sol 2 → Gel, or
2. Sol 2 → Gel

This process is illustrated in Figure 2.10. Four phase-inversion processes are discussed: the dry process, the wet process, the thermal process and the polymer-assisted process.

2.2.5.2.1 The dry process

The dry or complete evaporation process is the oldest and most simple of the phase-inversion processes. The final membrane thickness is only a fraction of the as-cast thickness owing to the loss of solvent and the resultant increase in the concentration of polymer per unit volume. Because of the voids in the structure, it is substantially thicker than the polymeric film containing an equivalent amount of polymer.

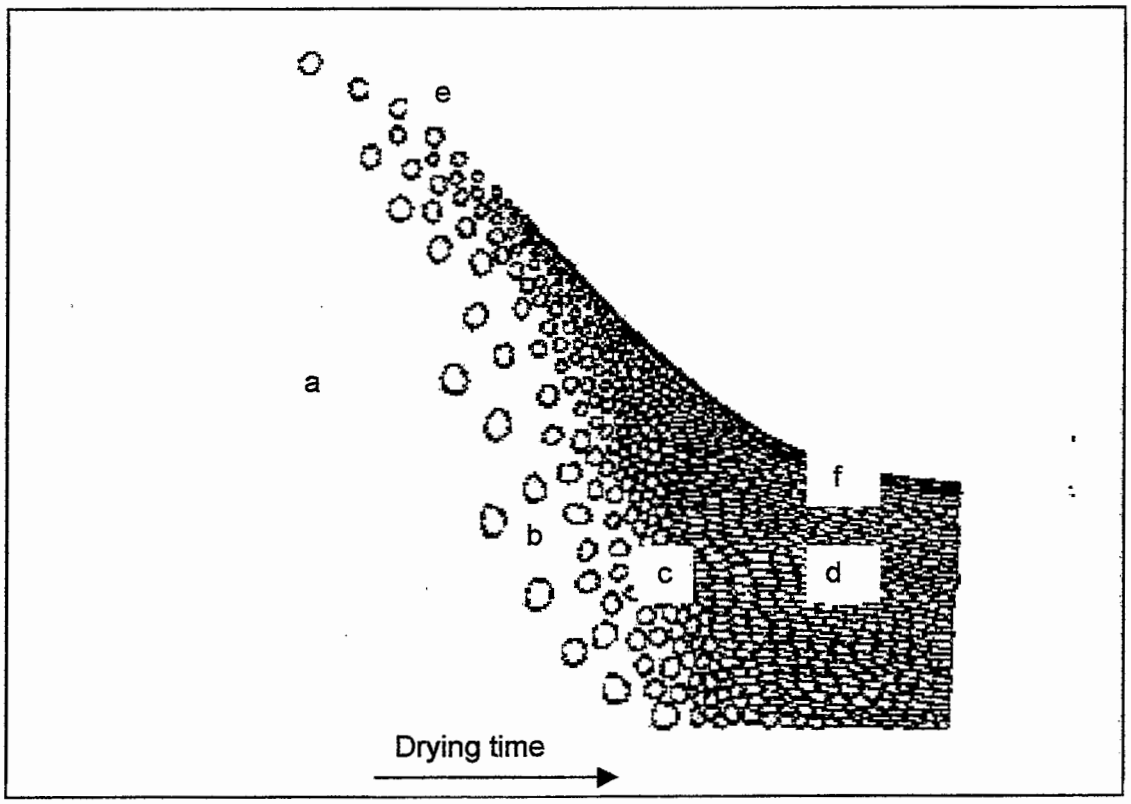

Figure 2.10 Mechanism of formation of phase-inversion membranes: (*a*) Sol 1; (*b*) Sol 2; (*c*) primary gel; (*d*) secondary gel; (*e*) air-solution interface; (*f*) skin

2.2.5.2.2 The wet process

The wet or combined evaporation-diffusion technique utilizes a viscous polymer solution in two ways. It is either allowed to partially evaporate after which it is immersed into a nonsolvent gelation bath where whatever is left of the solvent-pore-former system is exchanged for the nonsolvent or is immersed directly into the nonsolvent gelation bath for the exchange of the solvent system for nonsolvent. The membranes produced in the wet process are water-swollen; moreover, the water content of the membranes (the equivalent of porosity in the dry process) is a prime determinant of its functional performance characteristics (Barnes, 1993:20-31).

2.2.5.2.3 The thermal process

The thermal process is a recent development in the technology of phase-inversion membranes invented by Castro. It is applicable to a wide range of polymers, which are otherwise inaccessible to the phase-inversion approach because of their poor solubility. The thermal process utilizes a latent solvent (a solvent at elevated temperatures and a nonsolvent at low temperatures) and thermal energy to produce

a Sol 1, which on cooling inverts into a Sol 2 and on further cooling, gels. Both liquids and solids can serve as latent solvents. However, if a solid is employed, it must be a liquid at which Sol 2 appears. The latent solvents are removed from the final gel by extraction with a liquid, which is a solvent for the latent solvent and a nonsolvent for the polymer.

2.2.5.2.4 The polymer-assisted process

The polymer-assisted phase inversion process utilizes a solution consisting of a solution and two compatible polymers to cast a dense film with an interpenetrating polymer network. The solution is either completely or partially evaporated from this network, after which the film is immersed in a liquid, usually water, which is a solvent for one of the polymers and a nonsolvent for the other. The insoluble network, which remains after leaching, is a skinless microporous membrane. The leached polymer acts as a nonsolvent pore former, assisting the membrane polymer to assume a Sol 2 micellar structure prior to gelation. The membranes formed in the polymer-assisted process are usually skinless, isotropic with a narrow pore size distribution, of intermediate porosity (~ 50%), and characterized by excellent mechanical properties. The potential application for polymer-assisted phase-inversion membranes is to serve as microporous supports for thin-film composites (Kesting, 1985:237-265).

2.3 Statistical experimental design

2.3.1 Introduction

Most new chemical processes as well as improvements on existing ones, begin with small-scale laboratory investigations. In the early stages, these experiments may consist of simple experiments that offer small scope for what could be called an experimental design. One of the simplest and most common ways to investigate the effects of factors (or variables) on the response (or result of interest) is to sequentially change (or position) the level of each factor and observe the response change. When one factor is changed in the experiment, all others remain constant. This reasoning may work well in some instances. Take as an example Figure 2.15. A response surface topology has been plotted versus two independant variables, temperature and pressure. Temperature was chosen as the first factor to be varied, and line segment A-B was traversed. The best response is observed at point C. Next, in a sequential fashion, temperature is held constant while the pressure is varied. The result is that segment D-E is traversed with the best response observed at point X, which is the maximum for this surface.

This sequential method generally yields good results in practice, but unfortunately rarely yields optimum conditions. This is explained by the fact that real surfaces are rarely as ideal as the one in Figure 2.11. The example shown in Figure 2.12 will bear this out. Beginning with temperature, segment A-B is traversed and C is found to give the best response. Traversing segment D-E still yields point C as the best result. However, point C is far removed from the optimum at point X. Figure 2.12 represents what is routinely called a ridge. Ridged systems occur frequently in practice. The sequential method fails on the following important points:

- It does not always find the optimum.
- It tells nothing about interaction. That is, it assumes that each factor contributes individually to the response, but that factors combined in some way have no effect.

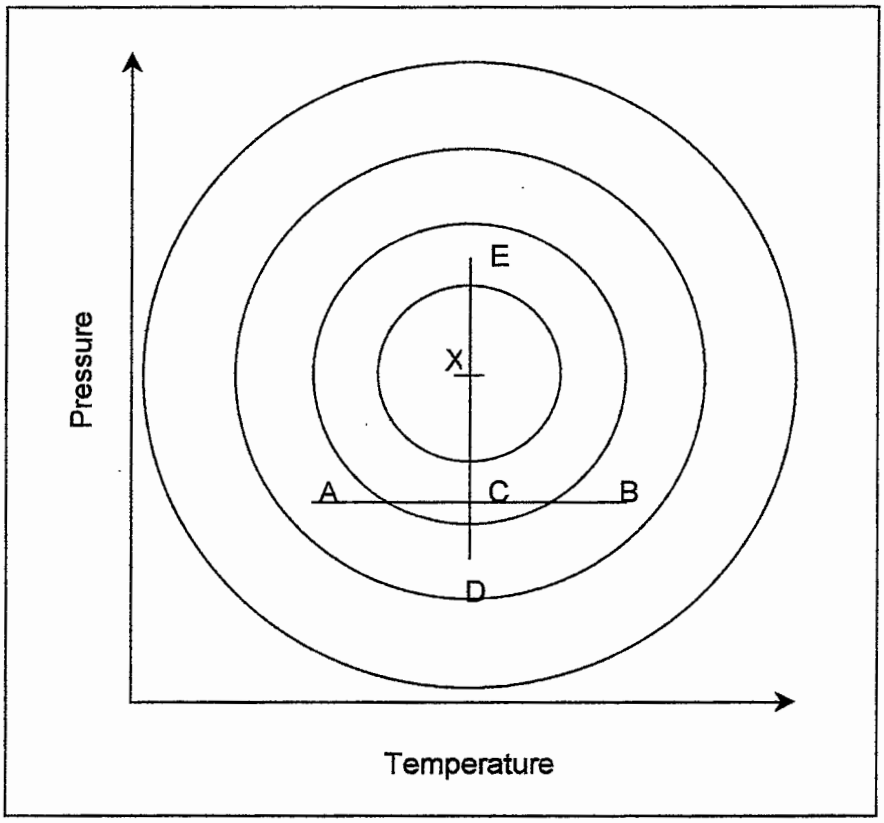

Figure 2.11 Simple response surface

- The result obtained is a function of both the starting levels and the factor chosen as the one to be varied initially (Currie, 1984:12-16).

2.3.2 Response surfaces

Response surface methodology consists of a group of techniques used in the empirical study of relationships between one or more measured responses, such as yield, on the one hand and a number of input variables (or factors), such as temperature and pressure, on the other (Box, 1978:510). A response surface is used for approximating the surface in the optimum region and characterizes a response that depends on K factors by a surface in K + 1 dimensions. For a small domain of

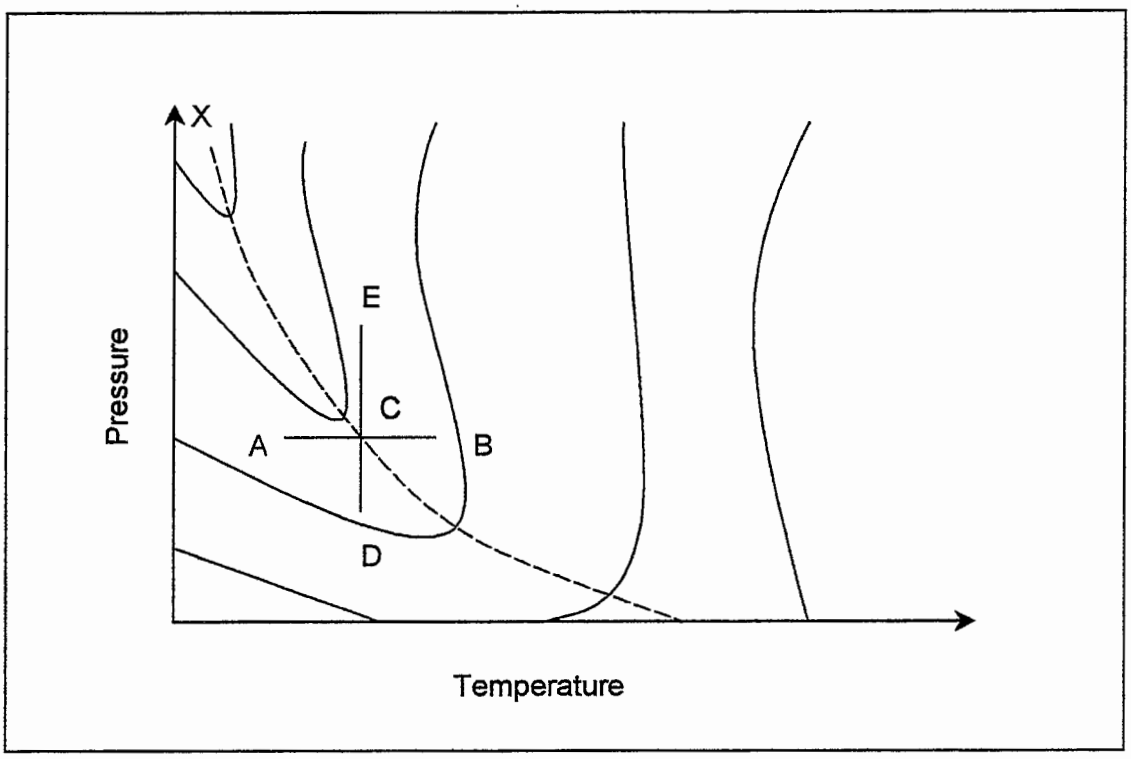

Figure 2.12 Ridged response surface

interest, a surface can usually be approximated by a plane or first-order polynomial. Larger regions of interest may have to account for curvature, and a second-order polynomial may be utilized. This curvature is usually detected during optimization experiments. The purpose of this experimental design is to design a set of experiments that will yield a mathematical relationship between the different factors and the responses.

CHAPTER 3 EXPERIMENTAL IRRADIATION OF POLYETHYLENE

"The greatest pleasure in life is doing what people say you cannot do."
- Walter Bagehot -

The raw material, polyethylene, was irradiated at an industrial facility to enhance its properties (crosslinking and melting temperature). Soxhlet extraction was used to determine the extent to which the crosslinking was increased, and DSC measurements determined the increase in melting temperatures.

3.1 Polyethylene material

Three polyethylene samples with different densities were received from Plastomark (Midrand, South Africa). They consisted of low-density polyethylene (LDPE), high-density polyethylene (HDPE) and ultra-high molecular weight polyethylene (UHMWPE). The former two polymers were manufactured by Safripol (Sasolburg, South Africa), while the latter was imported from Hoechst in Germany.

3.2 Size distribution

The size distribution of the polymer powder is of critical importance in the manufacturing of sintered membranes. The smaller the size of the polymer particles, the smaller the pore size of the membrane will be.

The size distributions for the different polymers were determined with a Sympatec Particle Size Analyzer (SPSA). The cuvet method was used to determine the particle size for the different polyethylene samples. These size distributions are summarized in Table 3.1. The complete size distribution curves are included in Appendix A.

3.3 Irradiation of polyethylene

The polyethylene samples were irradiated at Iso-Ster (Kempton Park, South Africa) using its industrial gamma irradiator (Figure 3.1). Iso-Ster's industrial irradiator consists of a room with concrete walls two meters thick, which contain the cobalt-60 radiation source. A conveyor system automatically moves the products into the room for irradiation, and again removes them after irradiation has taken place. When personnel must enter the room, the irradiation source is lowered to the bottom of a pool, where water absorbs the radiation energy and protects the workers.

Table 3.1 Size distributions

Sample	D_{10}, μm	D_{50}, μm	D_{90}, μm	Mean Particle Diameter, μm
LDPE	190.89	281.49	400.75	290
HDPE	217.16	312.00	432.17	320
UHMWPE	67.02	128.91	213.43	140

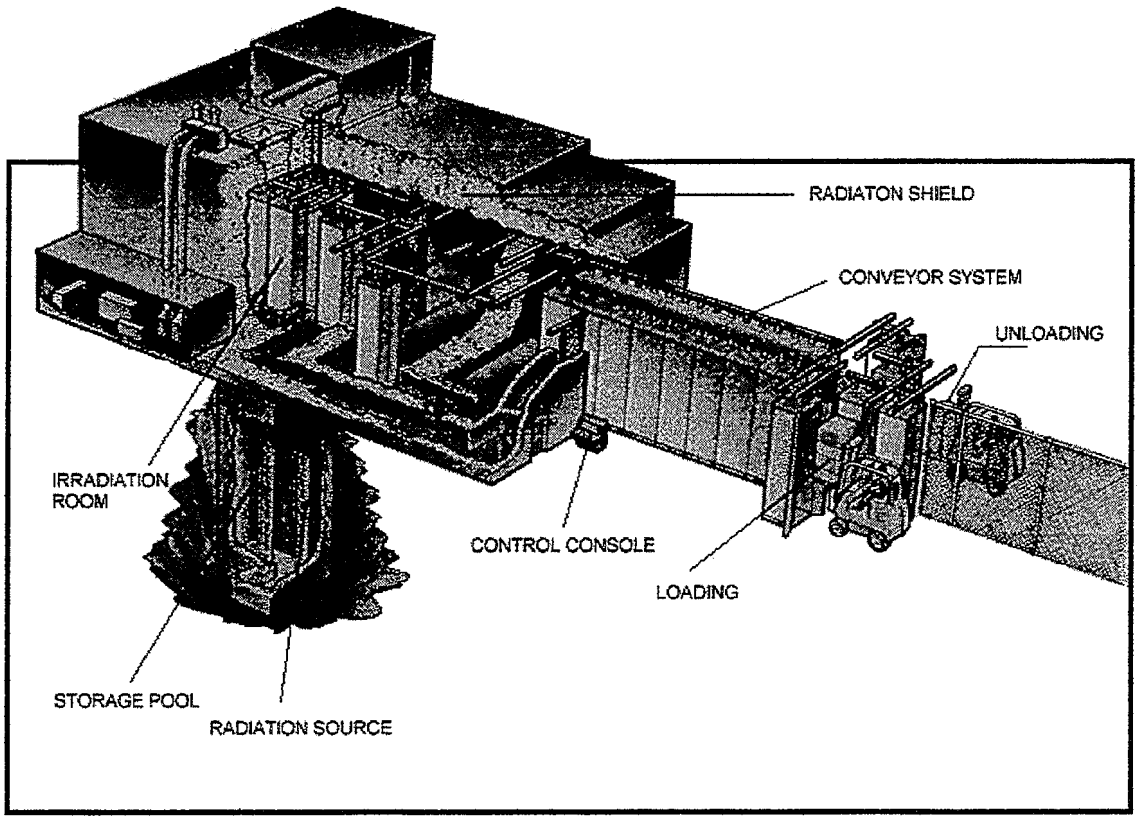

Figure 3.1 Industrial irradiator

The samples were sealed in polyethylene/polyester laminate bags to prevent oxygen degradation during irradiation. Two atmospheres were used: nitrogen as an inert gas (reference) and acetylene as the crosslinking agent. It is important to use an excess amount of acetylene; if too little is used, the acetylene will only react with some of the polyethylene and a vacuum will form in the sample bag. All the samples that had to be irradiated at the same dose, were sealed into a large container. Therefore, every container comprised of six samples:

1. LDPE in a nitrogen atmosphere.

2. LDPE in an acetylene atmosphere.
3. HDPE in a nitrogen atmosphere.
4. HDPE in an acetylene atmosphere.
5. UHMWPE in a nitrogen atmosphere.
6. UHMWPE in an acetylene atmosphere.

The specific dose received during irradiation was determined by red polymethyl methacrylate dosimetry, which is intercalibrated annually through the National Physical Laboratory in the United Kingdom as a primary standards laboratory. These values are shown in Table 3.2.

Table 3.2 Dose received

Container	Dose, kGy
Container 1	0 (Control)
Container 2	11.0
Container 3	31.5
Container 4	52.6
Container 5	73.5
Container 6	104.1
Container 7	150.2

3.4 Free radical destruction

The free radicals produced during irradiation, will remain in the irradiated polymer sample bags and must be destroyed before opening the bag to prevent it from reacting with oxygen in the air. All the sample containers were heated in an oven at 90°C for 12 hours to ensure that all the free radicals were destroyed.

3.5 Property enhancement

3.5.1 Gel formation

3.5.1.1 Experimental setup

The crosslinked portion of a polymer is equivalent to the percentage gel present in the polymer and is insoluble in conventional polymer solvents. The percentage gel can be determined by dissolving the soluble fraction from the polymer sample. Polyethylene has no solvents at temperatures lower than 100°C, therefore the polyethylene samples had to be heated to a higher temperature before the sol

dissolved into the solvent. A Soxhlet extractor was used to isolate the gel fraction of the polyethylene samples and is shown in Figure 3.2.

The solid polyethylene sample is placed in the porous thimble A (which is made of tough filter paper), and the latter is inserted into the wider inner tube. The extractor is then fitted to flask C, containing the solvent. Decahydronaphthalene (DHN or decalin) was used as solvent during the investigation. A double surface type reflux condenser (D) is attached to the top of the extractor. The DHN is boiled gently on a heater (B), the vapour passes through the tube E, is condensed by the condenser D, and the condensed solvent falls into the thimble A and slowly fills the body of the extractor. It is important

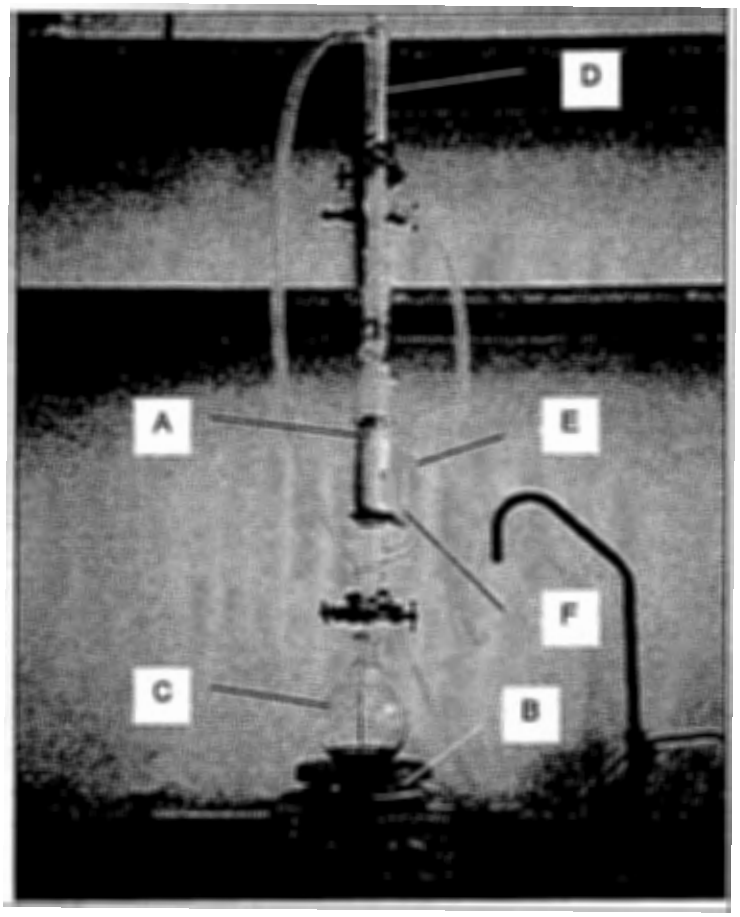

Figure 3.2 Soxhlet extractor

to use a thimble with a top higher than the siphon tube F, otherwise the polyethylene might float out of the thimble and pass down the siphon tube.

When the solvent reaches the top of the tube F, it siphons over into the flask C, and removes the portion of the substance which was extracted in A. This process is

repeated continuously until complete extraction is effected. The advantage of this apparatus is that the temperature in A remains near the boiling point of the solvent; extraction is effected by the hot solvent. The extraction time for each polyethylene sample was 60 hours for this investigation. The percentage gel was calculated using the following equation:

$$\text{Gel \%} = \frac{m_f}{m_i} \times 100 \qquad (3.1)$$

with m_f = mass of sample after extraction (g)

m_i = mass of sample before extraction (g).

3.5.1.2 Results and discussion

The effect of irradiation dose on gel formation is illustrated in Figure 3.3.

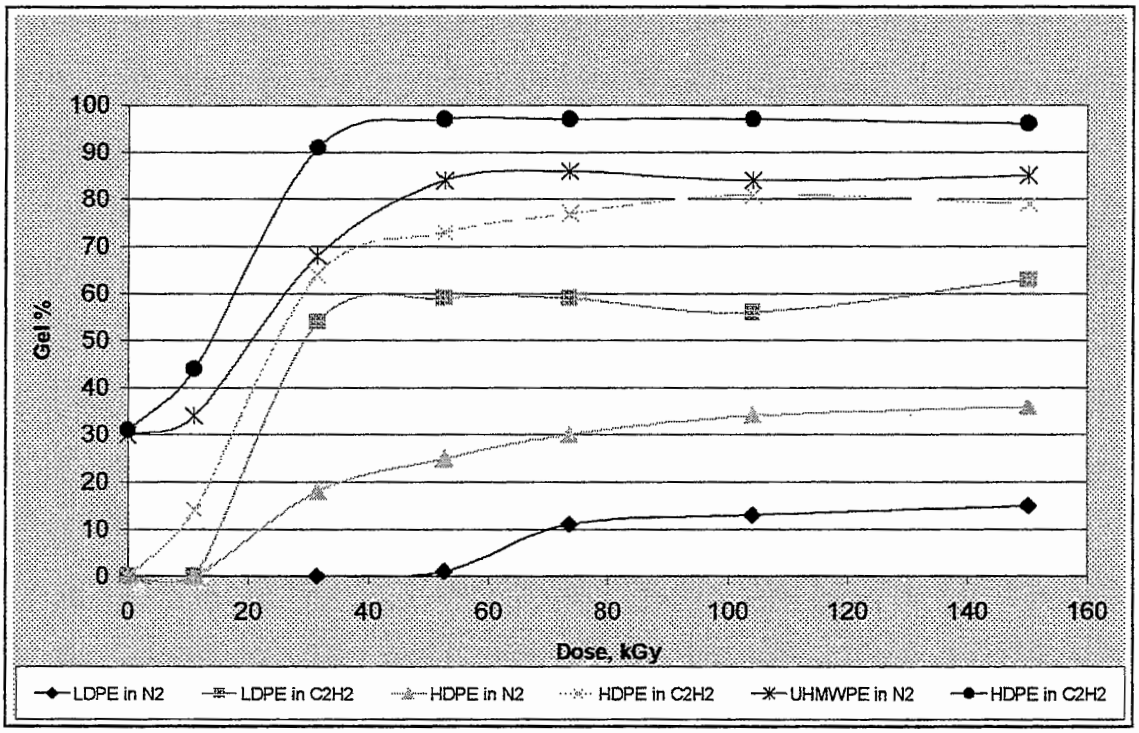

Figure 3.3 The effect of irradiation on gel formation

It is clear from Figure 3.3 that gel formation was enhanced by irradiation. The following are also evident:

1. The increased gel formation on irradiation dose observed in the testwork, is in agreement with the results obtained in the literature survey. The gel percentage

increased with increased irradiation dose for all samples in both nitrogen and acetylene atmospheres.

2. Acetylene proved to be a good crosslinking agent. The gel percentage for LDPE, HDPE and UHMWPE in acetylene atmospheres had higher values compared to the corresponding samples in nitrogen at the same dose.
3. There is a steep initial increase in gel formation on dose received, which tends to level out at a critical irradiation dose. This phenomenon is more pronounced in HDPE and UHMWPE.

The Soxhlet extraction identified a dose of 60 kGy as sufficient for maximum gel formation for the three membrane materials. LDPE, HDPE and UHMWPE samples of 1 kg each were irradiated at this dose to be used for membrane manufacture (refer to Chapter 4).

A mathematical equation is required to relate the gel fraction of the polyethylene sample to the irradiation dose received. After studying the different gel fraction curves, it was decided to fit the following equation through the obtained experimental data:

$$\text{Gel \%} = c_1 - c_2 e^{-c_3 \cdot \text{dose}} \tag{3.2}$$

with c_1, c_2 and c_3 constants. The ultimate percentage crosslinking can be determined with equation 3.2 by calculating Gel % at time t=∞.

$$\begin{aligned} \text{Gel \%}\big|_{t=\infty} &= c_1 - c_2 e^{-c_3 \cdot \infty} \\ &= c_1 - c_2(0) \\ &= c_1 \end{aligned} \tag{3.3}$$

The initial rate of crosslinking can be determined as follows:

$$\begin{aligned} \text{Rate} &= \frac{d}{dt}\left(c_1 - c_2 e^{-c_3 \cdot t}\right) \\ &= c_2 c_3 e^{-c_3 t} \\ \text{If } t = 0 & \\ \text{Rate} &= c_2 c_3 (1) \\ &= c_2 c_3 \end{aligned} \tag{3.4}$$

Equation 3.2 was used to fit the observed values for the Soxhlet extraction experiments using the different polyethylene samples. These curves are presented in Appendix B. The most important values obtained from the mathematical model are summarized in Table 3.3.

Table 3.3 Important observations on gel formation

Observation	LDPE		HDPE		UHMWPE	
	In N_2	In C_2H_2	In N_2	In C_2H_2	In N_2	In C_2H_2
Initial gel percentage	0	0	0	0	30	30
Ultimate gel percentage	14.4	59.4	36.1	82.3	85.9	96.9
Initial gel forming dose (kGy)	> 53	> 11	> 11	> 0	> 0	> 0
Maximum effective dose (kGy)	80	40	90	60	60	40
Initial rate of gel formation	20.4	25.2	1.5	3.4	5.7	18.8

3.5.2 Melting temperature

The effect of irradiation on the melting temperature of polyethylene was also investigated.

3.5.2.1 Experimental method

It is important to consider the thermal analysis of materials before they are utilized in new applications. Differential scanning calorimetry (DSC) is the most popular technique in thermal analysis. Two types of DSC are used in analysis: heat-flux DSC and power-consumption DSC. Heat-flux DSC is eminently suited for quantitative measurements to be performed. A schematic drawing of a heat-flux DSC cell is shown in Figure 3.4. The sample and reference substance are placed in small aluminium crucibles and positioned on a heat-flux plate. This plate generates a very controlled heat-flow from the furnace wall to the crucibles. The temperature measurements also take place at this plate, directly below the crucibles. In this way, the influence of changes in thermal resistance of the sample is eliminated. A characteristic DSC curve is shown in Figure 3.5.

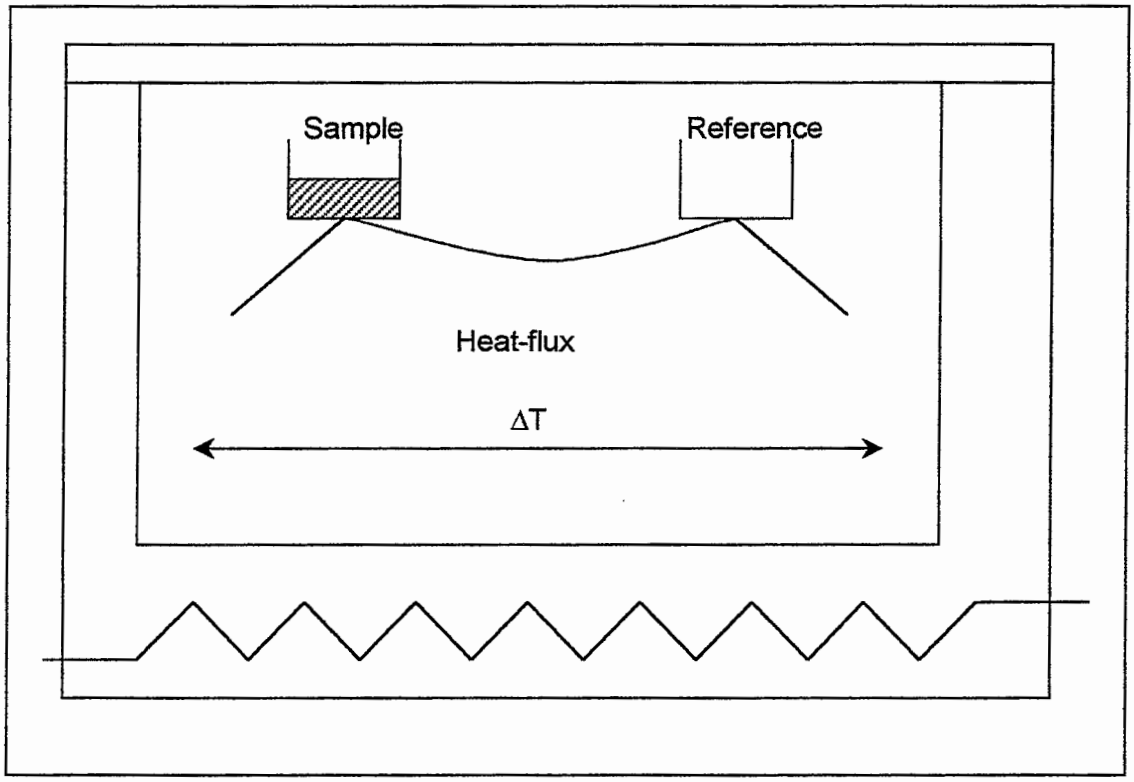

Figure 3.4 Heat-flux DSC cell

The temperature is always displayed on the X-axis, while $\dot{q}\left(\frac{dq}{dt}\right)$ is shown on the Y-axis. The peak corresponds to the melting of the polymer (T_M). Endothermic peaks are always plotted downward, while exothermic peaks are plotted upward. The DSC curves were used to determine the melting points of the irradiated polyethylene samples.

3.5.2.2 Results and discussion

The results of the DSC measurements are shown in Table 3.4. Irradiation caused a definite increase in the melting temperature of all the polyethylene samples. This is an important effect of irradiation on polymers, which is used on a large scale in industrial applications. The irradiation caused the stabilizer in the polyethylene samples to degrade, therefor 1% of industrial stabilizer (IRGANOX 1010) was added before the DSC measurements were done.

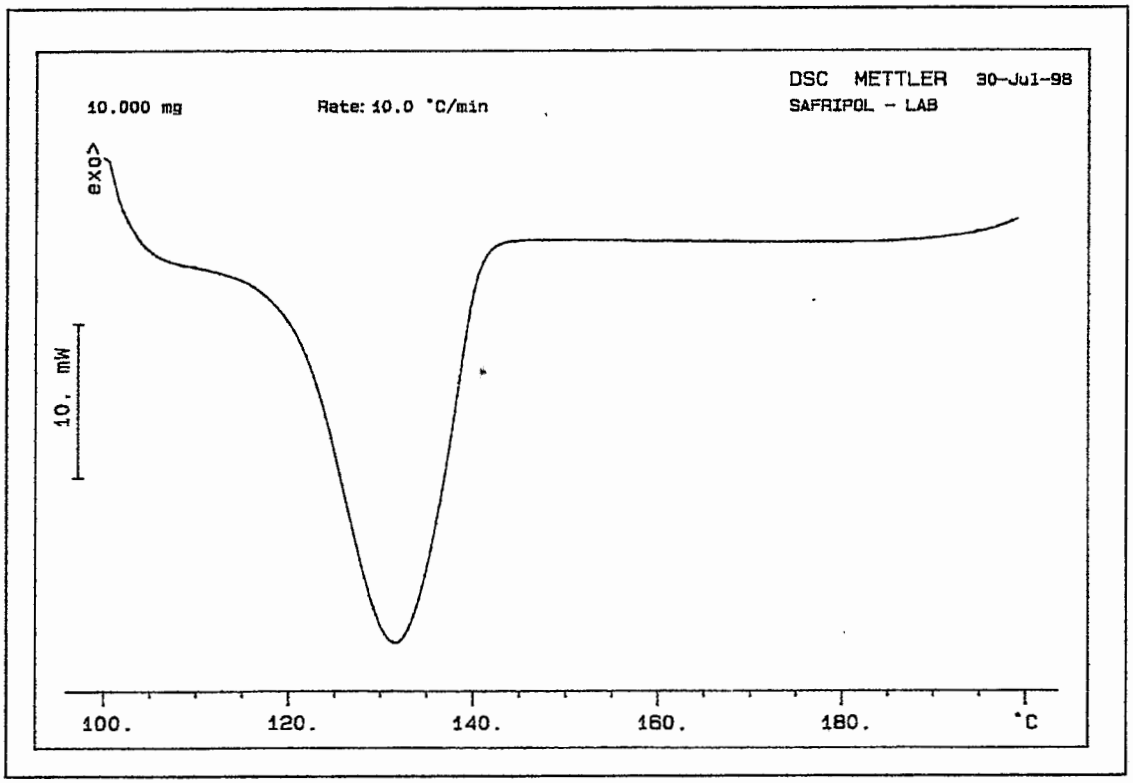

Figure 3.5 Characteristic DSC curve

Table 3.4 Results of DSC measurements

Sample	Dose, kGy	Melting temperature, °C
LDPE	0 (unirradiated)	128.4
	60.0	132.4
HDPE	0 (unirradiated)	130.4
	60.0	133.4
UHMWPE	0 (unirradiated)	139.5
	60.0	142.6

The complete DSC curves generated during the measurements are included in Appendix C.

3.6 Conclusions

Noncrosslinked polyethylene can not be used for the production of sintered membranes because it will form a film that is not permeable. The radiation crosslinking of the polymer, however, is a viable modification treatment because it alters the properties of polyethylene to prevent it from melting at its usual melting

temperature. The following conclusions were made from the results obtained in this chapter:

1. Gel formation is enhanced by gamma-irradiation. The higher the molecular weight of the polyethylene sample, the more pronounced is this effect. The results have shown that an increase in molecular weight of the sample, results in a higher ultimate gel fraction in the sample. The literature survey has shown that impact strength decreased with increased dose, and therefore it is important to irradiate the polyethylene at a dose that will increase the crosslinking but is not too high to cause brittleness in the membrane. The results also showed that the ultimate gel fraction has been reached for the samples at a dose of approximately 60 kGy. It was therefore decided to take samples of the three polyethylenes and irradiate them at a dose of 60 kGy. These irradiated samples were used as raw material for membrane manufacture.
2. The results showed conclusively that acetylene is an effective crosslinking agent. At a dose of 60 kGy, 97% of the UHMWPE sample irradiated in an acetylene atmosphere was crosslinked, compared to 86% of the same material irradiated in a nitrogen atmosphere. Similar results were observed for LDPE and HDPE: respectively 60% and 75% were crosslinked in the acetylene environment compared to 5% and 26% in the nitrogen atmosphere. Therefore, a polyethylene sample irradiated in acetylene will achieve the same crosslinking as a similar sample irradiated at a higher dose in the absence of acetylene. This may result in lower membrane production costs as radiation at a higher dose is more expensive.
3. The melting temperatures of all the samples increased after irradiation. This phenomenon was expected as it was also described in the literature.

CHAPTER 4 MEMBRANE MANUFACTURING AND CHARACTERIZATION

"I have learned to use the word 'impossible' with the greatest caution."

- Werner von Braun -

The irradiated polyethylene was used for the production of membranes. An experimental design was used to identify the membrane with the optimum characteristics to be used in the permeation tests. The extraction of nickel through the new membrane was compared to the extraction through a commercial membrane.

4.1 Membrane manufacture

The LDPE, HDPE and UHMWPE samples irradiated at 60 kGy, were further processed into flat-sheet membranes. A Struess Protopress-2 heat-press, normally used in sample preparation, was used as the membrane press. The adjustable parameters on the press, as well as their operating ranges, are given in Table 4.1. A constant mass of 0.5 g polyethylene powder was used for each membrane sample, resulting in a membrane with a diameter of 3 cm and a thickness of approximately 0.5 mm. A typical membrane is shown in Figure 4.1.

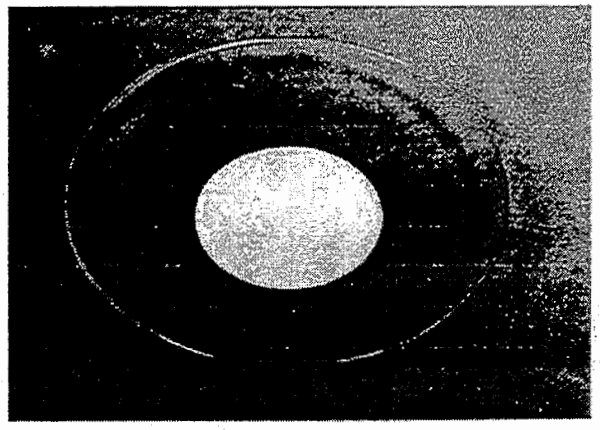

Figure 4.1 Membrane used in testwork

Table 4.1 Membrane heat-press

Parameter	Minimum value	Maximum value	Increment
Temperature, °C	105	185	5
Force, kN	10	40	2
Heating time, min	1	30	0.5
Cooling time, min	1	12	0.5

4.2 Theoretical Maximum Membrane Characteristics

The maximum theoretical pore size and porosity are useful to identify possible applications for the membrane under investigation. The calculated values can then be compared to the experimental values from the investigation.

4.2.1 Maximum pore size calculation

Figure 4.2(a) shows four polyethylene particles arranged in a cubic coordination polyhedron with the particles touching each other. The small sphere in the center represents the maximum theoretical pore size. The shaded triangle is shown enlarged in Figure 4.2(b), with r_{par} the radius of the particle and r_p the radius of the maximum theoretical pore size.

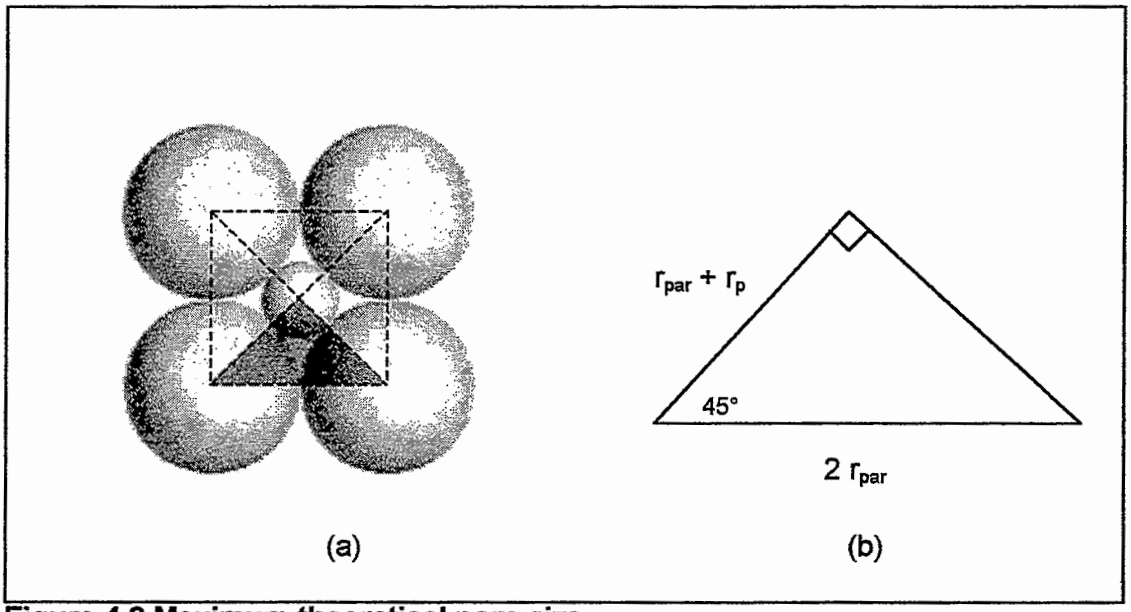

Figure 4.2 Maximum theoretical pore size

The value of r_{par} is obtained as follows:

$$\cos 45° = \frac{r_{par} + r_p}{2\, r_{par}}$$

$$\therefore 2\, r_{par} \cos 45° = r_{par} + r_p$$

$$\therefore r_p = r_{par}\left(2\cos 45° - 1\right)$$

$$\therefore r_p = 0.414\, r_{par}$$

or

$$d_p = 0.414\, d_{par} \qquad (4.1)$$

with d_{par} the diameter of the particle and d_p the diameter of the sphere representing the maximum theoretical pore size. Table 4.2 lists the mean diameters of the particles and theoretical pore sizes, calculated with equation 4.1.

Table 4.2 Maximum theoretical pore size

Characteristic	LDPE	HDPE	UHMWPE
Mean diameter, μm (d_{par})	200	120	200
Maximum theoretical pore size, μm (d_p)	83	50	83

The maximum theoretical pore sizes from Table 4.2 indicate that the LDPE, HDPE and UHMWPE membranes are suitable for normal membrane applications. These pore sizes are also suitable for microfiltration, the membrane process using membranes with the largest pores.

4.2.2 Maximum porosity calculation

Figure 4.3 shows the four polyethylene particles with another layer added. The void volume enclosed by the eight particles is surrounded by a cube, with the centres of each particle forming a corner of the cube. Each side of the cube has a length equal to the diameter of a single particle, d_{par}.

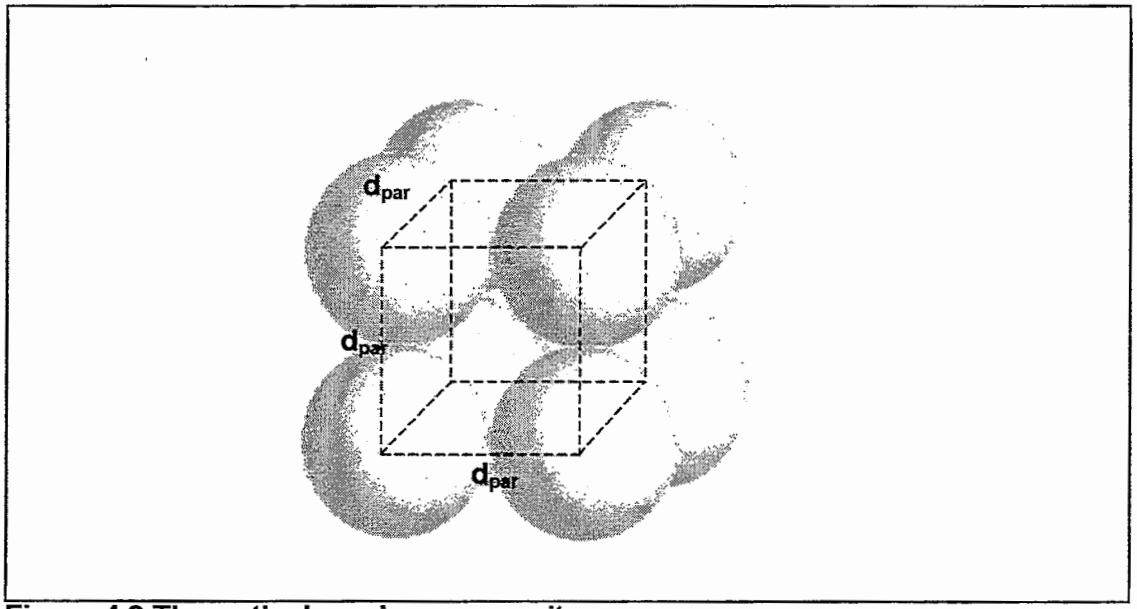

Figure 4.3 Theoretical maximum porosity

The total volume of the highlighted cube (V_{cube}) is calculated as follows:

$$V_{cube} = d_{par}^{\ 3} \tag{4.2}$$

Every corner of this cube includes an eighth of a sphere with diameter d_{par}. Therefore, the void volume (V_{void}) is calculated by subtracting the volume of a sphere (V_{sphere}) with diameter d_{par} from the total volume of the cube. The complete calculation of the porosity is given below.

$$\begin{aligned} \text{Porosity (max)} &= \frac{V_{void}}{V_{cube}} \times 100 \\ &= \frac{V_{cube} - V_{sphere}}{V_{cube}} \times 100 \\ &= \frac{d_{par}^{\ 3} - \frac{1}{6}\pi d_{par}^{\ 3}}{d_{par}^{\ 3}} \times 100 \\ &= \frac{d_{par}^{\ 3}(1 - 0.524)}{d_{par}^{\ 3}} \times 100 \\ &= 47.6\% \end{aligned} \tag{4.3}$$

The maximum porosity is independant on the size of the particle, and based on this value, all three membranes can be used as SLM and microfiltration membranes.

4.3 Experimental design

4.3.1 Response variables

The first step in experimental design is to list all applicable response variables that will be influenced by the design factors. The response variables selected for this investigation, are generally used for membrane characterization. The response variables are:

1. The porosity of the membrane.
2. The mean pore size of the membrane.
3. The pore size distribution of the membrane.

These observations were measured on a microscopic level.

4.3.2 Design factors

The next step in experimental design is to list all the factors (independant variables) that will be varied to determine their influence on the experimental observations. These variables are:

1. Temperature.
2. Pressure.

These factors were varied simultaneously during membrane manufacture. A response surface design is necessary to determine the relationships between these two factors.

4.4 Initial testwork

The first step in experimental design is to determine the range over which the variables must be varied for optimum results. Although one has an intuitive idea of how the dependant variable will respond to changes in the independant variables, it must be proven experimentally. This is done by varying one independant variable while keeping the other constant. The initial experiments are shown in Table 4.3.

Table 4.3 Initial experiments

Experiment no.	Constant factor	Value of constant factor	Variable factor	Values of variable factor
1.	Pressure	42.44 MPa	Temperature	110, 115, 120, 125, 130, and 140°C
2.	Temperature	125°C	Pressure	14.15, 21.22, 28.29, 35.37, and 56.59 MPa

4.4.1 Results of initial testwork

4.4.1.1 Effect of temperature and pressure on porosity

The porosities of the membranes were determined at Mintek (Randburg, South Africa) using a QuantaChrome porosimeter (Figure 4.4). This porosimeter uses mercury intrusion to determine the total pore volume intruded.

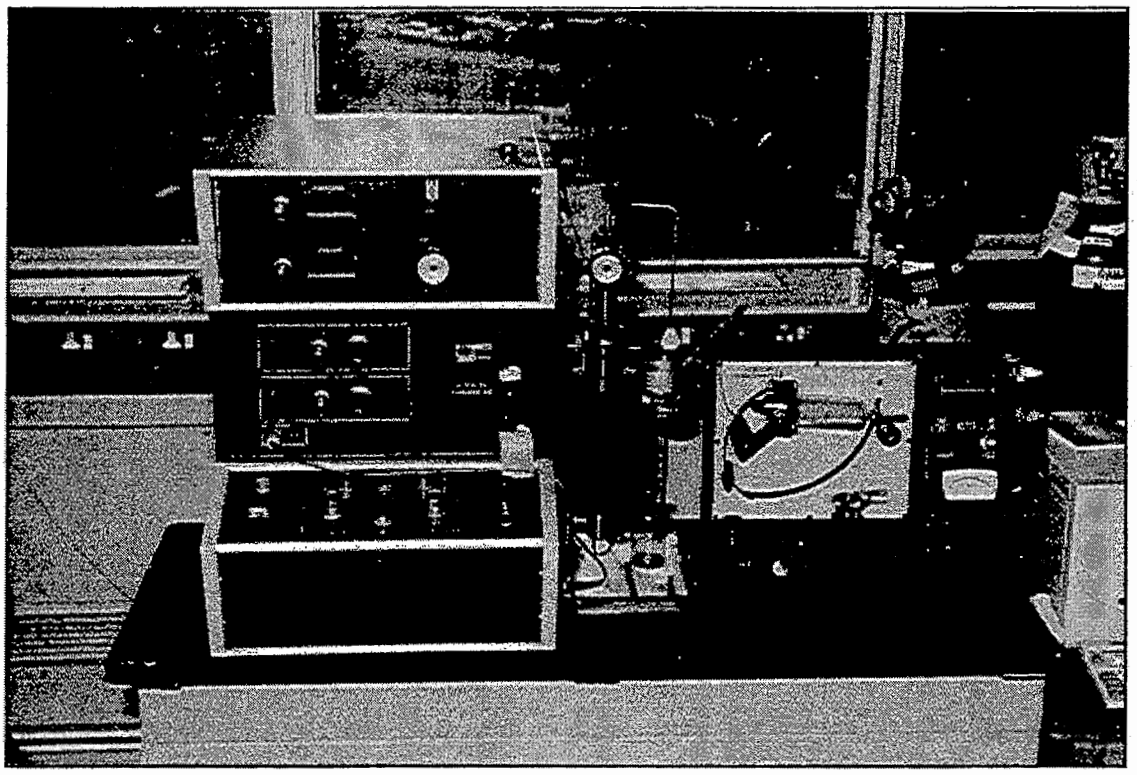

Figure 4.4 The QuantaChrome porosimeter

The porosities of the different polyethylene membranes were measured in terms of total pore volume intruded and reported in cm^3/g. The following equation was used to calculate the percentage porosity of each membrane:

$$\text{Porosity}(\%) = \frac{\text{Porosity}\left(\frac{cm^3}{g}\right)}{\rho_a} \times 100 \qquad (4.4)$$

with ρ_a the apparent density (measured with the instrument). The porosities for experiment 1 (constant pressure of 42.44 MPa, variable temperature) are shown in Figure 4.5.

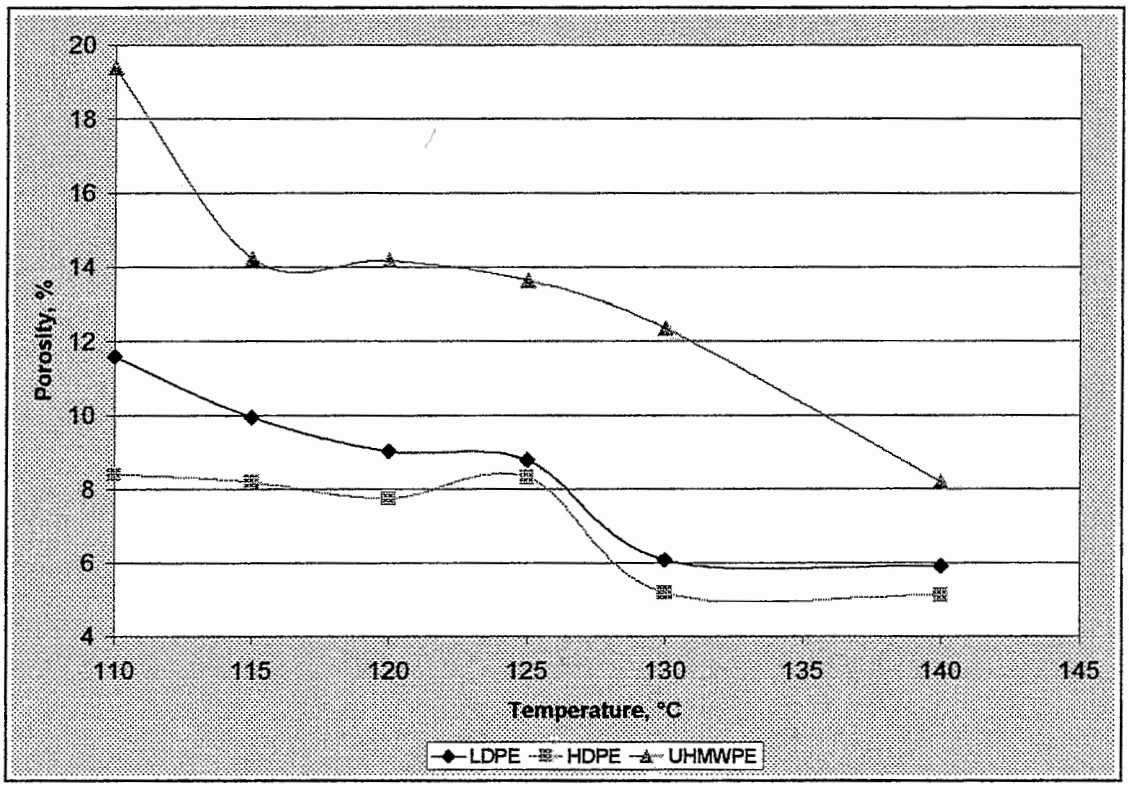

Figure 4.5 Effect of temperature on porosity

The results indicate that the porosities of the LDPE, HDPE and UHMWPE membranes decreased with increased temperature. The porosities of the membranes manufactured in experiment 2 (constant temperature of 125°C, variable pressure) are shown in Figure 4.6.

Figure 4.6 shows a decrease in porosity with an increase in pressure. The applied pressure forces the particles closer together, reducing the void volume between the particles. The full set of porosimetry curves are included in Appendix D. Although the polyethylene particles are almost entirely crosslinked, they still possess elastic properties. At high temperatures, the particles are softened and are pressed tightly against each other. This effect is more pronounced at higher temperatures.

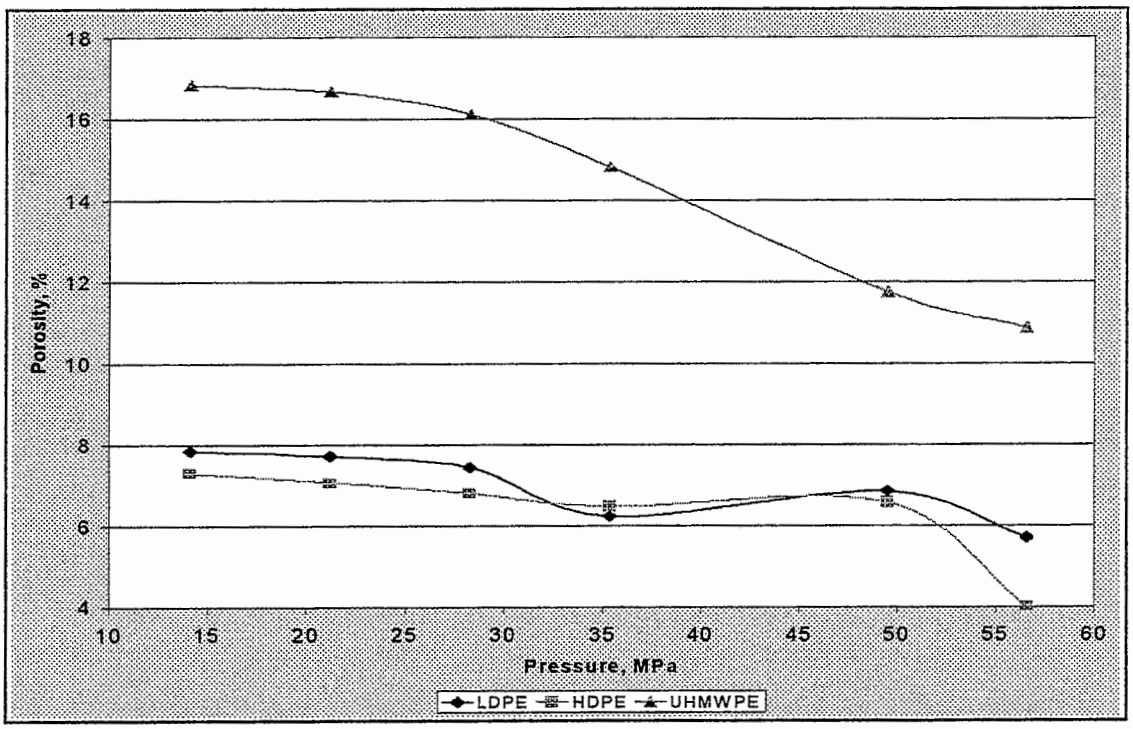

Figure 4.6 Effect of pressure on porosity

4.4.1.2 Effect of temperature and pressure on mean pore size

The mean pore size and maximum pore size of the membranes were also measured with the QuantaChrome porosimeter. The mean pore size determines the size of the particles or substances that can be separated by the membrane.

Three different types of pores are measured with the porosimeter: micropores, mesopores and macropores. These types are defined as:

1. Micropores, pores with a diameter smaller than 3.6 nm.
2. Mesopores, pores with a diameter between 3.6 nm and 59.6 nm.
3. Macropores, pores with a diameter greater than 59.6 μm.

All industrial membranes are characterized by macropores, and therefore the former two types of pores are not important for this investigation. The effect of a constant pressure (42.44 MPa) and different temperatures (experiment 1) on mean pore size are shown in Figure 4.7.

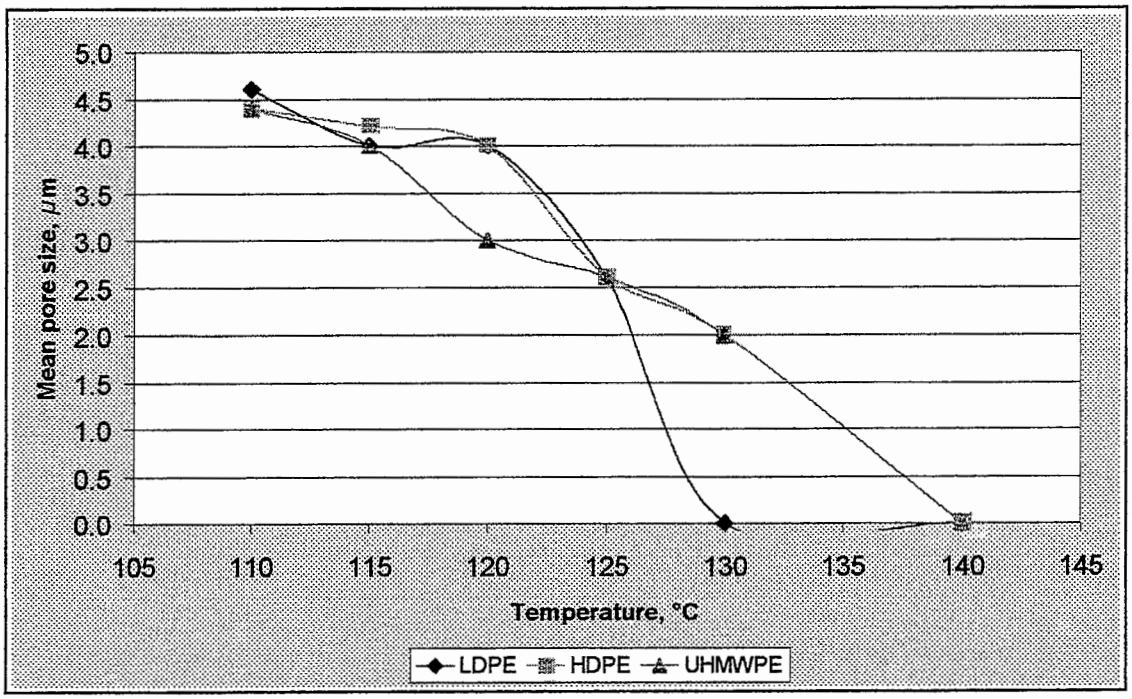

Figure 4.7 Effect of increased temperature on mean pore size

When the temperature is increased, the mean pore sizes of the membranes decrease sharply. Furthermore, no macropores are present at the higher temperatures for all three polyethylene materials. This was confirmed by the SEM photographs.

An increase in pressure at a constant temperature of 125°C (experiment 2), results in a small decrease in pore size (Figure 4.8). The constant temperature that was chosen (125°C), was below the melting point of any of the irradiated polyethylene materials, which may explain the results.

All the membranes produced during both initial experiments were investigated under the SEM. However, it is difficult to determine the mean pore size of a membrane under a microscope; the pore sizes determined with the porosimeter are more accurate. A typical SEM photograph of a membrane is shown in Figure 4.9. The SEM photographs of all the produced membranes are included in Appendix E.

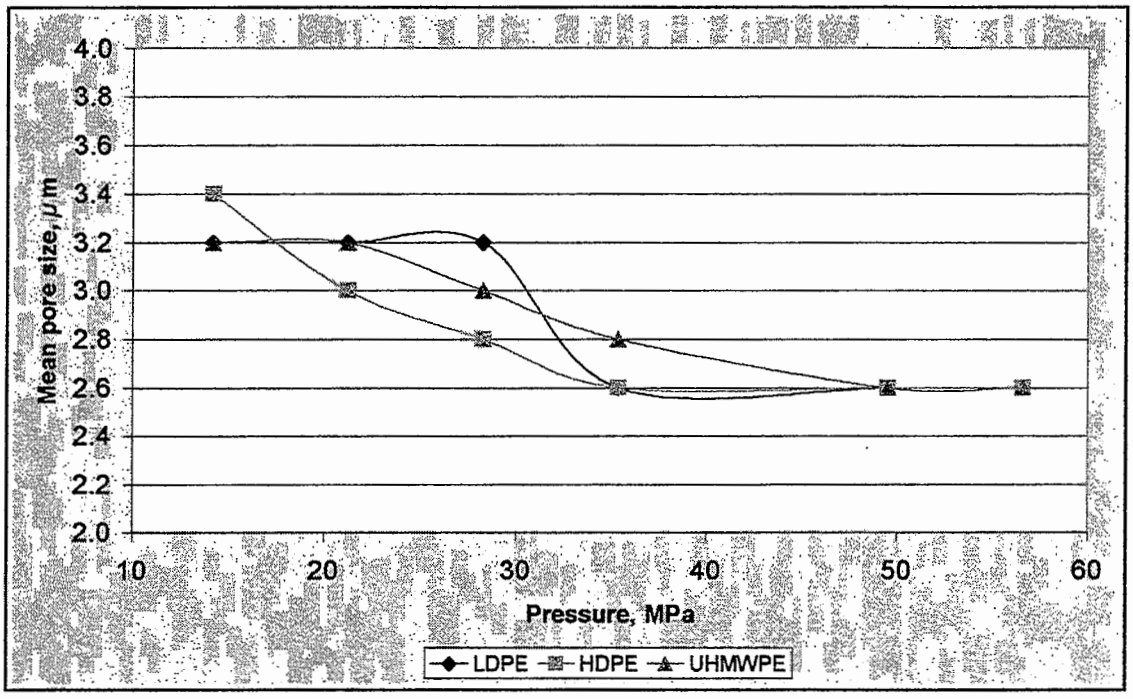

Figure 4.8 Effect of pressure on mean pore size

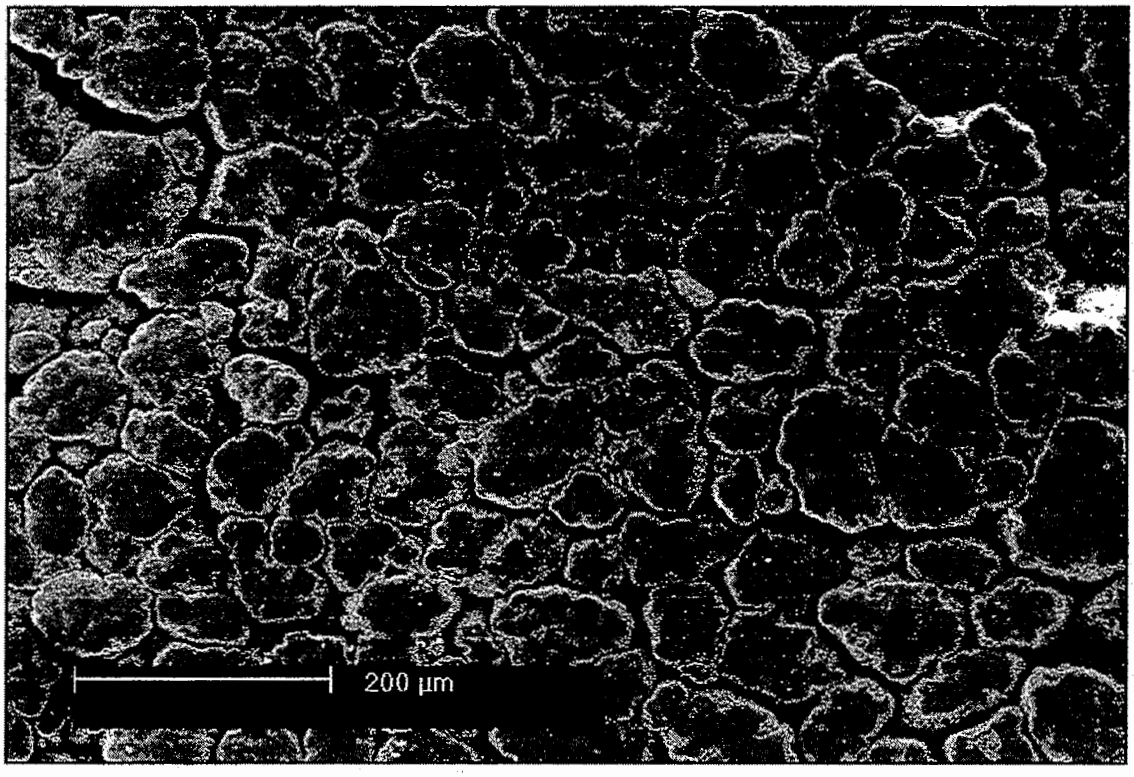

Figure 4.9 SEM photograph of UHMWPE membrane

The pore size distribution is an important characteristic of membranes. If a narrow pore size distribution can be achieved, the membrane can be used to separate two substances with different diameters. However, if the pore size distribution is too wide, the permeate will still contain unwanted particles.

The maximum pore size of a membrane relative to the mean pore size gives an indication of the pore size distribution of the membrane. The ideal membrane has a mean pore size that is very near the maximum pore size. The maximum pore sizes of the membranes from experiment 1 are shown in Figure 4.10.

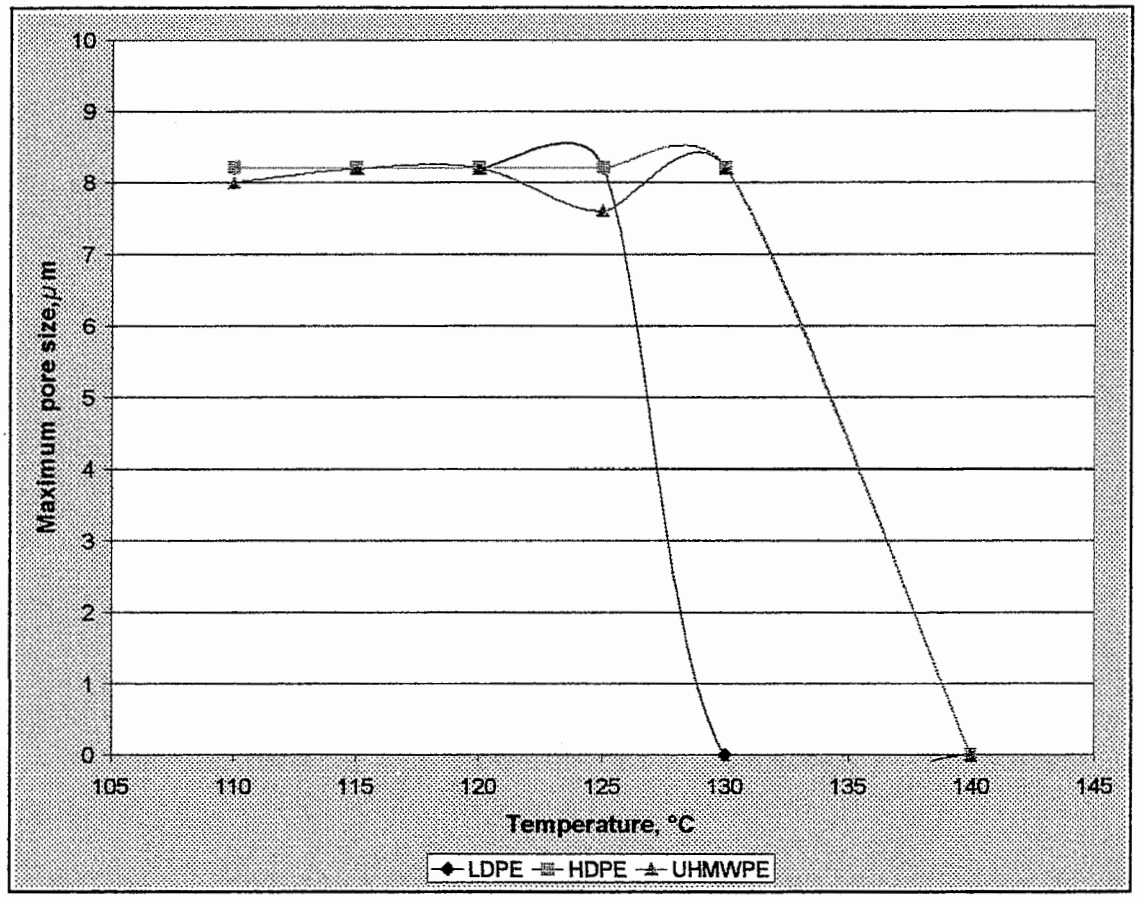

Figure 4.10 Effect of temperature on maximum pore size

Increased pressure had no effect on the maximum pore size of the membranes. The maximum pore size of all the membranes remained at 8.2 μm.

4.4.2 Central composite design

The results of the initial testwork identified the ranges of the factors to be used in the experimental design. These ranges are:

1. Temperature: 110 - 130°C.
2. Pressure: 14.15 - 42.44 MPa.

The computer program *Statistica* was used to generate the central composite design using response surface methods. A standard design with an input of two factors was chosen to generate an experiment with 10 runs. Two center points were added to the 2-level factorial design points to achieve rotatable and nearly orthogonal designs. The 12 experiments were used to fit a mathematical model. The experimental profile of these 12 experiments is shown in Table 4.4.

Table 4.4 The 2^2 central composite design

Standard run	Temperature	Pressure
1	-1.0	-1.0
2	-1.0	1.0
3	1.0	-1.0
4	1.0	1.0
5	-1.4	0.0
6	1.4	0.0
7	0.0	-1.4
8	0.0	1.4
9	0.0	0.0
10	0.0	0.0
11	0.0	0.0
12	0.0	0.0

The selected ranges for the different factors were translated into real values by *Statistica*. The actual values of the factors used in the experiments are shown in Table 4.5.

Table 4.5 Experimental values of the design factors

Factor	Level					Unit
	-1.4	-1.0	0.0	1.0	1.4	
Temperature	105.9	110	120	130	134.1	°C
Pressure	8.30	14.15	28.30	42.44	48.30	MPa

4.4.3 Response surfaces

The purpose of response surface design is to fit a multi-dimensional surface to the surface obtained from the results of the experimental design. This multi-dimensional surface is actually a mathematical relationship between the design factors and the response variables of the system. The results (porosity and mean pore size) obtained from the designed experiment are shown in Table 4.6. The results from the initial testwork were included (standard run 13 to 24).

Table 4.6 Experimental results

Standard run	Temperature, °C	Pressure, MPa	Porosity, %	Mean pore size, μm
1	110.0	14.15	16.6	4.2
2	110.0	42.44	16.0	4.2
3	130.0	14.15	17.1	4.0
4	130.0	42.44	11.9	2.1
5	105.9	28.30	15.7	4.2
6	134.1	28.30	11.5	2.1
7	120.0	8.30	14.9	4.0
8	120.0	48.30	14.6	3.8
9	120.0	28.30	15.2	4.0
10	120.0	28.30	15.6	4.0
11	120.0	28.30	15.8	3.7
12	120.0	28.30	14.7	4.2
13	110.0	42.44	16.0	4.4
14	115.0	42.44	15.4	4.0
15	120.0	42.44	14.2	3.0
16	125.0	42.44	13.6	2.6
17	130.0	4244	12.4	2.0
18	140.0	42.44	8.2	0.0
19	125.0	14.15	16.8	3.2
20	125.0	21.22	16.7	3.2
21	125.0	28.29	16.1	3.0
22	125.0	35.37	14.8	2.8
23	125.0	49.52	11.7	2.6
24	125.0	56.59	10.9	2.6

4.4.3.1 The effect of temperature and pressure on porosity

The interaction and main effects of the different design factors on membrane porosity were evaluated. The following second order function was fitted through the experimental data (Figure 4.11):

$$\text{Porosity (\%)} = -86.273 + 1.584T + 0.965P - 0.006T^2 - 0.0015P^2 - 0.0078TP \quad (4.5)$$

At the following conditions, the porosities of the membranes are maximized:

1. Temperature < 110°C and pressure > 10 MPa.
2. Temperature 110-115°C and pressures 10-30 MPa.
3. Temperature 120-130°C and pressure 10-20 MPa.

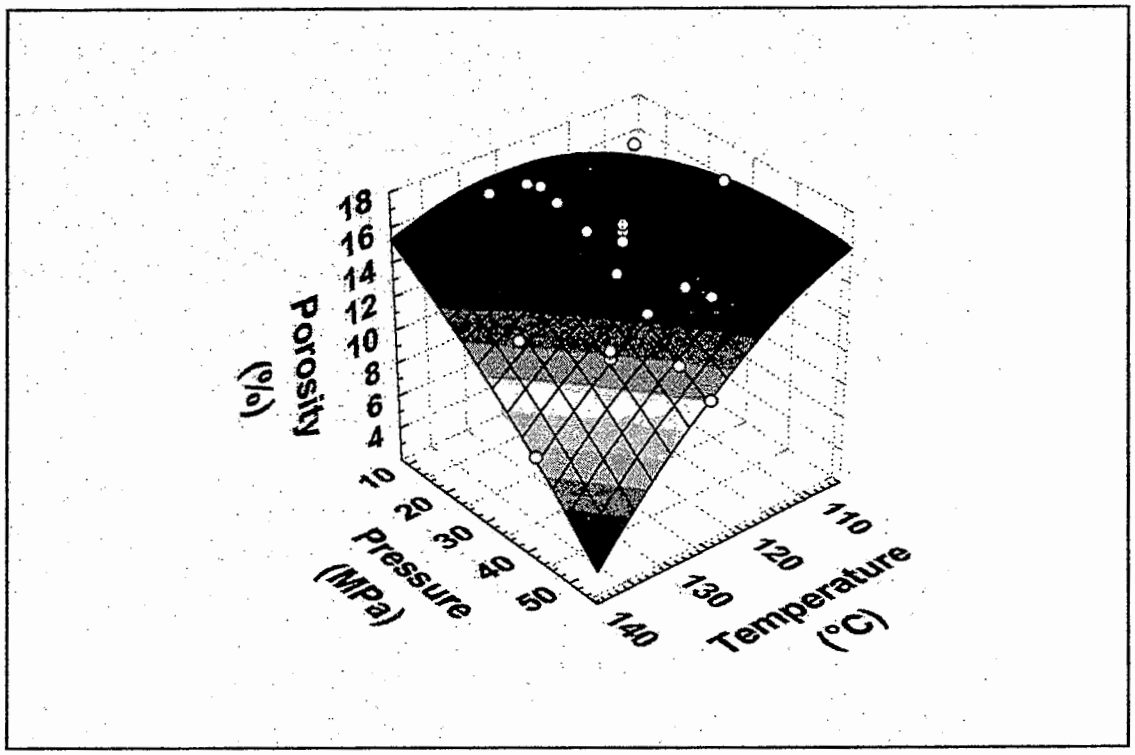

Figure 4.11 The effect of temperature and pressure on membrane porosity

The observed values and the values predicted by equation 4.5 are shown in Figure 4.12. A user-defined loss function

$$\text{Loss} = (\text{Observed value} - \text{Predicted value})^2 \quad (4.6)$$

was used to calculate the variance. The variance explained, was calculated as 89.0%.

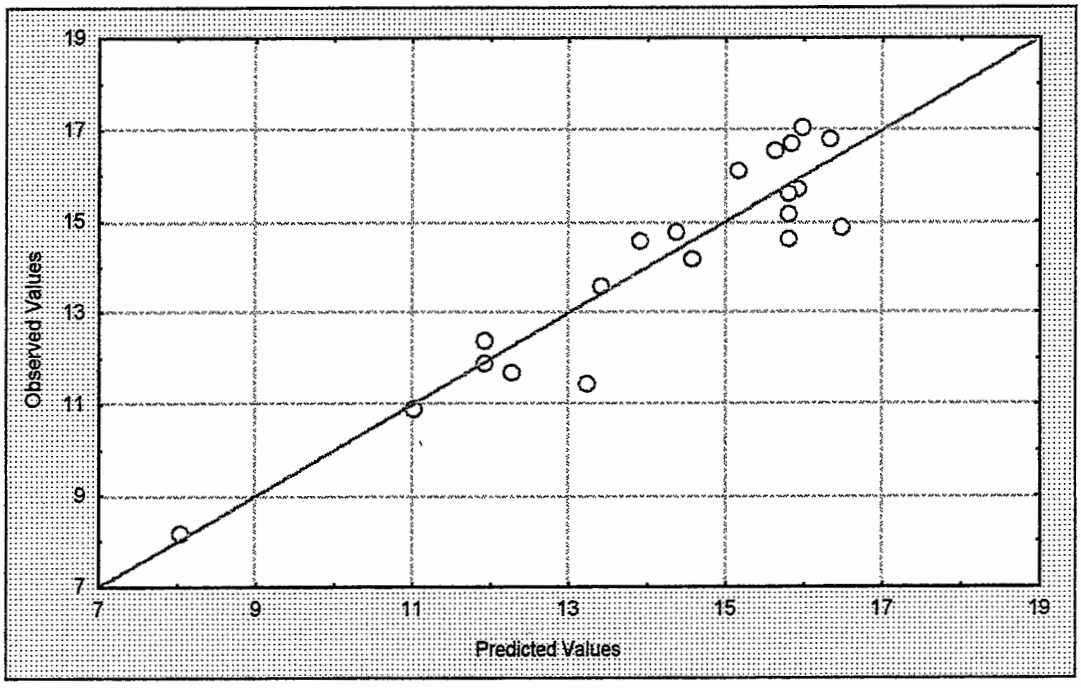

Figure 4.12 Predicted and observed values: porosity

4.4.3.2 The effect of temperature and pressure on mean pore size

A second order function was fitted through the experimental data to relate the mean pore size of the membranes with the design factors. The following function resulted:

$$d_{pore} = -34.314 + 0.637T + 0.329P - 0.0026T^2 + 0.00026P^2 - 0.003TP \quad (4.7)$$

This function is shown in Figure 4.13. The variance explained, was calculated with equation 4.6 as 92.5%. The observed and predicted mean pore sizes are shown in Figure 4.14.

Pore sizes below 4 μm is generally accepted for microfiltration. The conditions to produce pore sizes smaller than 4 μm, are

1. Temperature > 115°C and pressure 10-50 MPa.

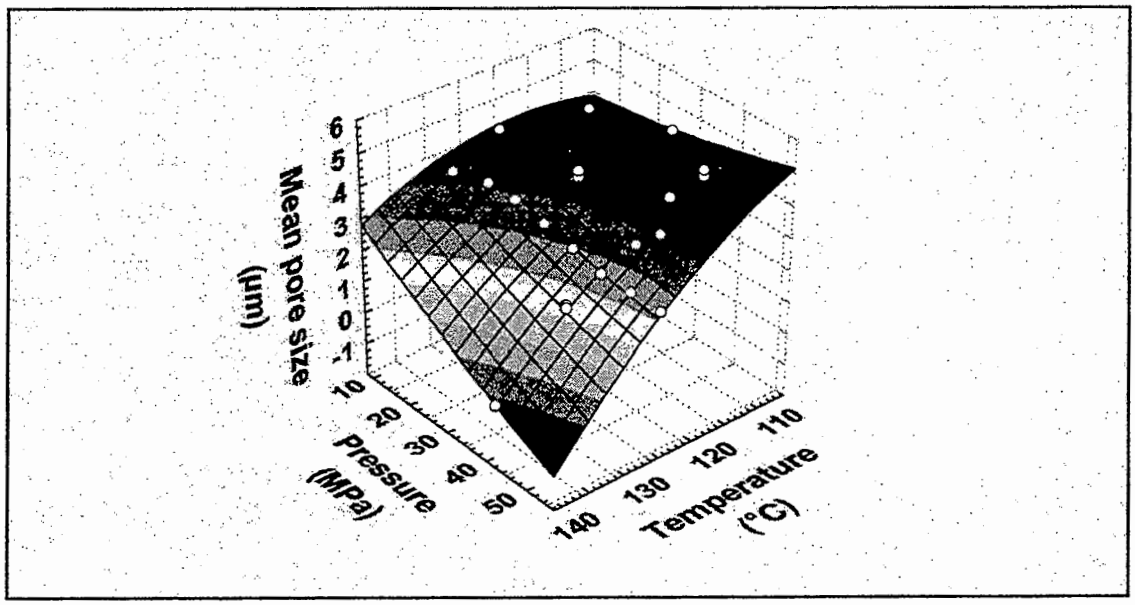

Figure 4.13 The effect of temperature and pressure on mean pore size

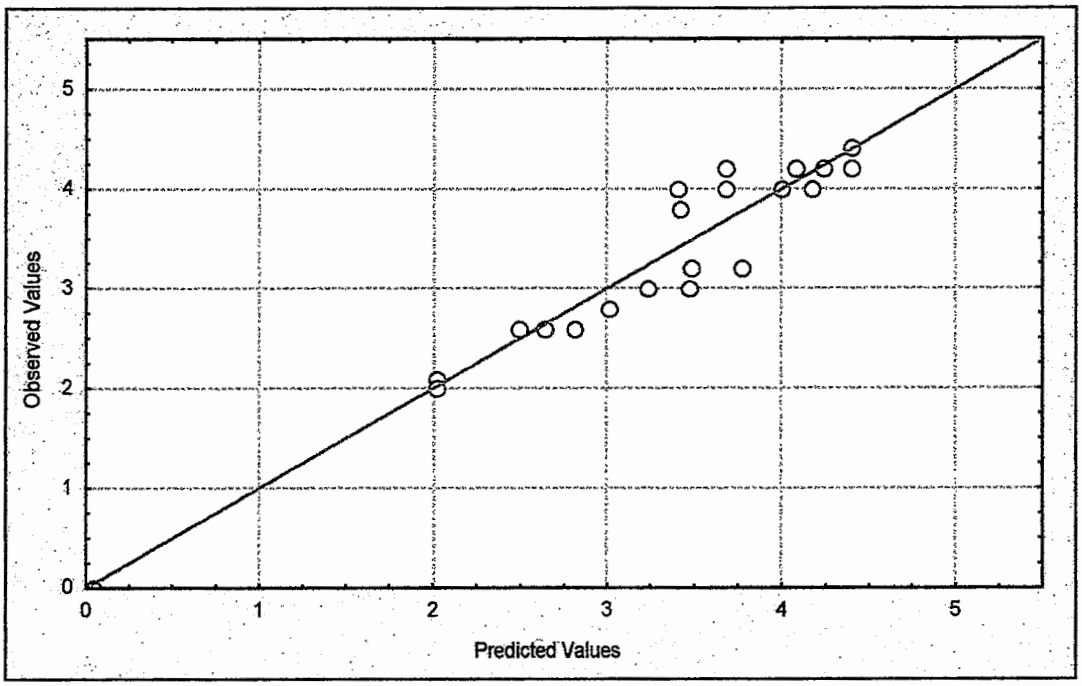

Figure 4.14 Predicted and observed values: mean pore size

4.5 Membrane extraction

Koekemoer (1996) did a detailed investigation into the extraction of nickel through a SLM. It was decided to compare the permeation of nickel through the sintered membranes with the results reported in Koekemoer's dissertation. SLM technology was used to test the performance of the membranes because of the low pressure drop across the membrane. The pressure-driven processes (MF, UF, and RO) could not be used because of the brittleness of the membranes.

4.5.1 Experimental set-up

The membrane tested in the SLM configuration, was produced from UHMWPE at a temperature of 120°C and a pressure of 28.29 MPa. This membrane was tested in a two-cell reactor (Figure 4.15) with the membrane forming the barrier between the two cells. The part of the membrane exposed to the two compartments in the reactor, was a circle with a diameter of 1 cm. The feed solution had a nickel concentration of 1000 mg/l and a strip solution of 2 mol/dm^3 H_2SO_4 was used. Both cells had a volume of 200 ml and contained synchronized mechanical stirrers. The sintered membrane was inserted into an Escaid 100 solution containing 60% DEHPA for 5 minutes. The pH of the feed solution was adjusted with a 10% NaOH solution every 30 minutes, and a sample of the strip solution was taken every 5 hours over a 20 hour period.

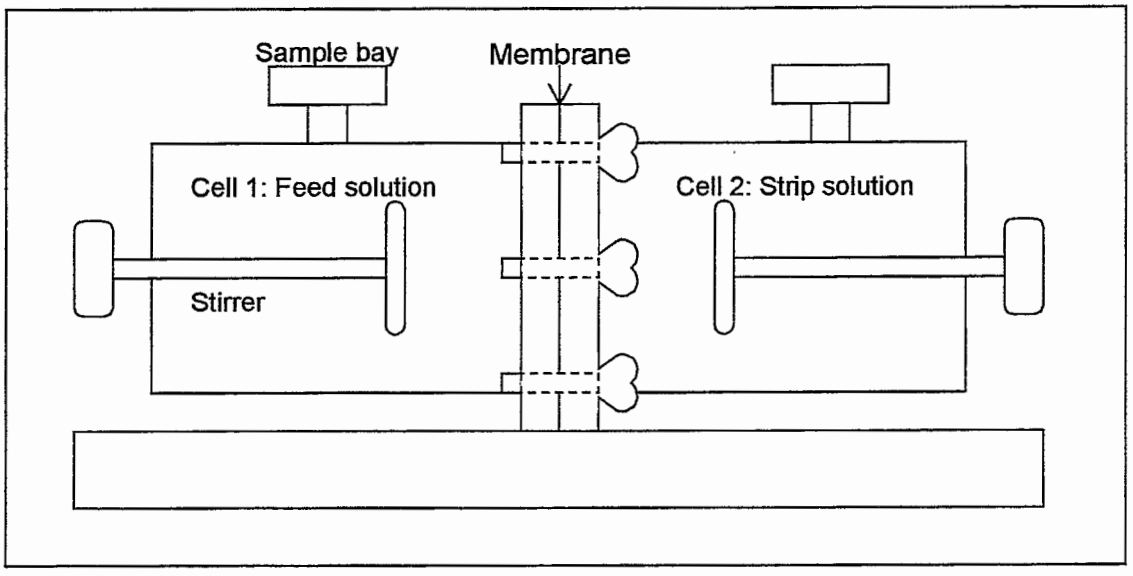

Figure 4.15 Two-cell reactor used in extraction studies

4.5.2 Experimental results

The Atomic Adsorption Spectrophotometer of the Potchefstroom University was used to determine the nickel concentration of samples taken periodically from the strip solution. The results were reported in mg/l nickel, and the cumulative extraction was calculated with the following equation:

$$\text{Cumulative extraction} = \frac{[Ni] \times V_{strip}}{1000 \times A_m} \qquad (4.8)$$

with [Ni] the nickel concentration (mg/l) in the strip solution, V_{strip} = 0.2 l the volume of the strip solution and $A_m = 7.85 \times 10^{-5}$ m^2 the area of the membrane exposed to the strip solution. The experimental results are shown in Table 4.7.

Table 4.7 Results of permeation studies

Time, h	[Ni], mg/l	Cumulative extraction, g/m^2
0	0.00	0.00
5	2.49	6.34
10	4.23	10.77
15	6.01	15.30
20	7.43	18.92

The cumulative extraction was plotted against time (Figure 4.16) and the least-squares method was used to fit a straight line through these data points.

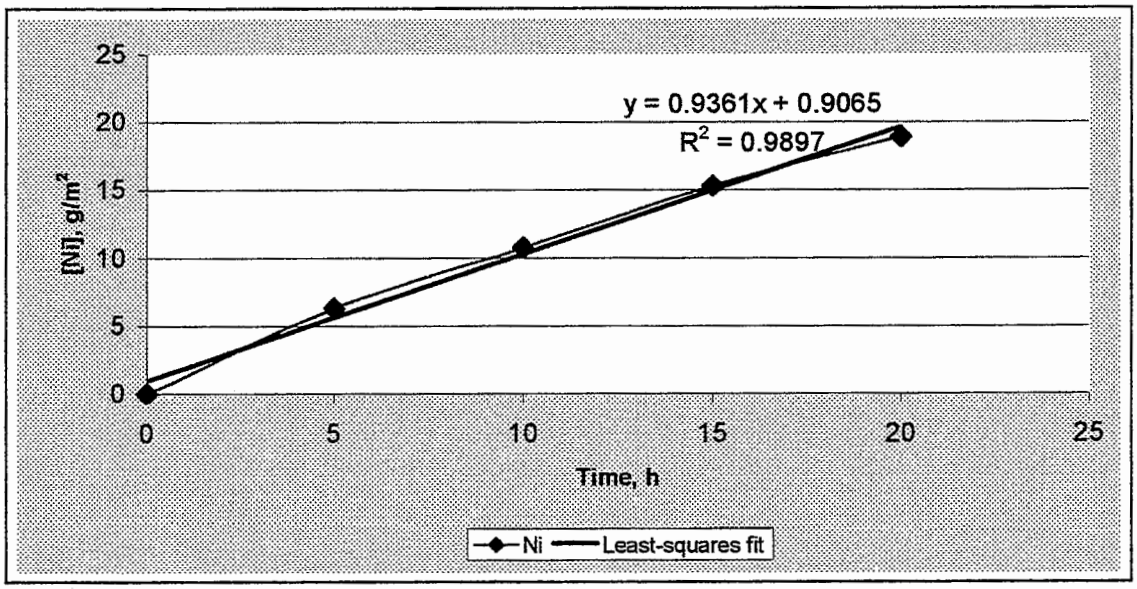

Figure 4.16 Cumulative extraction through the sintered membrane

The following equation was fitted through the experimental data:

$$y^* = 0.9361t + 0.9065 \qquad (4.9)$$

with y^* the cumulative extraction (g/m^2) obtained with the sintered membrane and t the time of extraction (h).

4.5.3 Comparative studies

The extraction of the sintered membrane was compared with the extraction of the Celgard 4500 membrane used by Koekemoer (1996) in his investigation. The following average function was fitted through the data obtained during his investigation:

$$y_{avg} = 49.652 - 27.4878e^{-0.02828t} - 22.165e^{-0.04335t} \tag{4.10}$$

with y_{avg} the cumulative extraction (in g/m^2) obtained with the Celgard membrane. The cumulative extraction of the sintered membrane relative to the Celgard membrane was determined as follows:

$$\frac{\int_0^{20} y^* dt}{\int_0^{20} y_{avg} dt} \times 100 = \frac{\int_0^{20} (0.9361t - 0.9065) dt}{\int_0^{20} \left(49.652 - 27.4878e^{-0.02828t} - 22.165e^{-0.04335t}\right) dt} \times 100$$

$$= 61.12\% \tag{4.11}$$

The deviation in cumulative extraction reported by Koekemoer may be attributed to the following:

1. Flux is inversely dependant upon the thickness of the membrane. The thickness of the Celgard 4500 membrane is 0.5 μm, compared to 500 μm of the sintered membrane.
2. The porosity of the Celgard membrane is also higher than the porosity of the sintered membrane; the porosity of the former is 45% compared to 14% of the sintered membrane.

The thickness of the membrane can be decreased using a smaller amount of polyethylene powder in the heat-press. The brittleness of the membranes prevented the use of smaller amounts of polyethylene to produce thinner membranes.

4.6 Preliminary economic evaluation

4.6.1 Introduction

It becomes possible to make accurate cost estimations as soon as the final process-design stage of a project is completed, because detailed equipment specifications and definite plant-facility information will then be available. Direct price quotations based on detailed specifications can be obtained from this information from various suppliers. The evaluation of costs in the preliminary design phases is sometimes called guesstimation, but the proper designation is *predesign cost estimation.* These estimates should be capable of providing a basis for company management or investigators to decide if further capital should be invested in the project (Peters & Timmerhaus, 1991:4-5). However, as a process design does not fall in the scope of this investigation, a detailed economic evaluation of the sintering process was not carried out. Only a guesstimation was performed to evaluate the economic feasibility of the new type of membrane.

4.6.2 Cost of membranes

The membranes supplied by Envig (Paarl, South Africa) were quoted as follows (Van der Merwe, 1998):

1. Membranes utilized in spiral wound configuration: R400/m^2
2. Membranes utilized as hollow fibers: R1500/m^2

In the overseas scenario, membrane processes are intensively applied in water purification processes. There are a great deal more membrane manufacturers and the close competition forces the membrane prices down. K.J. Hazelett (1998) from Osmonics, the suppliers of DESAL membranes, quoted for their flat sheet membranes as follows:

1. Thin film or CA reverse osmosis membranes: R373/m^2 - R435/m^2
2. Thin film nanofiltration membranes: R931/m^2
3. Thin film ultrafiltration membranes: R931/m^2
4. Polysulphone ultrafiltration membranes: R621/m^2
5. PVDF microfiltration membranes: R621/m^2
6. PTFE fluorocarbon microfiltration membranes: R1552/m^2 - R1862/m^2

These values exclude delivery cost and import tax and are based on an exchange rate of US$1.00 = R6.00.

4.6.3 Production cost of polyethylene membranes

Polyethylene was used as raw material for the sintered membranes. The price of the UHMWPE used in this investigation was quoted by R. Patmore (1998) as R12/kg. The next step in the production of the sintered membranes was the irradiation of the polyethylene powder. The cost of irradiation was quoted by M. Heidstra (1998) as R3.86/kg. Finally, the membranes must be pressed in a suitable heat-press.

A heat-press with diameter of 15 cm, was quoted as R65 000. If a pay-back period of 3 years is assumed (working 8 000 h/year), the operating cost of the press is

$$\text{Cost}_{\text{press}} = \frac{\text{R}65000}{8000 \times 3\,\text{h}}$$

$$= \text{R}2.71/\text{h} \qquad (4.12)$$

The labour cost for membrane production is another important component of the operating cost. It is assumed that the labour cost for a properly trained operator will be R50 000/year, with 1 year representing 2200 working hours. The labour cost is determined as:

$$\text{Cost}_{\text{labour}} = \frac{\text{R}50000}{2200\,\text{h}}$$

$$= \text{R}22.73/\text{h} \qquad (4.13)$$

If 4 membranes are manufactured per minute, the production rate is

$$\text{Production rate} = \frac{240 \times A_m}{\text{h}}$$

$$= 4.241\,\text{m}^2/\text{h} \qquad (4.14)$$

where A_m = 0.0177 m^2 is the surface area of a 15 cm membrane. The total operating cost of the membranes is:

$$\text{Total operating cost} = (\text{Cost}_{\text{polyethylene}} + \text{Cost}_{\text{irradiation}}) \cdot \rho_{PE} \cdot \delta_{membr} + \frac{(\text{Cost}_{\text{press}} + \text{Cost}_{\text{labour}})}{\text{production rate}}$$

$$= (\frac{R12}{kg} + \frac{R3.86}{kg}) \cdot \frac{940 kg}{m^3} \cdot 0.5 \times 10^{-3} m + \frac{(R2.71/hr + R22.73/h)}{4.241 m^2/h}$$

$$= R13.45/m^2 \qquad (4.15)$$

with ρ_{PE} = 940 kg/m^3 the density of polyethylene and δ_{membr} = 0.5 mm the thickness of the membrane. This value is significantly lower than the current retail price. The breakdown of the operating cost is given in Table 4.8.

Table 4.8 Contribution to operating cost

	Polyethylene cost	Labour cost	Radiation processing	Cost of heat-press
Percentage of total operating cost	41.93%	39.85%	13.49%	4.75%

The cost of the raw material (polyethylene) and the labour cost are the main contributors to the operating cost.

4.7 Conclusions

Microfiltration and SLM are membrane processes utilizing membranes with mean pore sizes up to 4.5 μm. The literature survey showed that microfiltration membranes have porosities lower than 50% (Kesting, 1985:237-265). The sintered membranes can therefore be used as microfiltration membranes or SLM, based on the porosity and mean pore size. Furthermore, the economic evaluation showed that polyethylene membranes could be produced at a cost far lower than the retail price of conventional membranes. By controlling the conditions of production, a membrane with a specific porosity and pore size can be tailor-made. The optimal conditions for the production of a sintered membrane, were found to be:

1. Temperature 115-120°C and pressure 20-30 MPa.
2. Temperature 120-125°C and pressure 10-30 MPa.

3. Temperature 125-130°C and pressure 10-20 MPa.

The extraction testwork showed a marked decrease in cumulative extraction between the Celgard and the manufactured membranes. However, this can be attributed due to the lower porosity and increased thickness of the manufactured membrane.

CHAPTER 5 FINAL CONCLUSIONS

"Nothing shocks me. I'm a scientist."
- Harrison Ford as Indiana Jones -

5.1 Final conclusions

The recent interest in environmental awareness across the world has forced companies to implement or extend their clean-up operations as far as effluents and waste are concerned. Membrane applications attracted a lot of attention in the past decade because it reduces the volume of waste that has to be treated, considerably. However, every clean-up operation has its price, and membrane processes are no exceptions. The cost of microfiltration membranes (excluding delivery) is presently R621/m^2 and upwards.

The aim of this dissertation was to investigate the production of cost-effective membranes made from an inexpensive material, polyethylene. The polyethylene was modified by irradiation, and used to produce membranes in a heat-press by controlling the temperature and pressure. These membranes were characterized to identify any current applications. The following conclusions were made on polyethylene irradiation:

1. Irradiation affects the properties of polyethylene. Gel formation is induced by irradiation, resulting in an increase of the melting temperature of the polyethylene. However, some of the new properties of the irradiated polyethylene have a negative influence on membranes. A good example is the increase of brittleness of the membrane.
2. Acetylene acts as a crosslinking agent for polyethylene. The acetylene is grafted onto the polymer leading to increased crosslinking.

The membranes that were manufacture in the heat-press were evaluated with respect to porosity and mean pore size. The following conclusions can be made:

1. The porosity and mean pore size of the membranes are dependent on both temperature and pressure. In general, an increase in temperature and pressure leads to lower porosities and lower mean pore sizes.
2. The type of polyethylene has an effect on membrane characteristics. The UHMWPE produced membranes with the highest porosity. This may be attributed

to the gel contents and the fact that it cannot easily reptate, the claims are too long to intermingle at pressure, adhesion contact areas.

3. The membranes produced can be utilized as microfiltration membranes and SLMs. However, they have a high brittleness and further research is necessary to find ways of increasing the elasticity of the membranes. The most-suited membranes as far as porosity and pore size are concerned, were produced at

   - Temperature 115-120°C and pressure 20-30 MPa.
   - Temperature 120-125°C and pressure 10-30 MPa.
   - Temperature 125-130°C and pressure 10-20 MPa.

4. The microfiltration membranes and SLMs currently available, are expensive and funds invested in future research will be worthwhile.
5. The manufactured membrane was compared to a commercial membrane in extraction studies involving nickel. Although the extraction rate achieved with the manufactured UHMWPE membrane was 39% lower than with the Celgard membrane, it can be explained by the decrease in porosity and increase in thickness of the HDPE membrane. This can be confirmed by more controlled manufacturing conditions using a more reliable heat-press.

5.2 Recommendations

5.2.1 Introduction

This project was a joint venture between a University, a Government Council and a Polymer Marketing Company. The knowledge and academic guidance was supplied by the University, the polymers were provided by the Polymer Marketing Company, the irradiation was done by the irradiation company and the Government Council supplied the equipment and manpower for the testwork. Every shareholder was a leader in his field of knowledge. From the author's point of view, similar projects must be undertaken to ensure that meaningful research is done.

5.2.2 Future research

This dissertation is only the first step in the development of a sintered membrane for industrial application. This investigation has identified the possibility to produce membranes from irradiated polyethylene by controlling the temperature and pressure during manufacturing. The following problems have been identified and will be the focus areas during further research:

1. *The brittleness and low tensile strength of the membranes.* There are several ways to increase the elasticity of the membranes. Firstly, the polyethylene can be subjected to a lower irradiation dose, which will ensure that the sol fraction of the sample will be high enough to melt and produce some elasticity. Alternatively, irradiated and unirradiated polyethylene can be mixed in a certain ratio to ensure that there will be a sol fraction in the sample when the membranes are pressed. Different polymers may be irradiated and evaluated to determine how their elasticity is influenced by irradiation.
2. *The configuration of the membranes.* Hollow-fiber, tubular and spiral-wound membrane configurations are the most popular configurations available today because of the available membrane area. Extrusion or similar production methods must be investigated.
3. *The manufacturing of a membrane heat-press.* The membranes manufactured with the Prontopress are not big enough to test permeation accurately. Ideally, membranes with diameters of ± 20 cm are required for this type of tests. A heat-press with a sensitive temperature and pressure control system will be used in further testwork.

5.3 Closing remarks

The objectives for this investigation, were:

1. The production of water treatment membranes from irradiated polyethylene.
2. The identification of applications for the membranes produced in the testwork.

The membranes manufactured during the testwork, were characterized according to their porosity and mean pore size. These properties are used by membrane suppliers to characterize water treatment membranes. These membranes have similar pore sizes found in commercial microfiltration membranes and SLMs. The preliminary cost evaluation showed a low production cost, which justifies investment into further research.

BIBLIOGRAPHY

"In your thirst for knowledge, be sure not to drown in all the information."
- Anthony D'Angelo -

ALVAREZ, V., ANDRES, L.J., RIERA, F.A. & ALVAREZ, R. 1996. Microfiltration of applejuice using inorganic membranes. *The Canadian journal of chemical engineering*, 74:156-162.

ANON. 1997. Diffusion dialysis. [Available on internet:] http://ww2.gpu.com/bitec/recycle/diffusion.htm [Date of use: 12 Aug. 1998].

ANON. 1998. Liquid membrane recovers nickel. *International newsletter: membrane technology*. 99:4. Jul.

ANON. 1998. Reagan advisor joins Sam Nunn at Commodore. *International newsletter: membrane technology*. 97:4. May.

APTEL, P. & BUCKLEY, C.A. 1996. Categories of membrane operations. (*In* Water treatment membrane processes. New York : McGraw-Hill. p. 2.1-2.24.)

BARNES, D.E. 1993. Supported liquid membranes in flow systems. Pretoria : Pretoria University. (Thesis - Ph. D.)

BILLMEYER, F.W. 1971. Textbook of polymer science. London : Wiley 598 p.

BIRD, R.B., STEWART, W.E. & LIGHTFOOT, E.N. 1960. Transport phenomena. New York : Wiley 779 p.

BOVEY, F.A. 1958. The effects of ionising radiation on natural and synthetic high polymers. London : Interscience Publishers. 287 p.

BOX, G.E.P. 1978. Statistics for experimenters. New York : Wiley. 653 p.

BOYSEN, B.L. 1981. High pressure (low and intermediate density) polyethylene. (*In* Encyclopedia of Chemical Technology, 16:402-420.)

BUNGA, H. 1995. Charged membranes. [Available on Internet:] http://www.rpi.edu/dept/chem-eng/Biotech-Environ/Membranes/eldial.htm [Date of use: 15 Jul. 1998].

CHAPIRO, A. 1962. Radiation chemistry of polymeric systems. London : Wiley 712 p.

CHERYAN, M. 1986. Ultrafiltration handbook. Lancaster : Technomic 375 p.

CURRIE, J.T. 1984. A response surface methodology approach to optimization in flow injection analysis. Virginia : Virginia Polytechnic Institute and State University. (Dissertation - Ph. D.) 352 p.

DANESI, P.R. 1985. Separation of metal species by supported liquid membranes. *Separation science and technology*, 19 (11 & 12) p. 857-894.

DU PLESSIS, T.A. 1997. The Raprex process and its potential in the radiation processing of polymers. (Training guidelines for radiation processing of polymers presented at the IAEA Conference, July 1997. Vienna. (Unpublished.)

DU PLESSIS, T.A. 1978. The place of radiation processing in polymer technology. *Plastics southern africa*:19-31, April.

FRANKEN, T. 1998. Membrane selection - more than material properties alone. *International newsletter: membrane technology*. 97:7-10. May.

GROBBELAAR, C.J., DU PLESSIS, T.A. & MARAIS, F. 1978. The radiation improvement of polyethylene prostheses: a preliminary study. *The Journal of bone and joint surgery*, 60-B(3):370-374.

HALLIDAY D. & RESNICK, R. 1988. Fundamentals of physics. 3rd ed. New York : Wiley. 1149 p.

HAZELETT, K.J. (info@osmonics.com) 1998. Discussion on flat sheet membrane prices. [E-mail to:] Van Wyk, A.M. (albertvw@mintek.ac.za) Oct. 21.

HEIDSTRA, M. 1998. Verbal communication with author. Kempton Park.

HO, S.V. 1992. A new membrane process for recovering organics from aqueous wastes, *Industrial Environmental chemistry*, p. 229-245.

KESTING, R.E. 1985. Synthetic polymeric membranes: a structural perspective. Irvine, CA : Wiley. 348 p.

KOEKEMOER, L.R. 1996. The extraction of nickel with membrane capsules. Potchefstroom : Potchefstroom University for CHE (Dissertation - M. Ing.)

MALLEVIALLE, J., ODENDAAL, P.E. & WIESNER, M.R. 1996. The emergence of membranes in water and wastewater treatment. (*In* Water treatment membrane processes. New York : McGraw-Hill. p. 1.1-1.10.)

MELLER, F.H. 1984. Electrodialysis - electrodialysis reversal technology. Watertown, MA : Ionics. 66 p.

PATMORE, R. 1998. Verbal communication with author. Midrand.

PEAVY, H.S., ROWE, D.R. & TCHOBANOGLOUS, G. 1985. Environmental engineering. New York : McGraw-Hill. 699 p.

PETERS, S. M. & TIMMERHAUS, K.D. 1991. Plant design and economics for chemical engineers. New York : McGraw-Hill. 910 p.

SCHULTZ, J. 1974. Polymer materials science. New Jersey : Prentice-Hall. 524 p.

SCHUTTE, F. 1997. Membrane technology introductory course. (Course presented on 21 October 1997 by the Membrane Technology Division of WISA.) Badplaas. (Unpublished.)

SHORT, J.N. 1981. Low pressure linear (low-density) polyethylene. (*In* Encyclopedia of Chemical Technology, 16:385-401.)

SMITH, W.F. 1990. Principle of materials science and engineering. New York : McGraw-Hill. 864 p.

SOUTH AFRICA. 1998. Water Act no. 54 of 1956 as amended by the Portfolio Committee on Agriculture, Water Affairs and Forestry of the National Assembly (B34B-98.)

TULASI, L. 1997. (tulasi@chemeng.iisc.ernet.in) 1997. Discussion on SLM. [E-mail to:] Van Wyk, A.M. (albertvw@mintek.co.za) Nov. 8.

VAN DER MERWE, W. 1998. (wimpie@envig.co.za) 1998. Discussion on membrane prices. [E-mail to:] Van Wyk, A.M. (albertvw@mintek.co.za) Oct. 20.

VAN DER PLAATS, G. 1992. The practice of thermal analysis. Schwerzenbach, Switzerland : Mettler Toledo. 101 p.

WAGNER, J. 1996. Membrane filtration handbook: Practical tips and hints. Gentofte, Denmark : Wagner Publishing. 62 p.

WHITELEY, K.S. 1992. Polyethylene. (*In* Ullmann's Encyclopedia of Industrial Chemistry, A21:488-517.)

APPENDIX A
Particle Size Distribution

Three different polymer powders were used. The size distribution of the polymer powder is of crucial importance for the manufacturing of the membranes. The smaller the size of the polymer particles, the smaller the pore size of the membrane. The size distributions for the different polymers were done with a Sympatec Particle Size Analyser (SPSA). The principle of operation of the analyzer is laser scattering and the resulting diffraction patterns are analysed via the Fraunhofer theory. The scattered light from the wet dispersion is focussed via a lens onto a 31-channel multielement detector. The instrument measures particle size in the range of 0.1-875 μm.

The cuvette method was used to measure the size distributions of the samples. The results are summarised in Table A1. The cuvette attachment comprises of a glass cuvette which is used for minute samples and samples that can be measured neither wet (soluble in water) nor dry (insufficient amounts of sample). The sample is dispersed in the solvent which does not dissolve the material.

Table A1 Particle size distributions

Sample	D_{10}, μm	D_{50}, μm	D_{90}, μm	Mean Particle Diameter, μm
LDPE	190.89	281.49	400.75	290
HDPE	217.16	312.00	432.17	320
UHMWPE	67.02	128.91	213.43	140

The complete size distributions are presented in Figures A1 to A3.

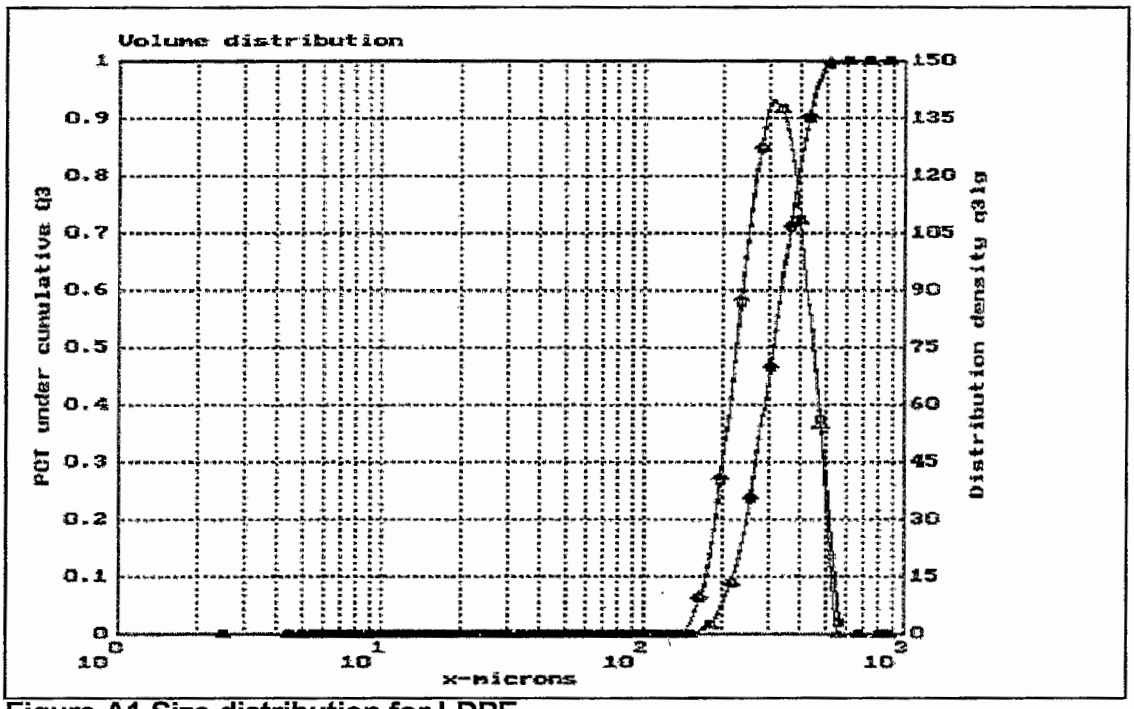

Figure A1 Size distribution for LDPE

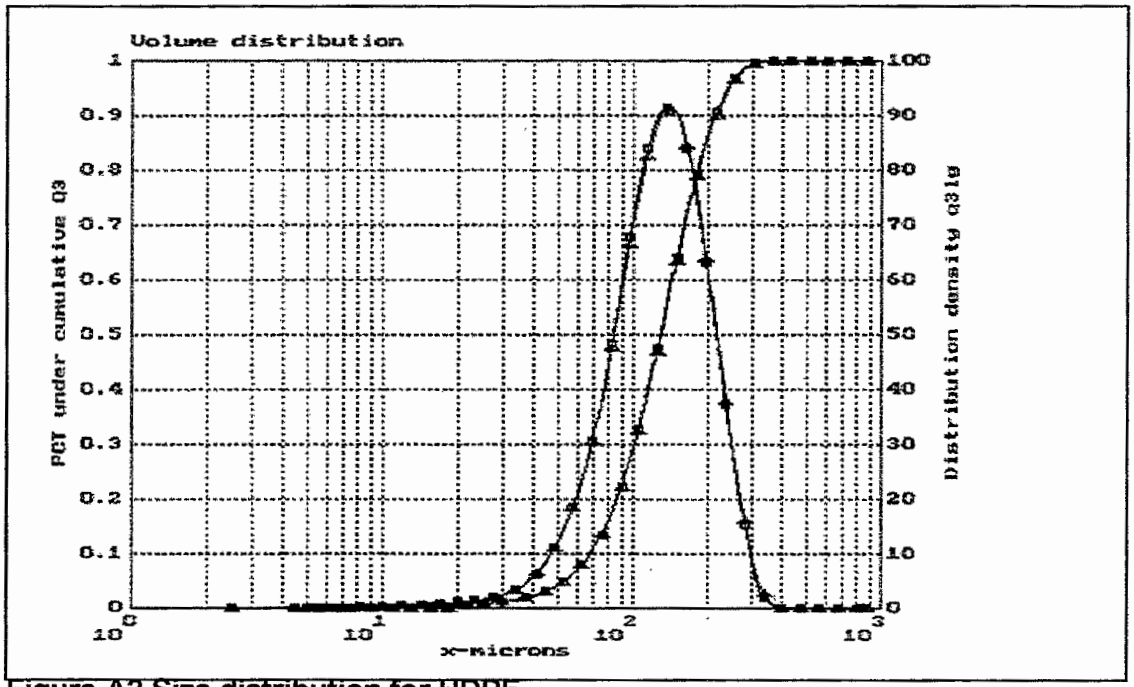

Figure A2 Size distribution for HDPE

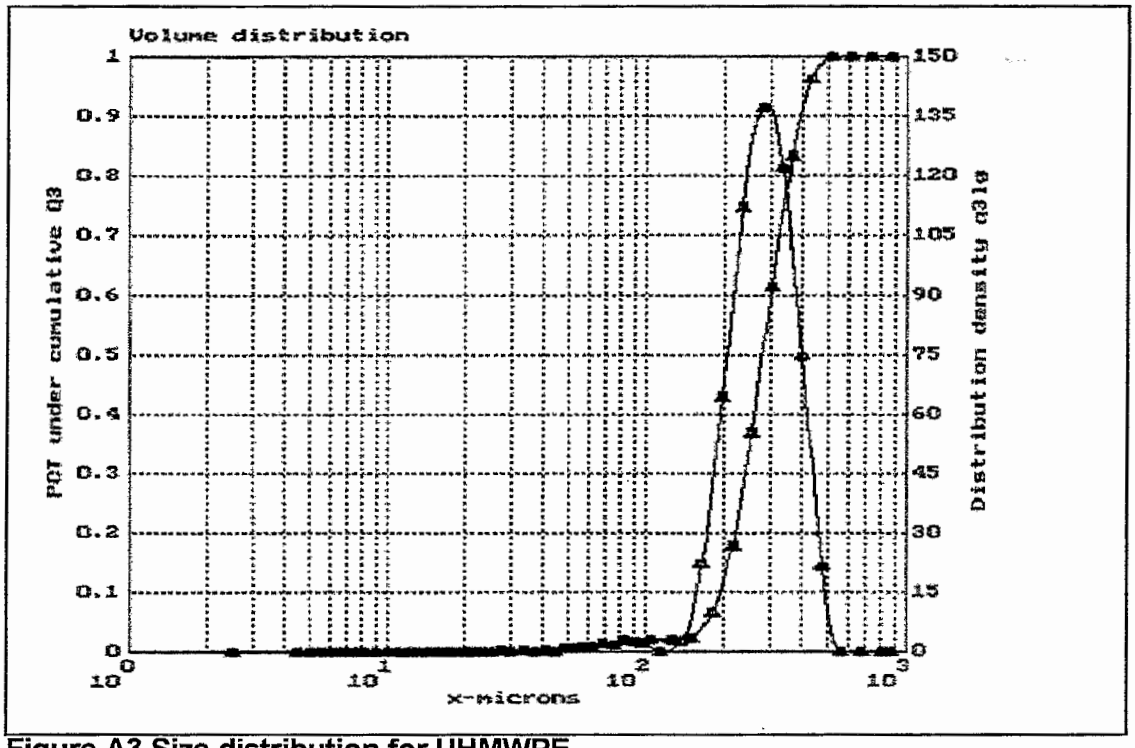

Figure A3 Size distribution for UHMWPE

APPENDIX B

Soxhlet Extraction Curves

Soxhlet extraction was used to determine the gel percentage of each irradiated polymer sample. Extraction curves were fitted through the experimental values, from which the ultimate crosslinking and initial rate of crosslinking were determined.

The fitted curves and the experimental data values are shown in Figures B1 to B6. The equations of the fitted graphs are indicated at the top of the figures.

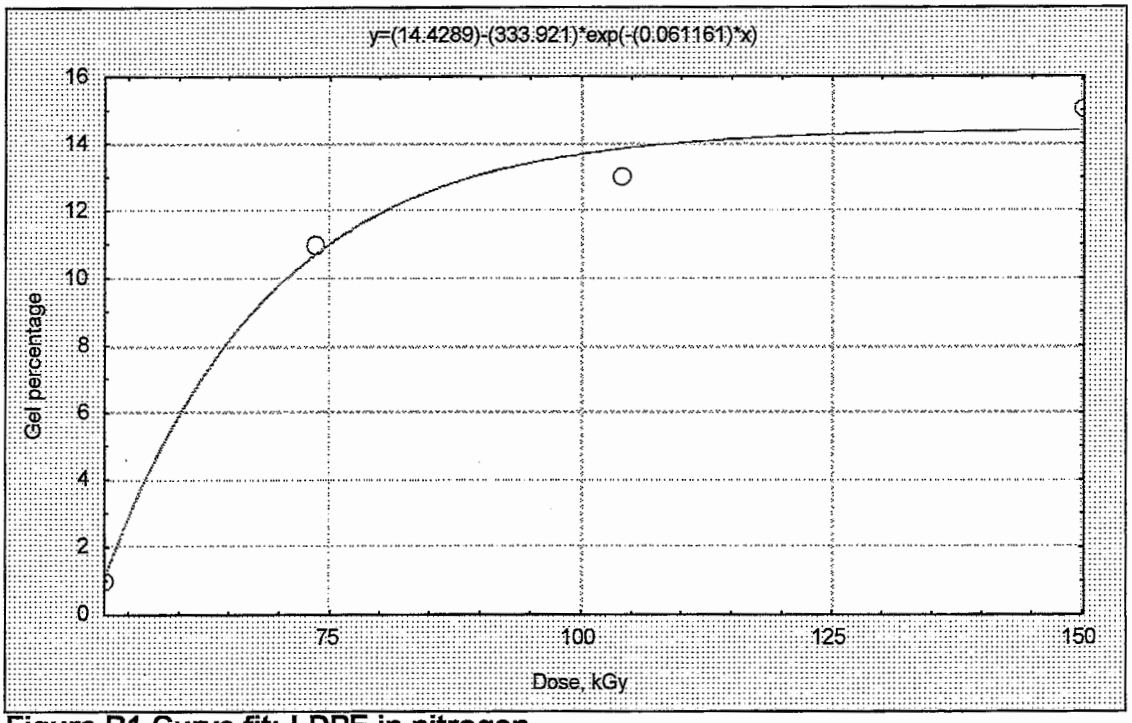

Figure B1 Curve fit: LDPE in nitrogen

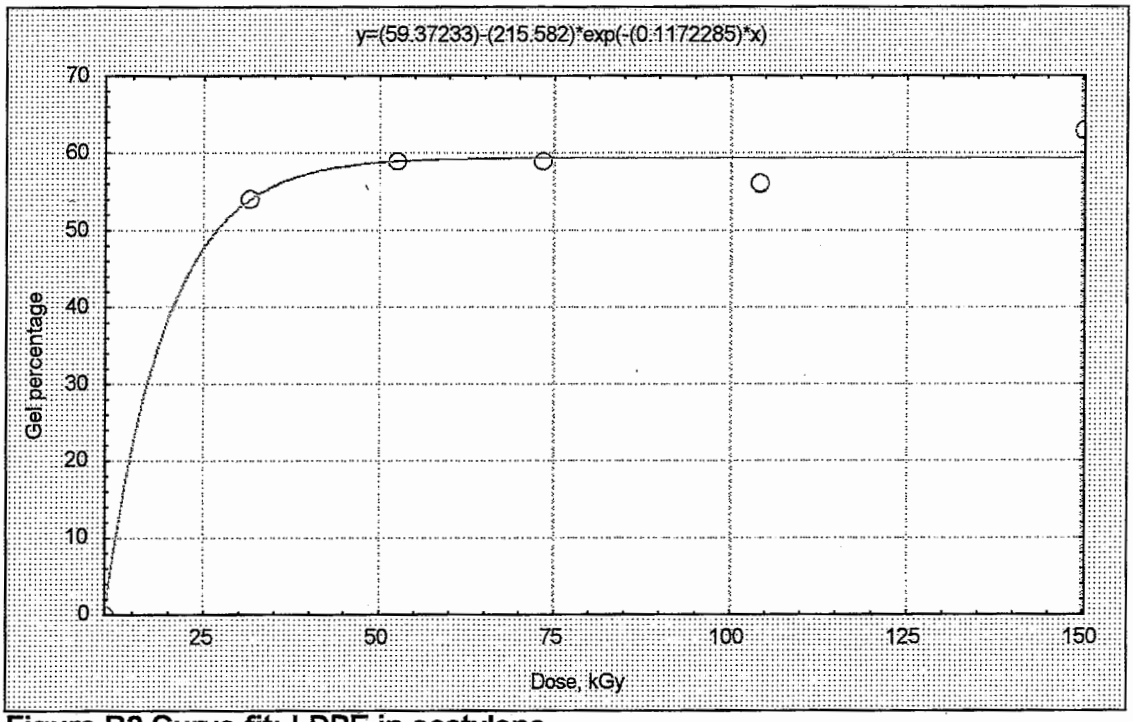

Figure B2 Curve-fit: LDPE in acetylene

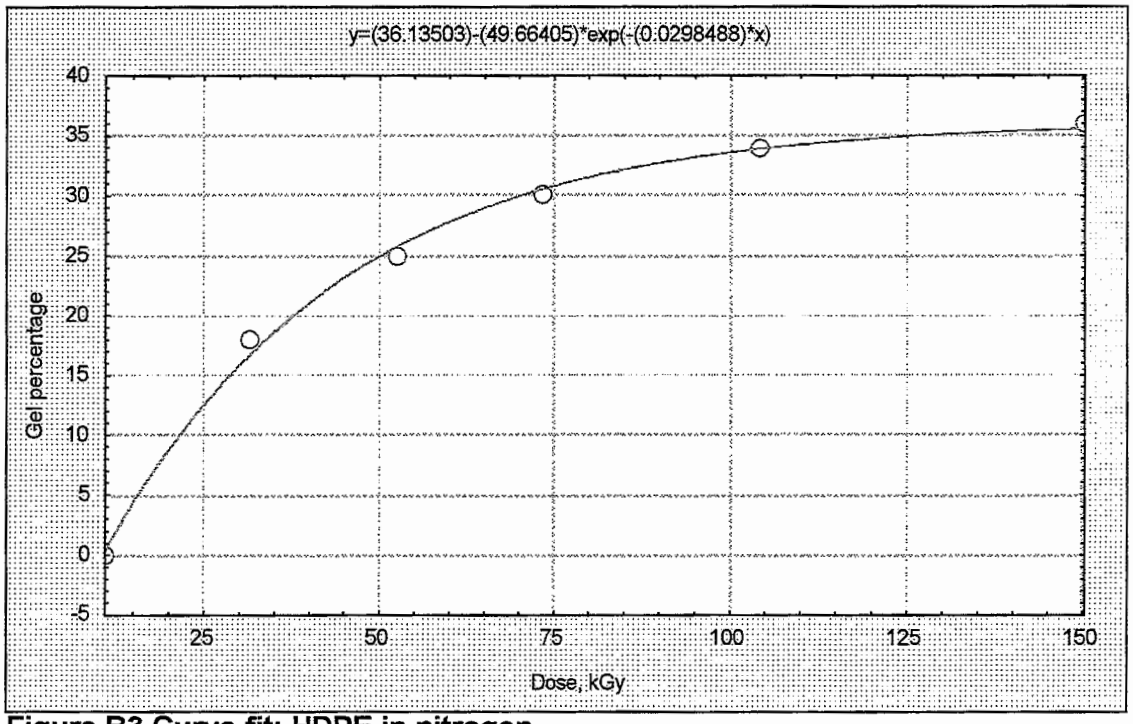

Figure B3 Curve-fit: HDPE in nitrogen

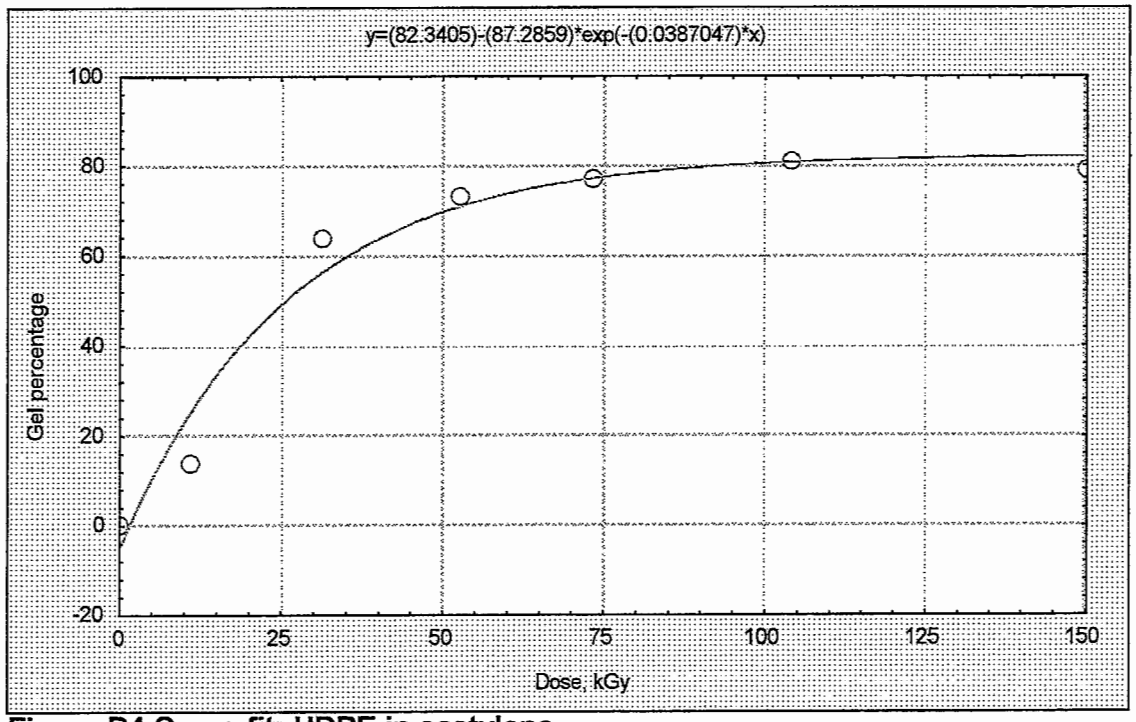

Figure B4 Curve-fit: HDPE in acetylene

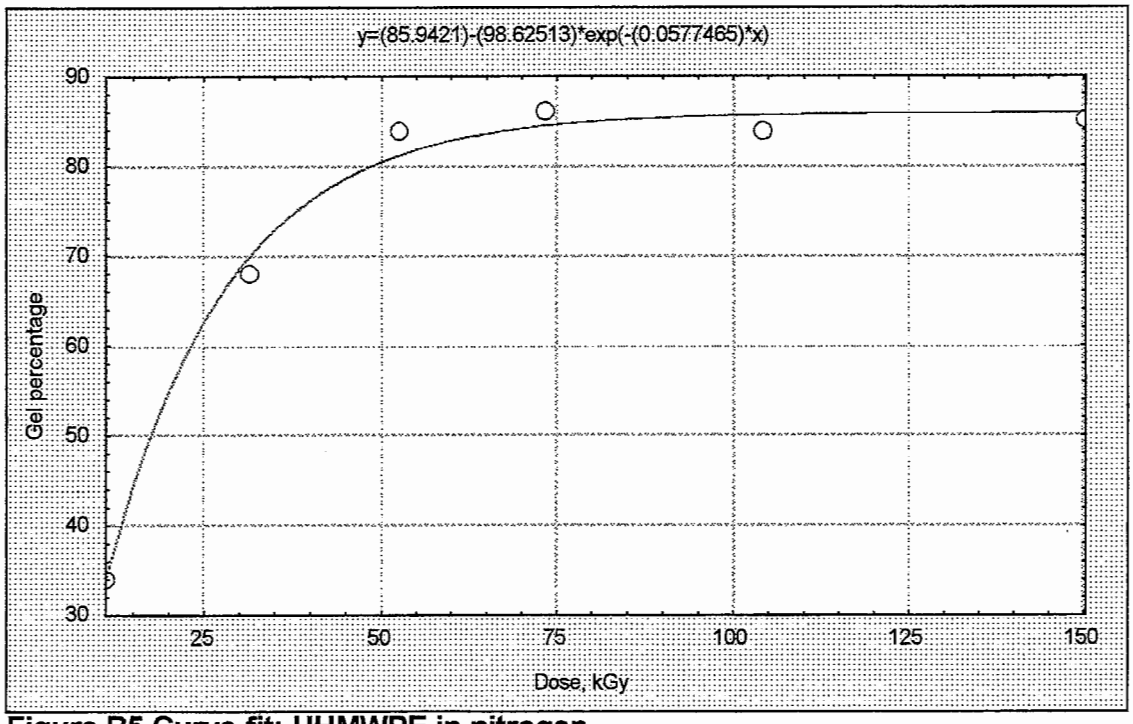

Figure B5 Curve-fit: UHMWPE in nitrogen

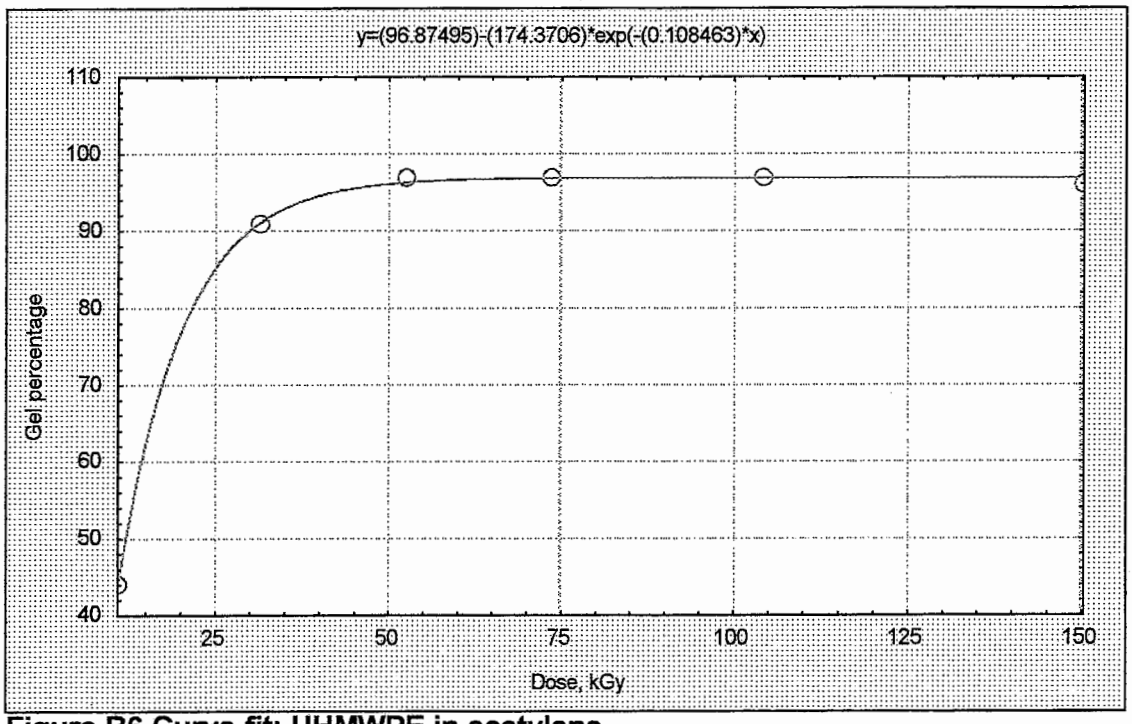

Figure B6 Curve-fit: UHMWPE in acetylene

APPENDIX C

Differential scanning calorimetry (DSC) Measurements

DSC measurements were done to determine the melting temperature of the different polymer samples, both before and after irradiation. These measurements showed that the melting temperature of the polyethylene powder increased after irradiation.

The DSC curves on the unirradiated LDPE, HDPE and UHMWPE samples are shown in Figures C1, C3 and C5. The DSC curves of the irradiated LDPE, HDPE and UHMWPE samples (Figures C2, C4 and C6) show a marked increase in melting temperature.

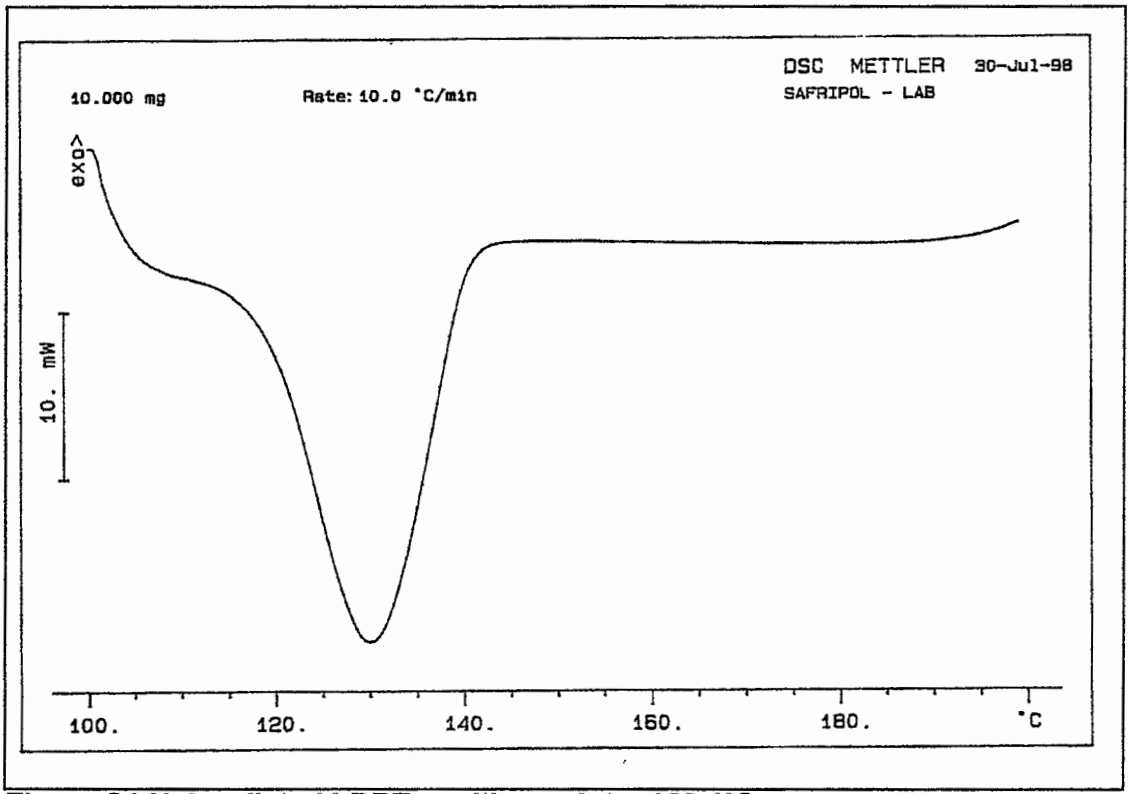

Figure C1 Unirradiated LDPE: melting point = 128.4°C

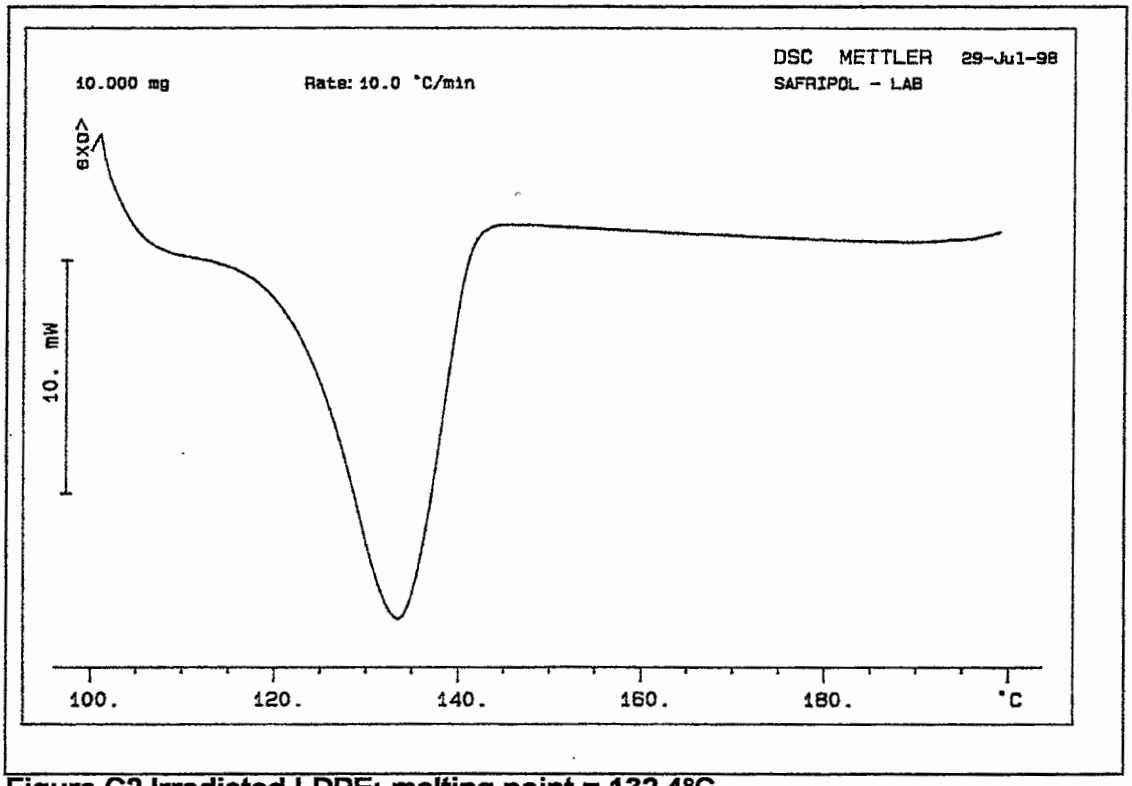

Figure C2 Irradiated LDPE: melting point = 132.4°C

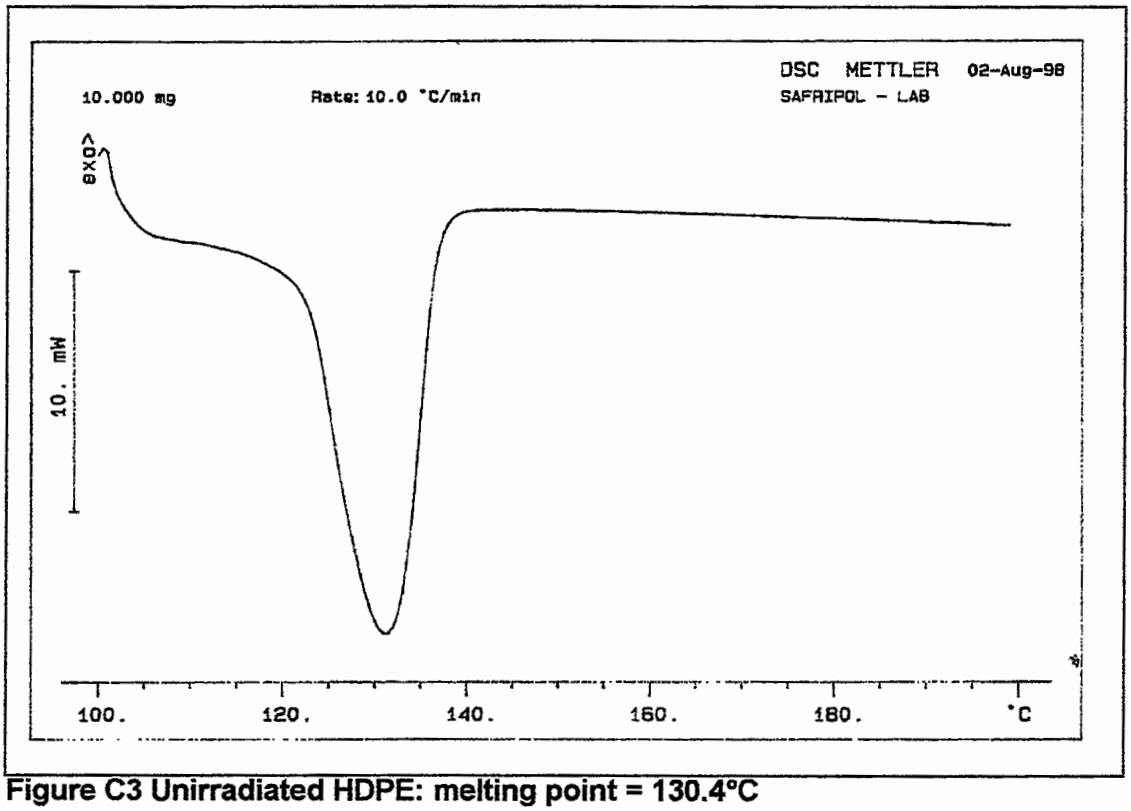

Figure C3 Unirradiated HDPE: melting point = 130.4°C

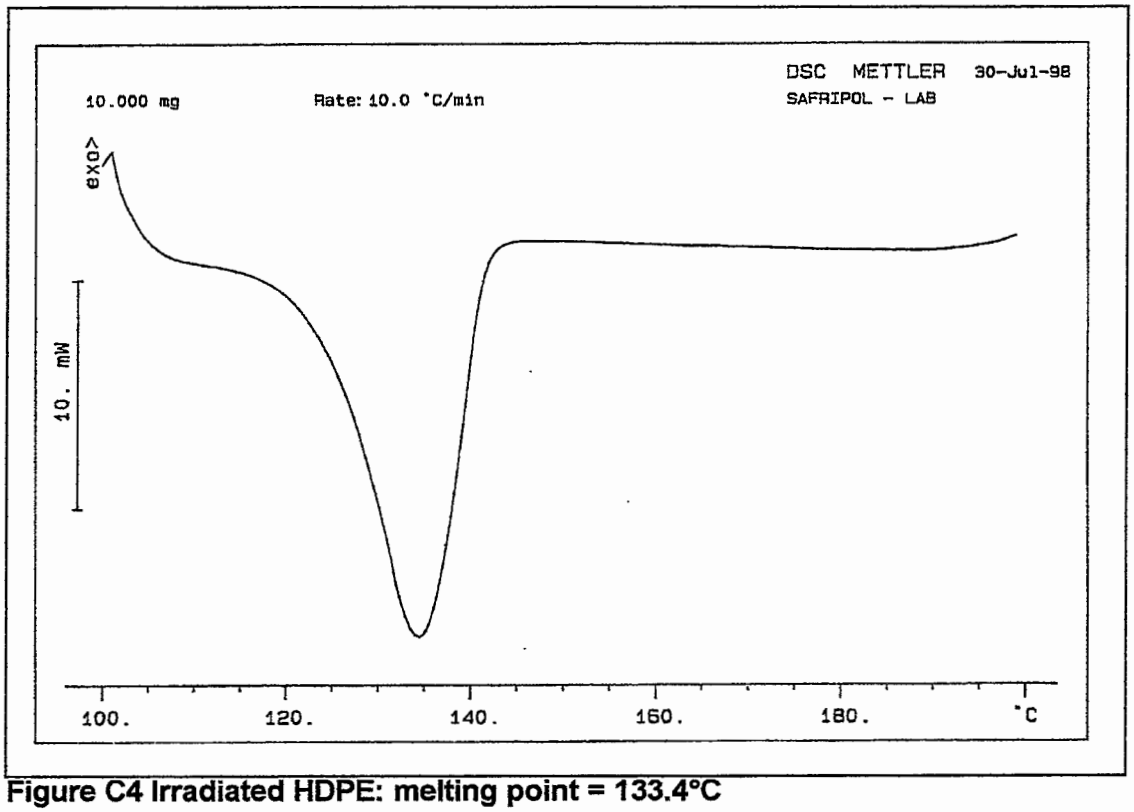

Figure C4 Irradiated HDPE: melting point = 133.4°C

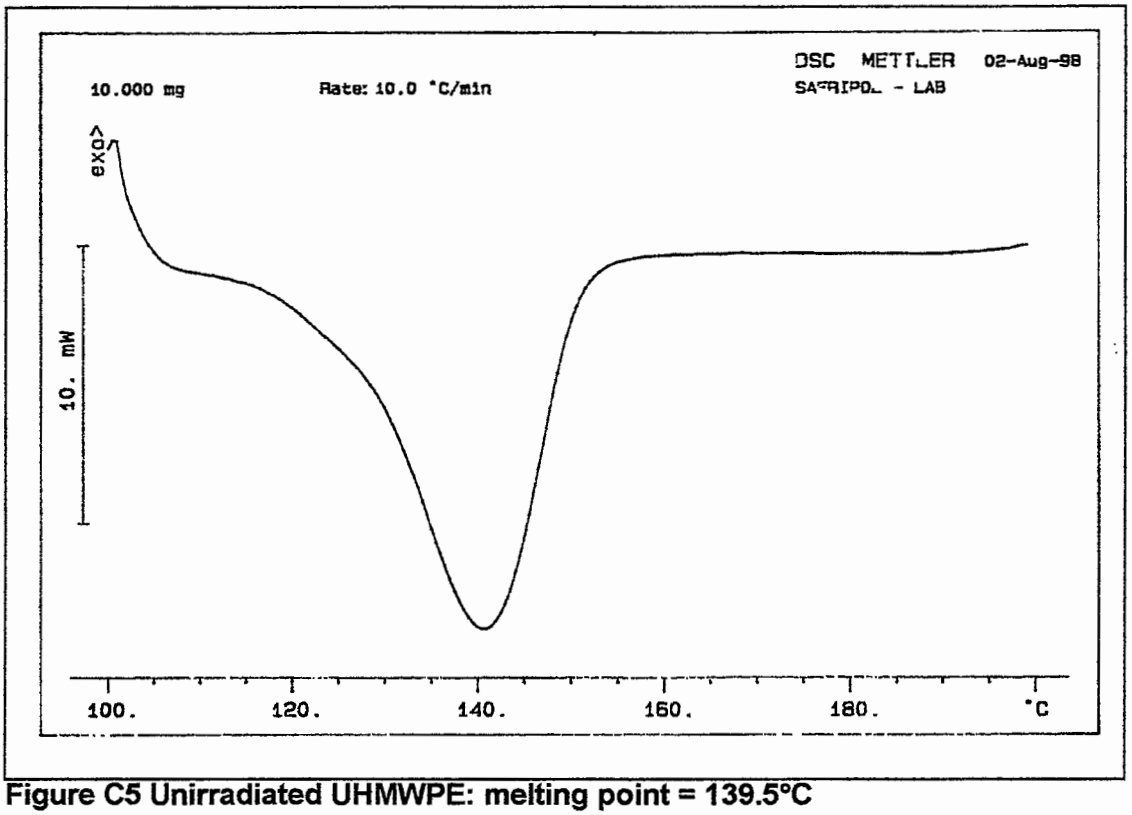

Figure C5 Unirradiated UHMWPE: melting point = 139.5°C

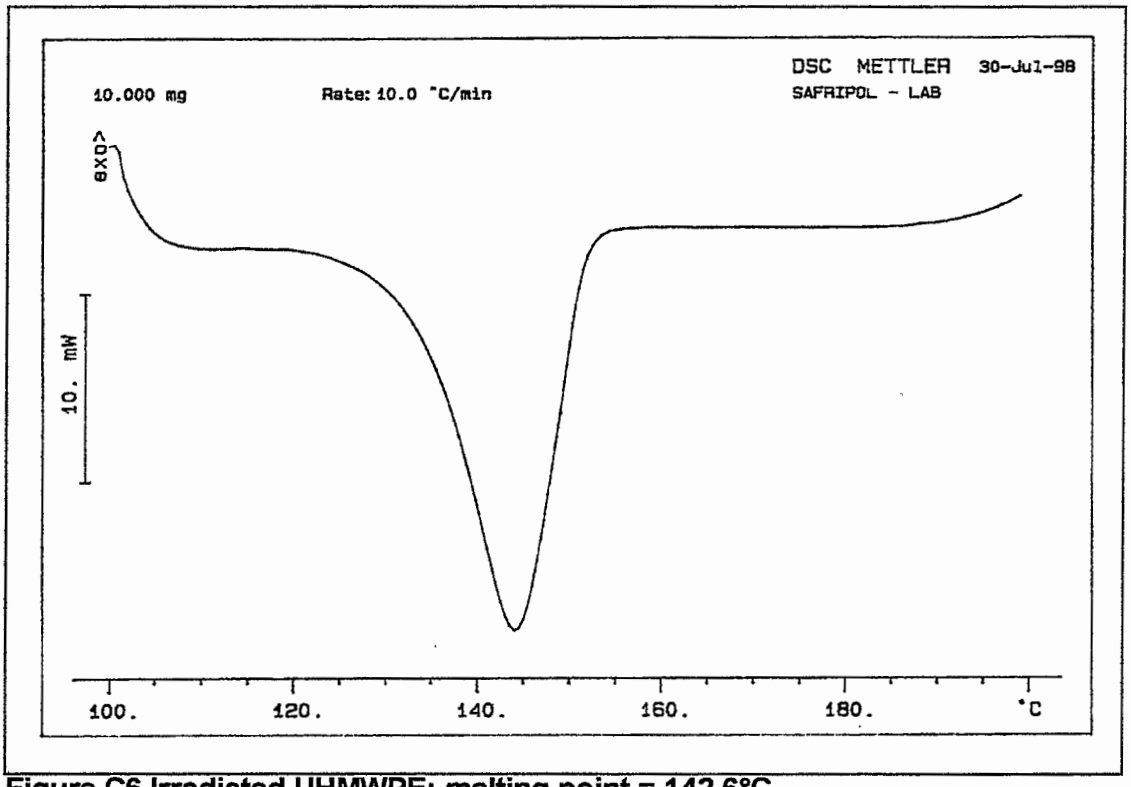

Figure C6 Irradiated UHMWPE: melting point = 142.6°C

APPENDIX D
Porosity Curves

D1 Initial experiments

D1.1 Constant pressure, different temperatures

Initial experiments were done to confirm that both porosity and mean pore size decrease with temperature when the pressure is kept constant. The corresponding porosity curves are given below.

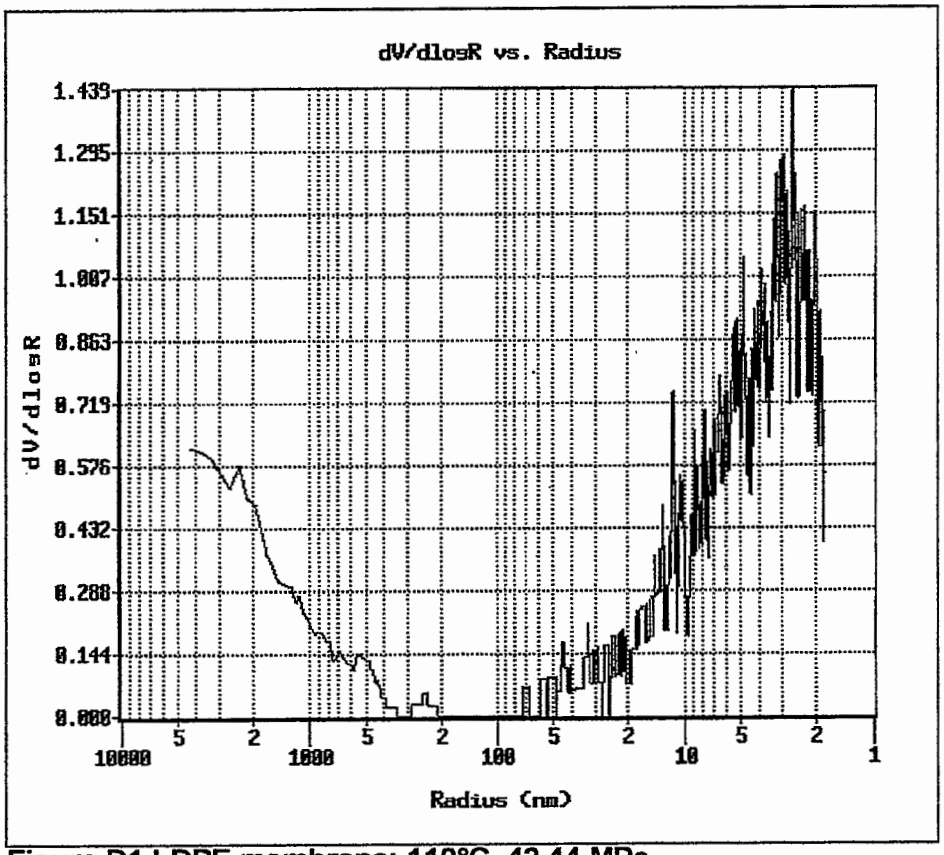

Figure D1 LDPE membrane: 110°C, 42.44 MPa

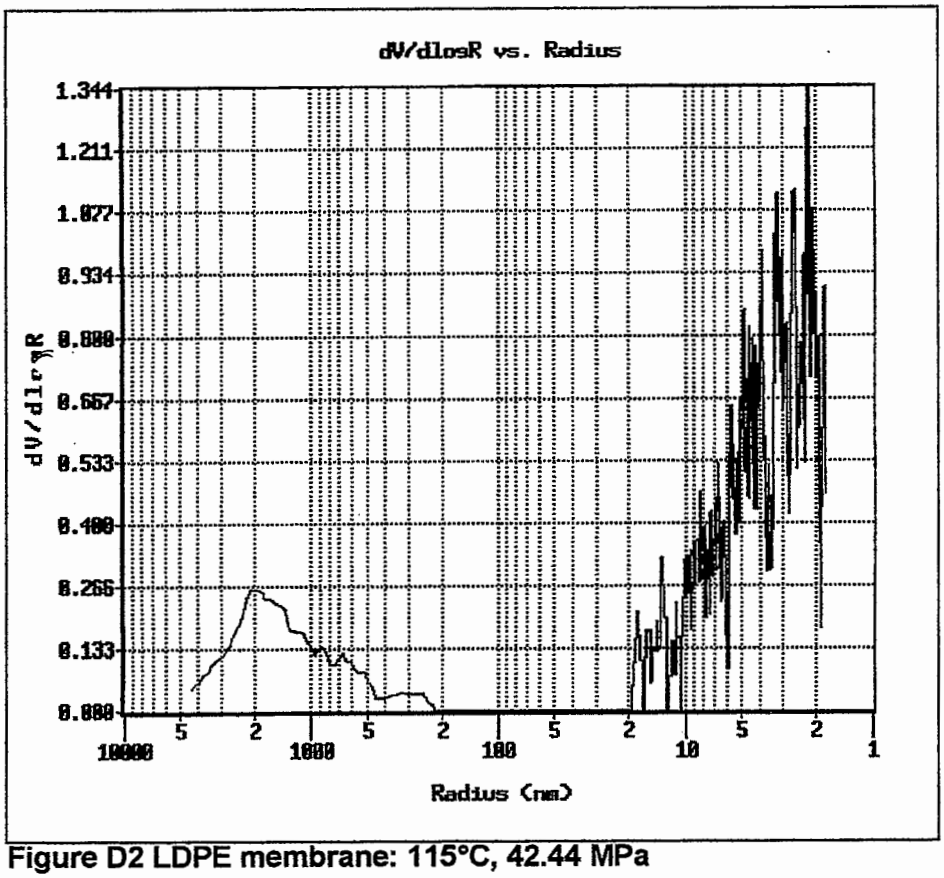

Figure D2 LDPE membrane: 115°C, 42.44 MPa

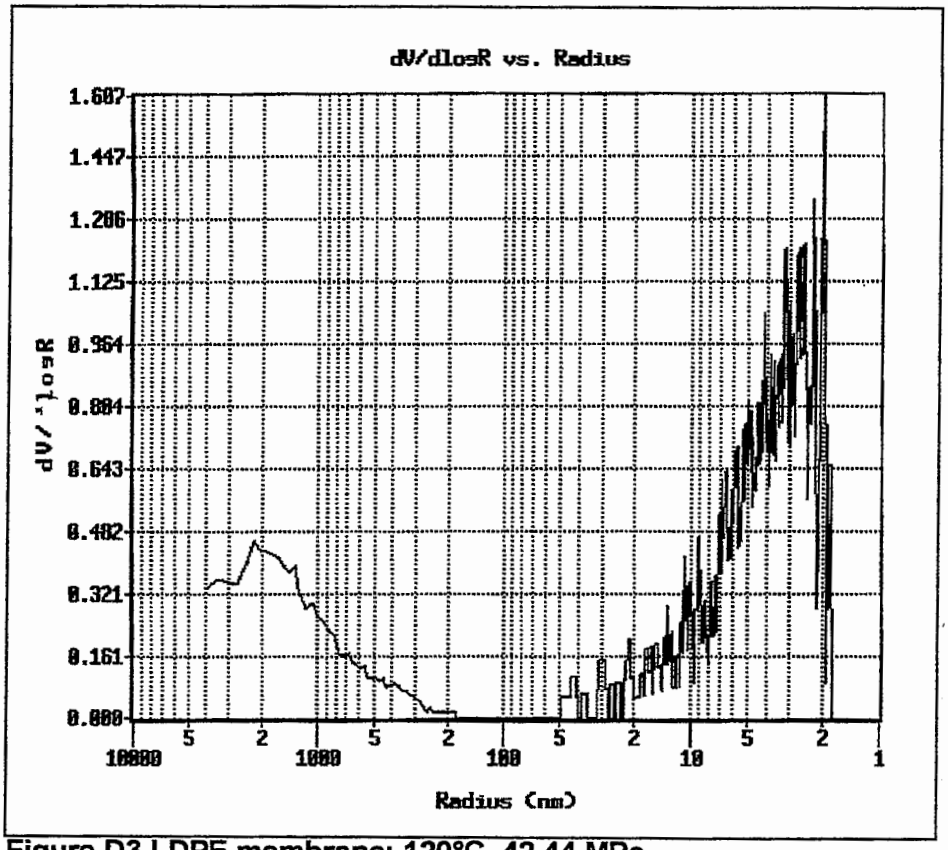

Figure D3 LDPE membrane: 120°C, 42.44 MPa

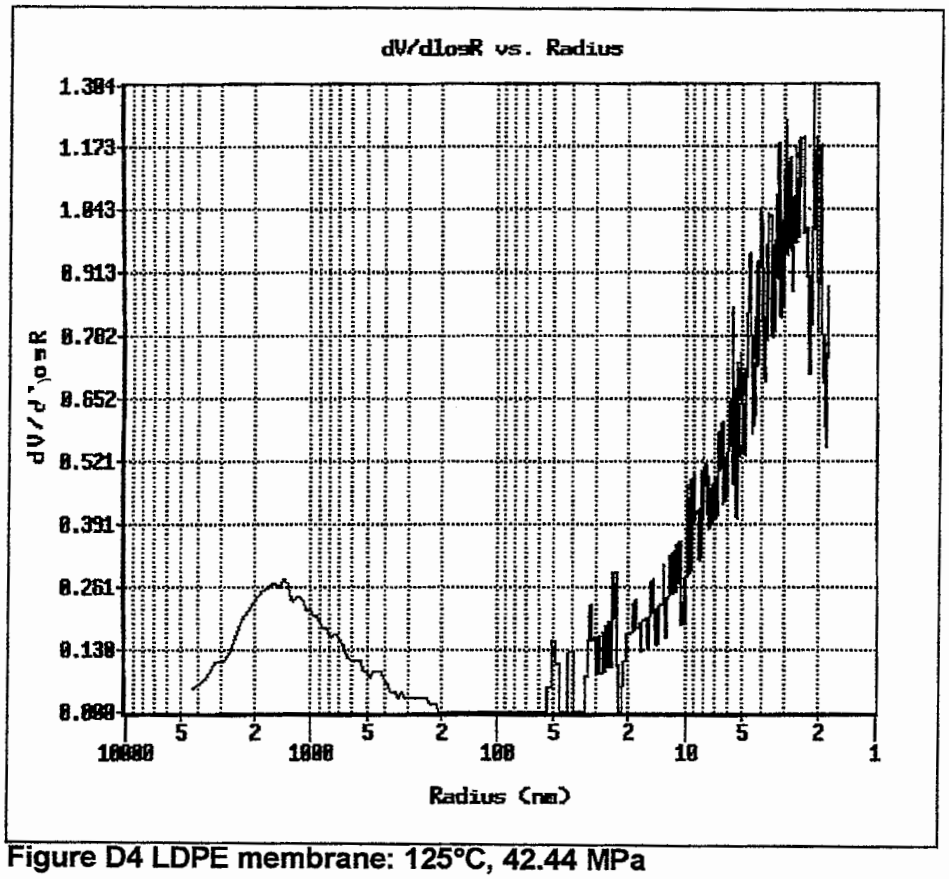

Figure D4 LDPE membrane: 125°C, 42.44 MPa

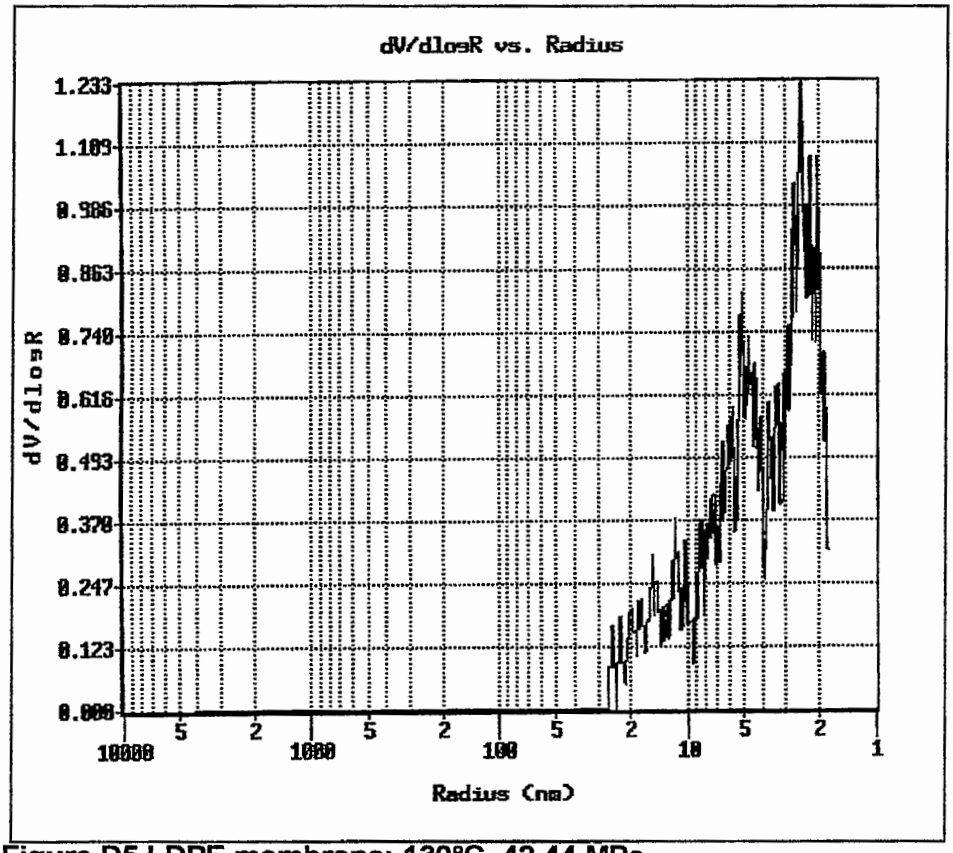

Figure D5 LDPE membrane: 130°C, 42.44 MPa

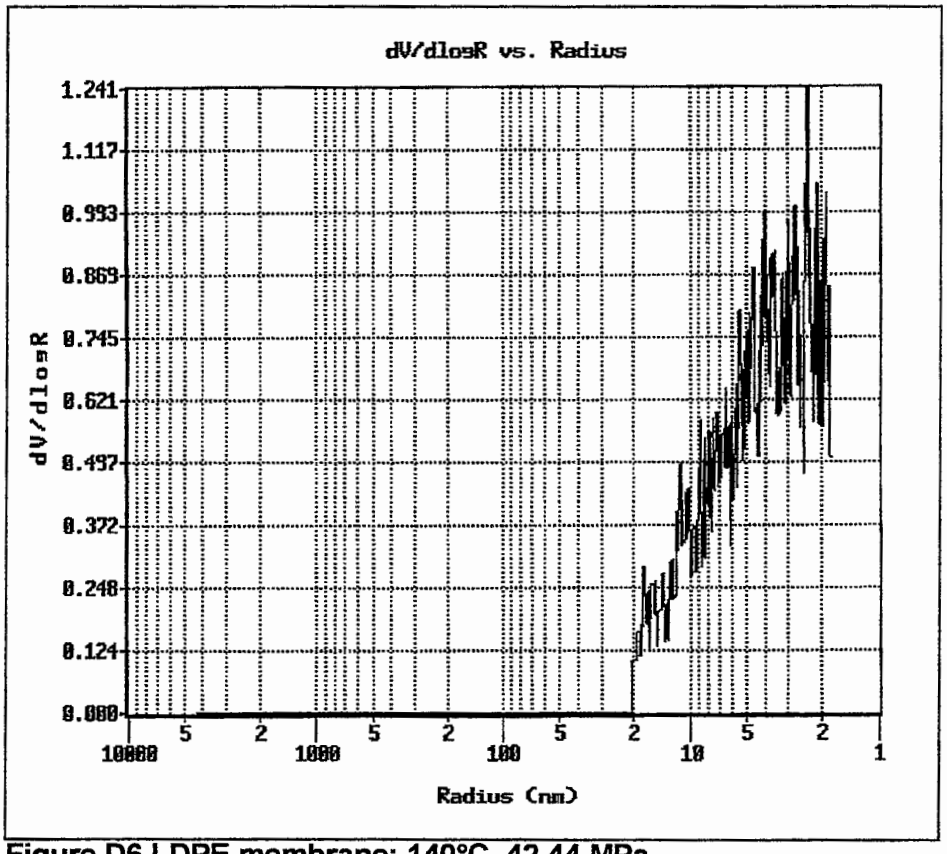

Figure D6 LDPE membrane: 140°C, 42.44 MPa

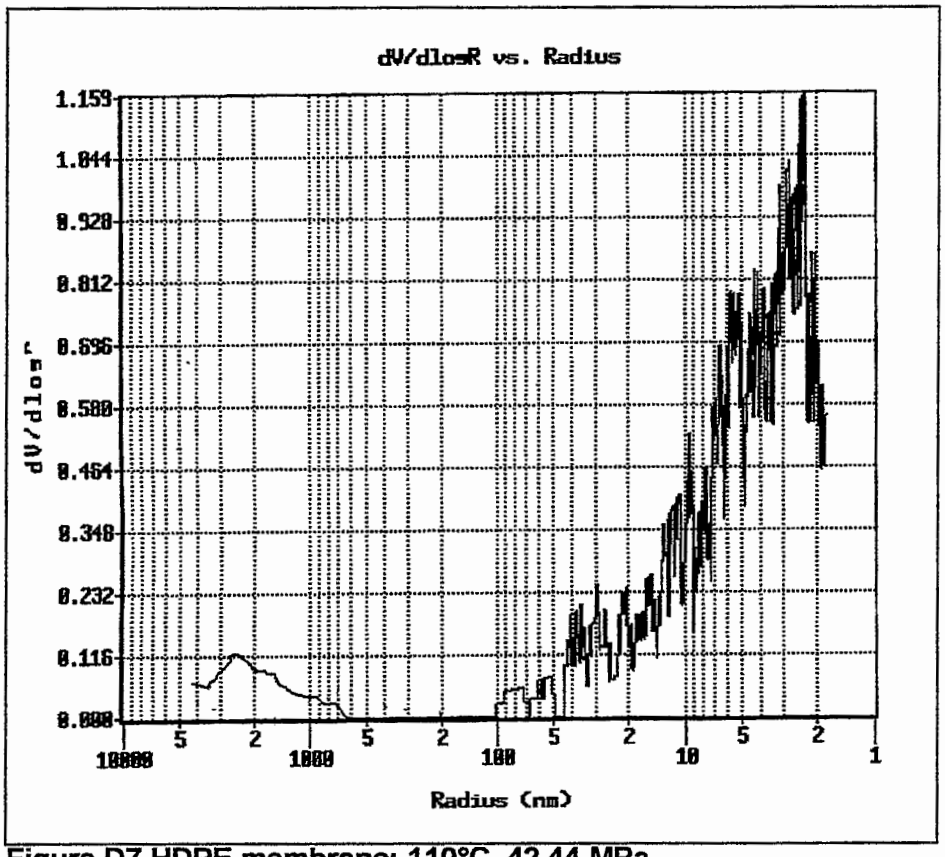

Figure D7 HDPE membrane: 110°C, 42.44 MPa

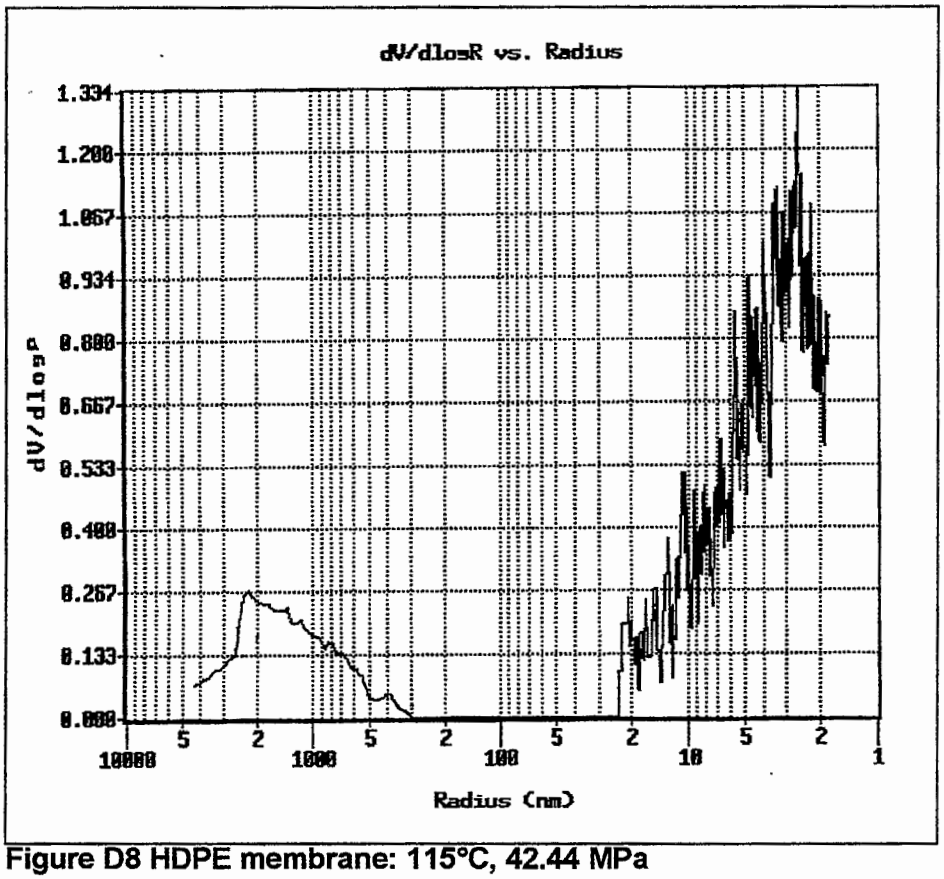

Figure D8 HDPE membrane: 115°C, 42.44 MPa

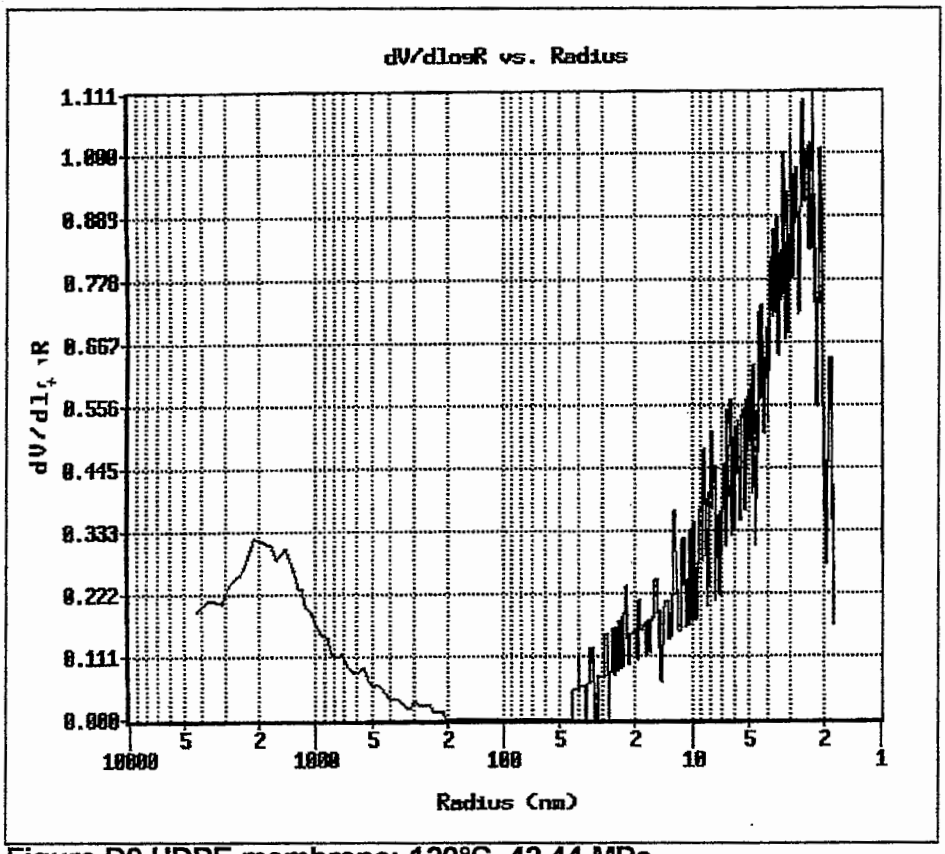

Figure D9 HDPE membrane: 120°C, 42.44 MPa

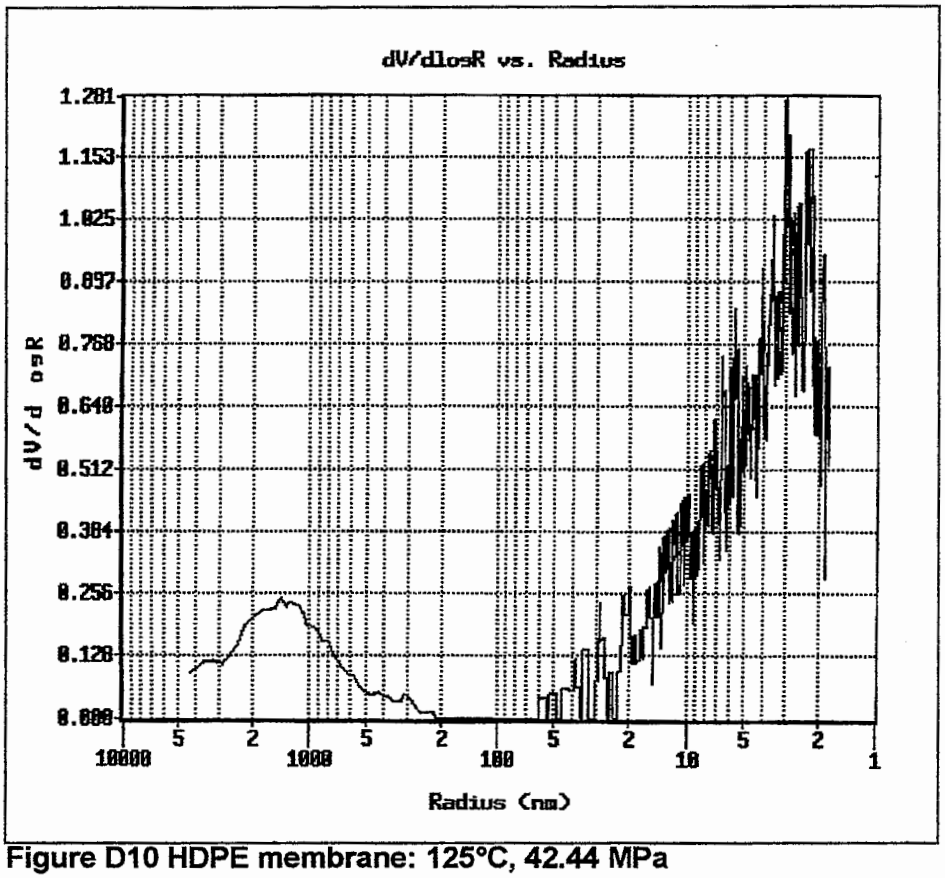

Figure D10 HDPE membrane: 125°C, 42.44 MPa

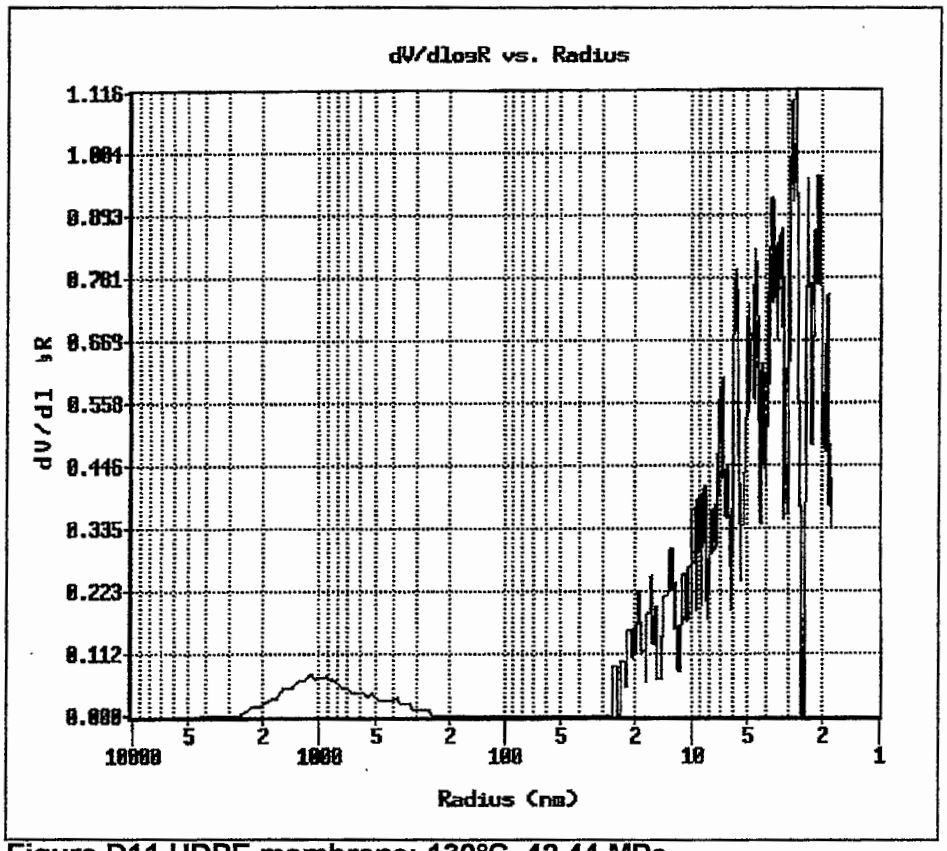

Figure D11 HDPE membrane: 130°C, 42.44 MPa

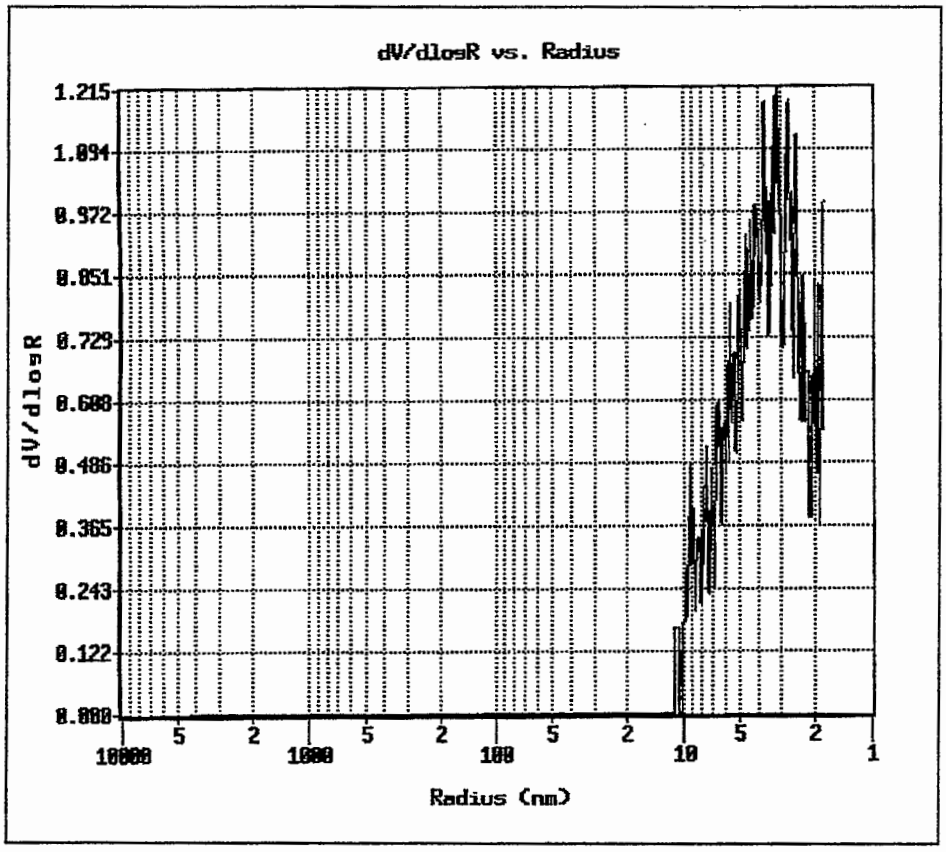

Figure D12 HDPE membrane: 140°C, 42.44 MPa

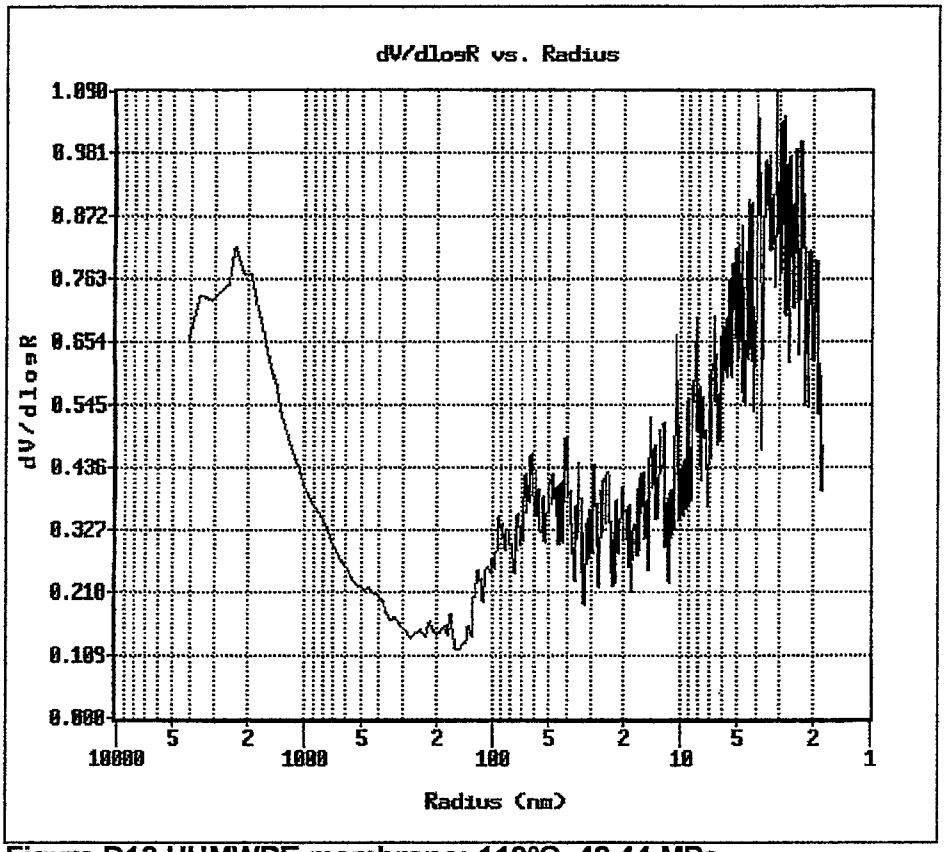

Figure D13 UHMWPE membrane: 110°C, 42.44 MPa

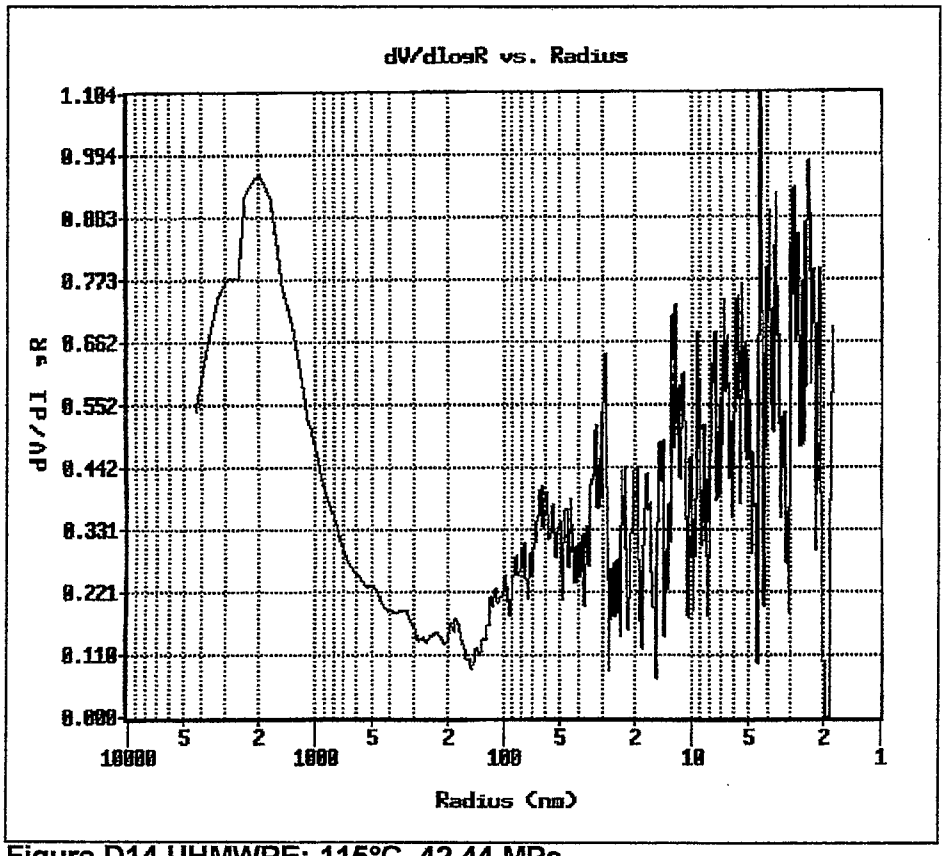

Figure D14 UHMWPE: 115°C, 42.44 MPa

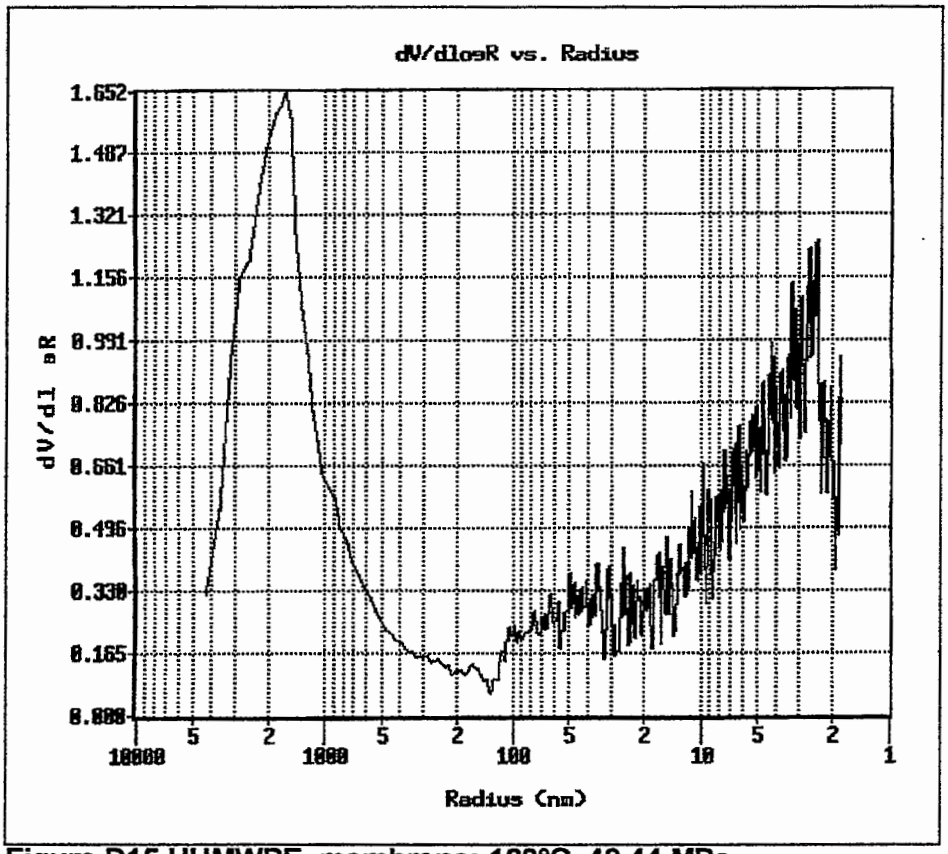

Figure D15 UHMWPE membrane: 120°C, 42.44 MPa

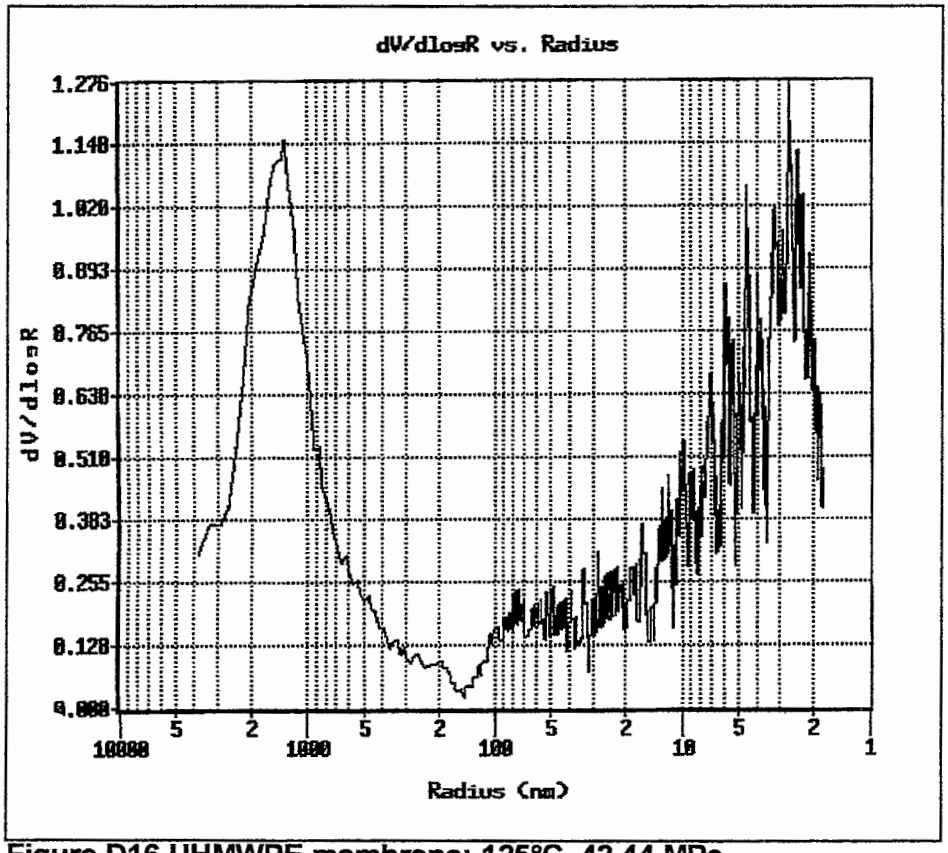

Figure D16 UHMWPE membrane: 125°C, 42.44 MPa

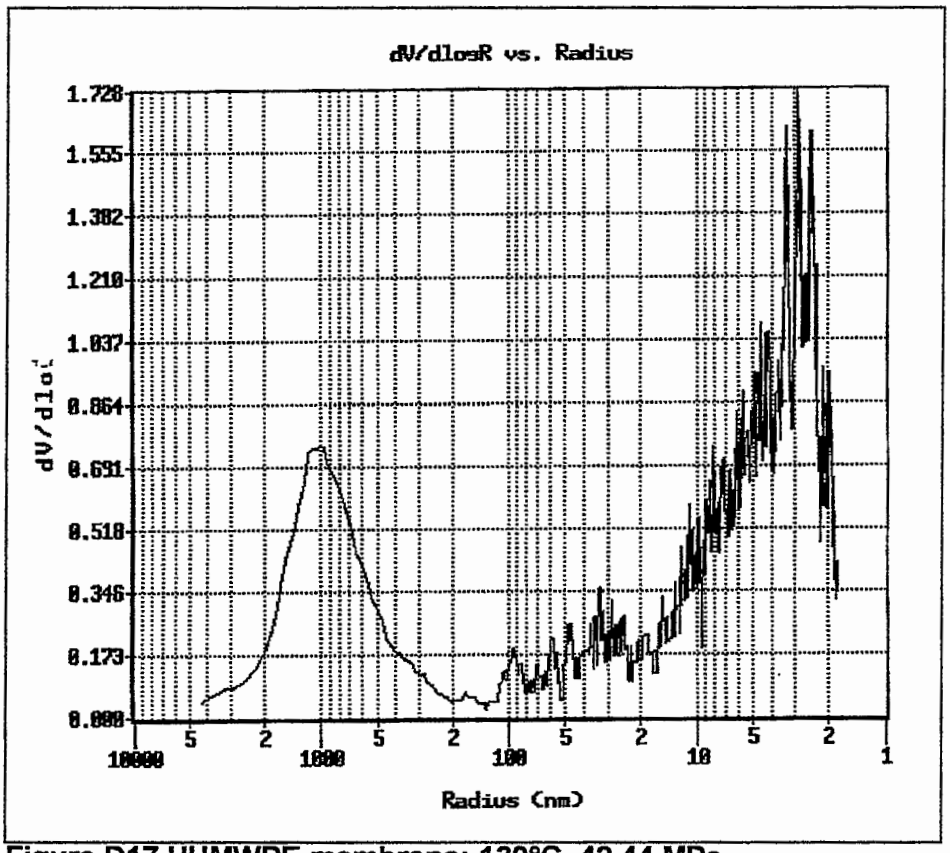

Figure D17 UHMWPE membrane: 130°C, 42.44 MPa

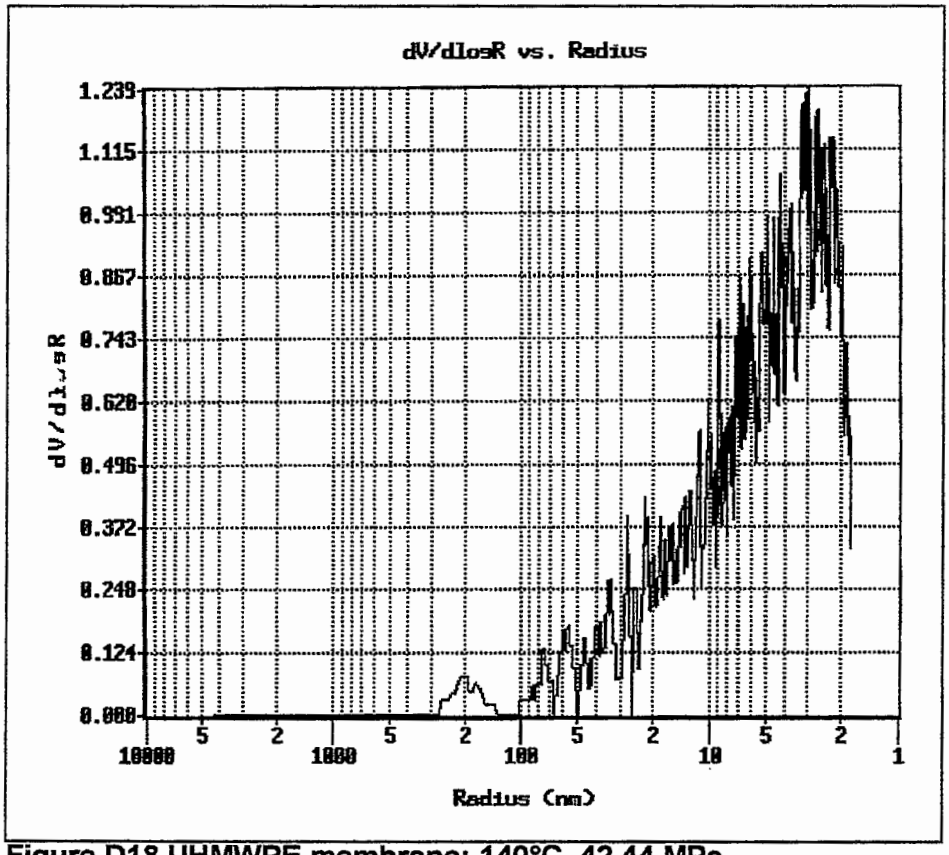

Figure D18 UHMWPE membrane: 140°C, 42.44 MPa

D1.2 Constant temperature, increasing pressures

Initial experiments were done to confirm that both porosity and mean pore size decreases with increased pressure at constant temperature. The corresponding porosity curves are given below.

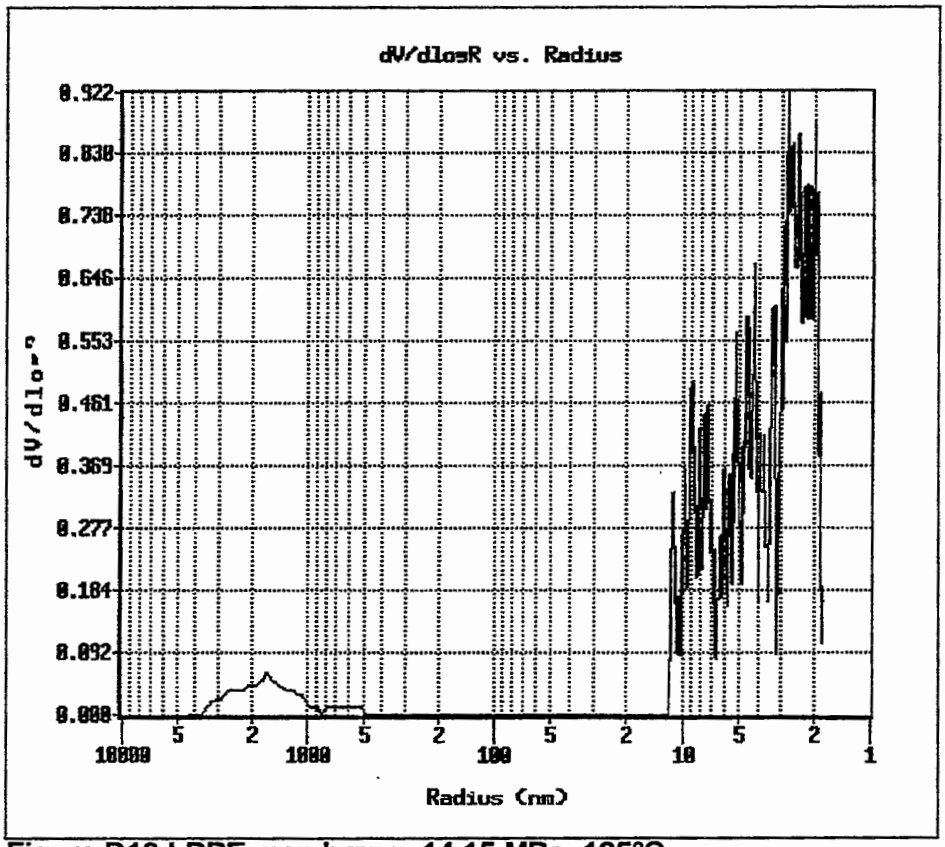

Figure D19 LDPE membrane: 14.15 MPa, 125°C

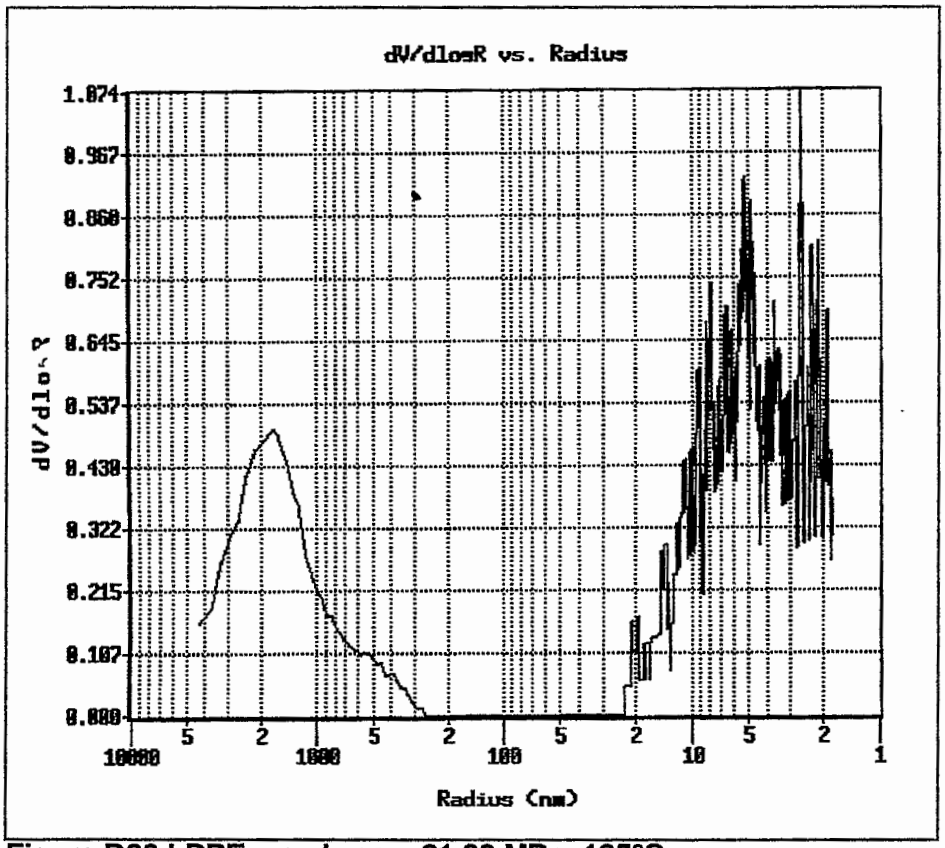

Figure D20 LDPE membrane: 21.22 MPa, 125°C

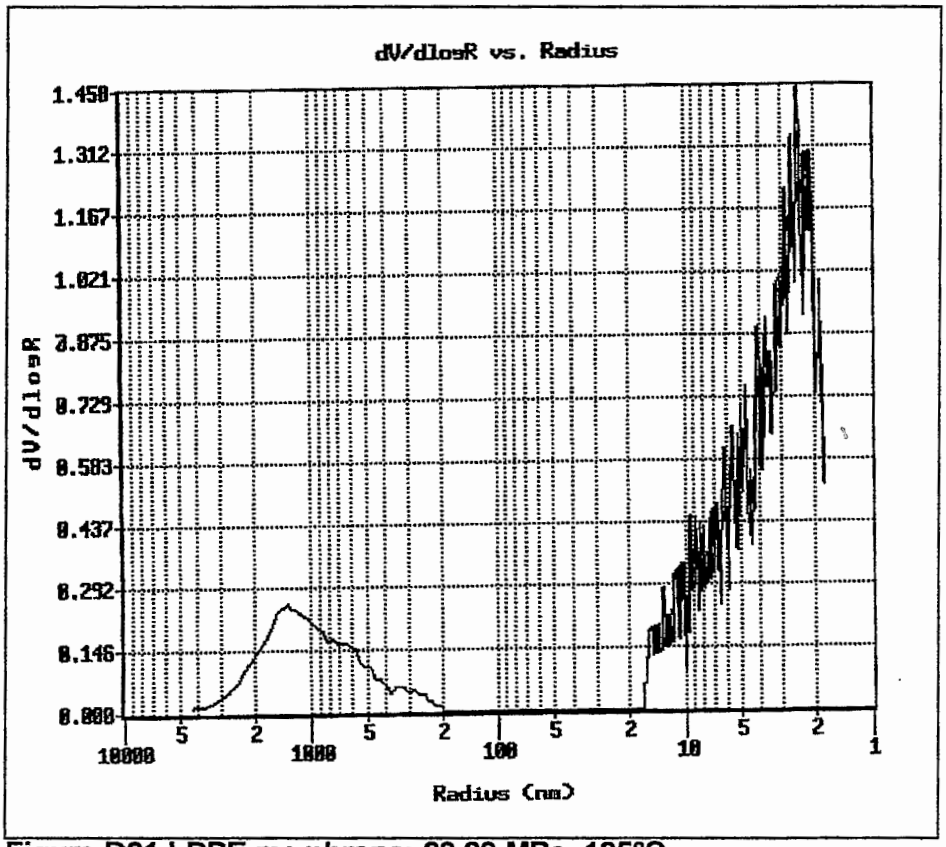

Figure D21 LDPE membrane: 28.29 MPa, 125°C

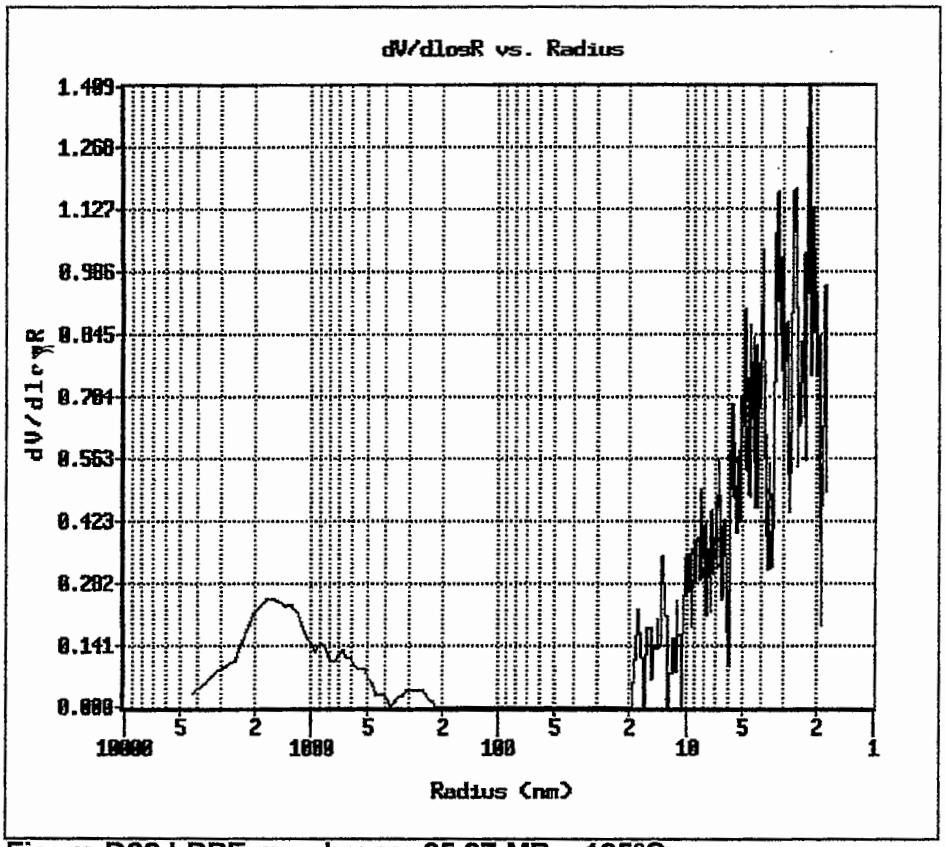

Figure D22 LDPE membrane: 35.37 MPa, 125°C

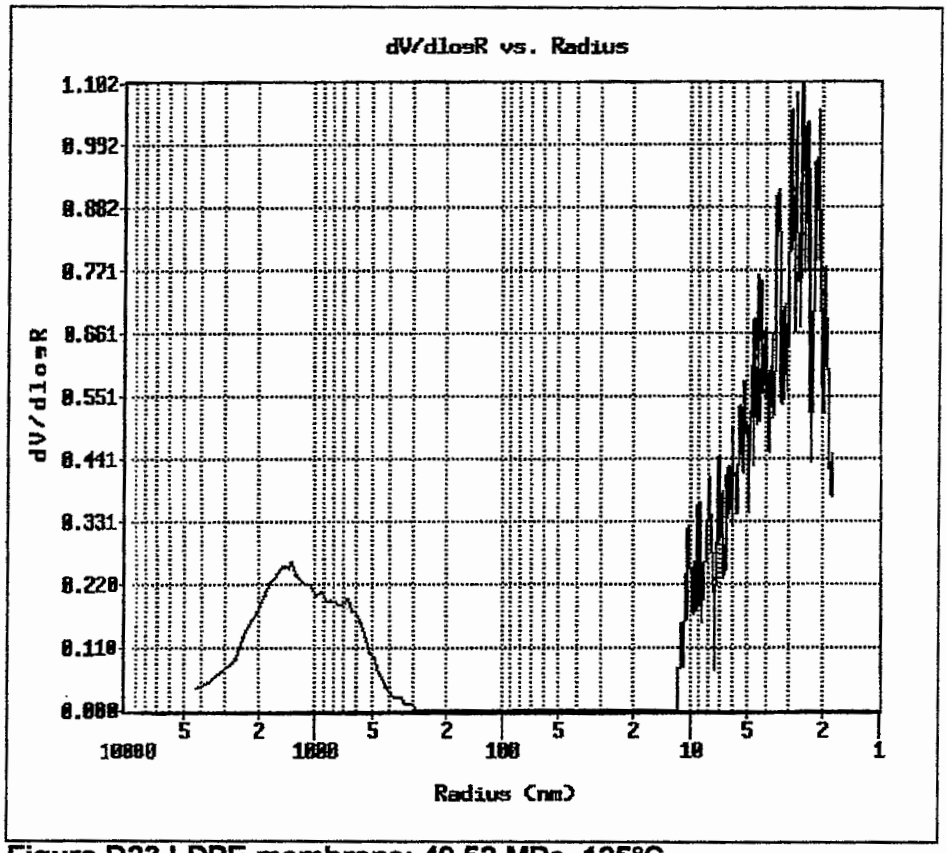

Figure D23 LDPE membrane: 49.52 MPa, 125°C

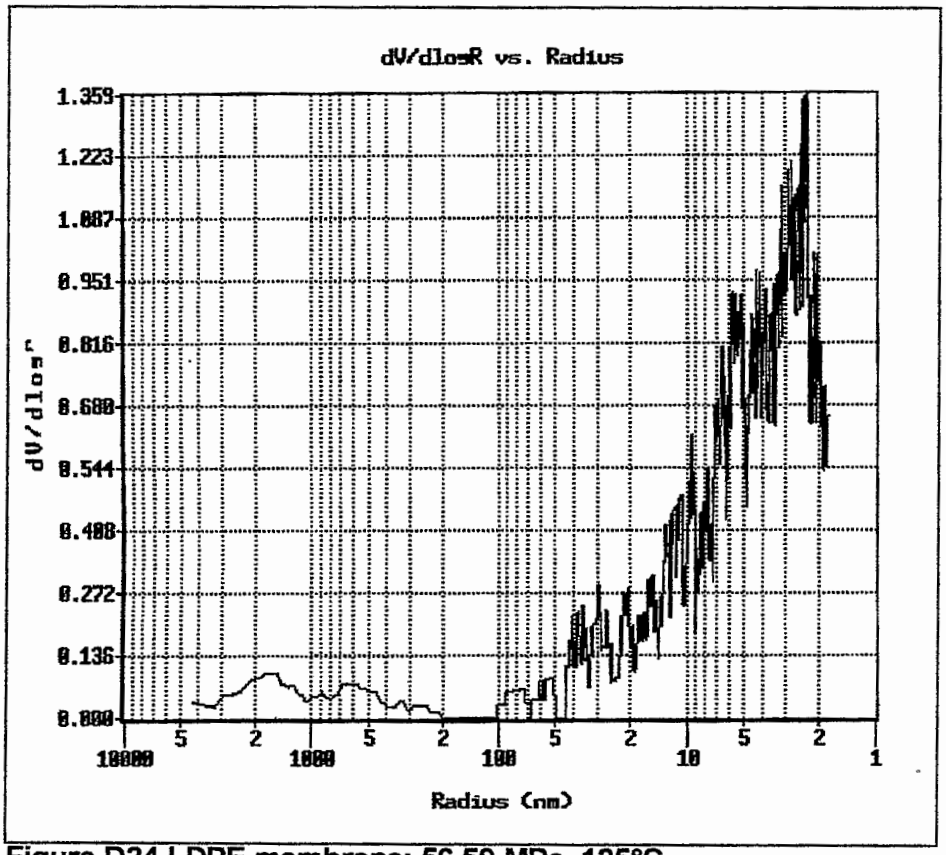

Figure D24 LDPE membrane: 56.59 MPa, 125°C

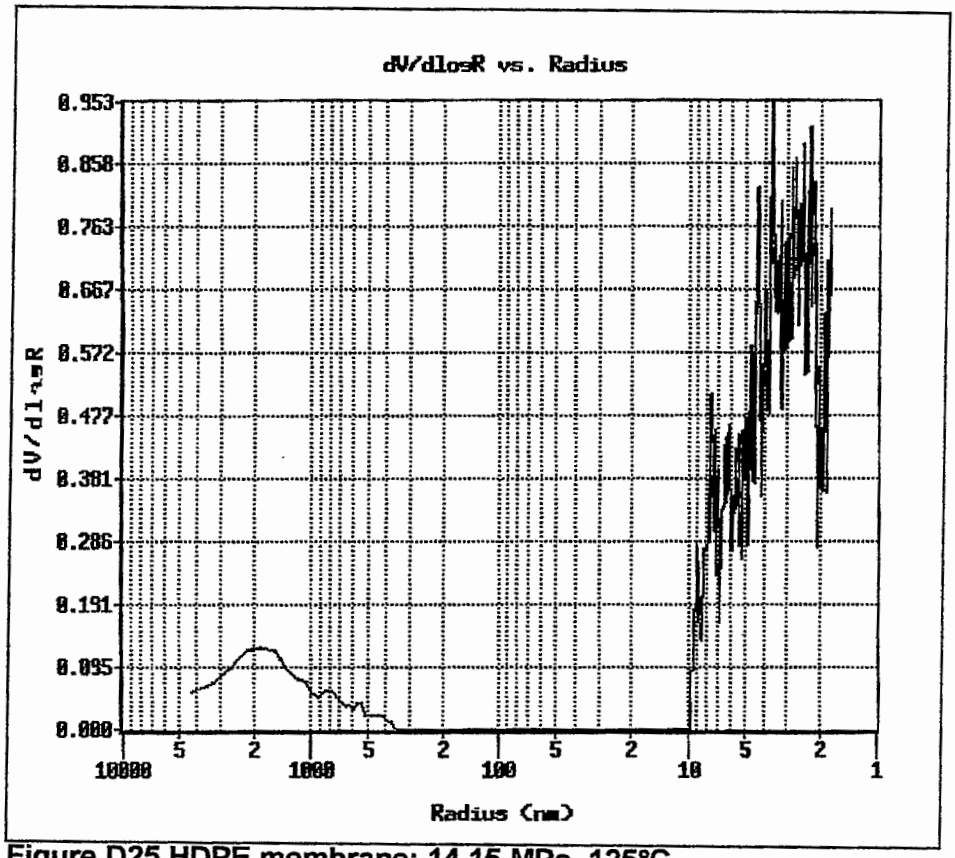

Figure D25 HDPE membrane: 14.15 MPa, 125°C

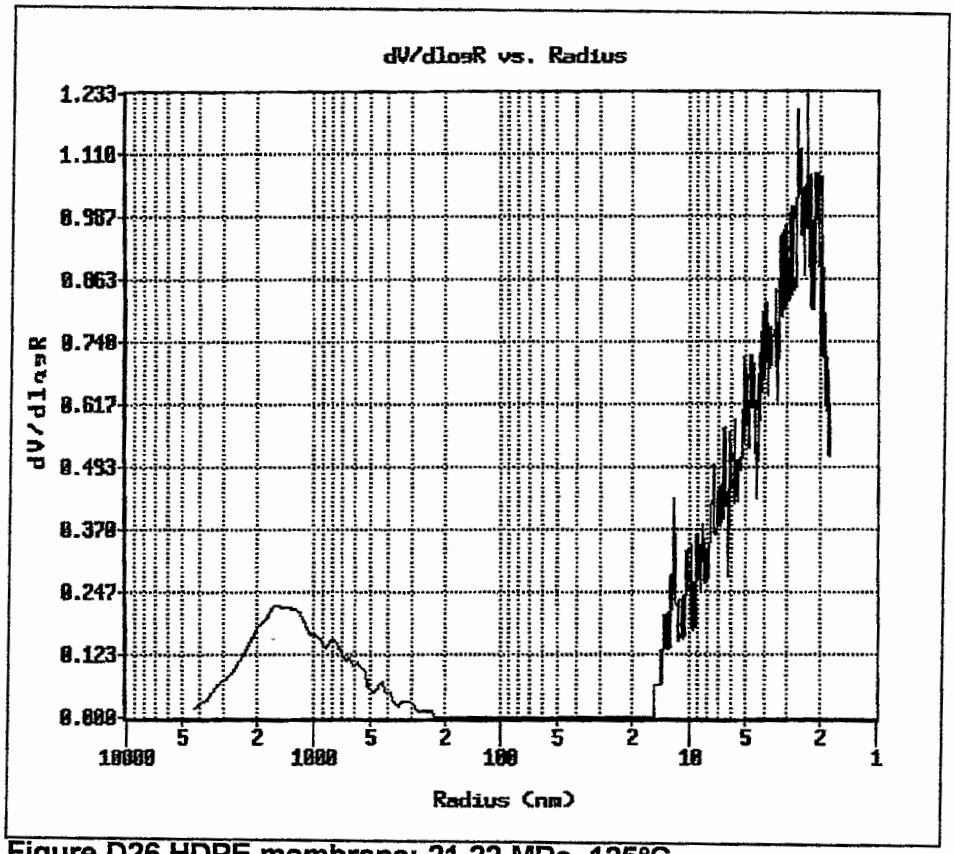

Figure D26 HDPE membrane: 21.22 MPa, 125°C

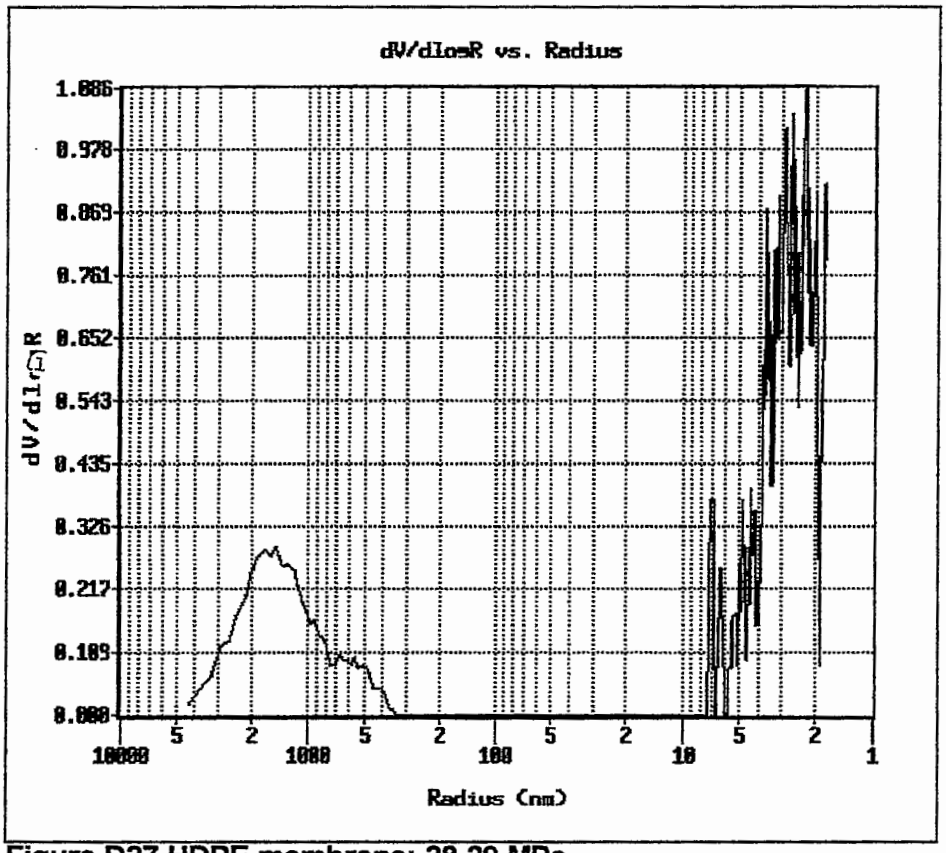

Figure D27 HDPE membrane: 28.29 MPa

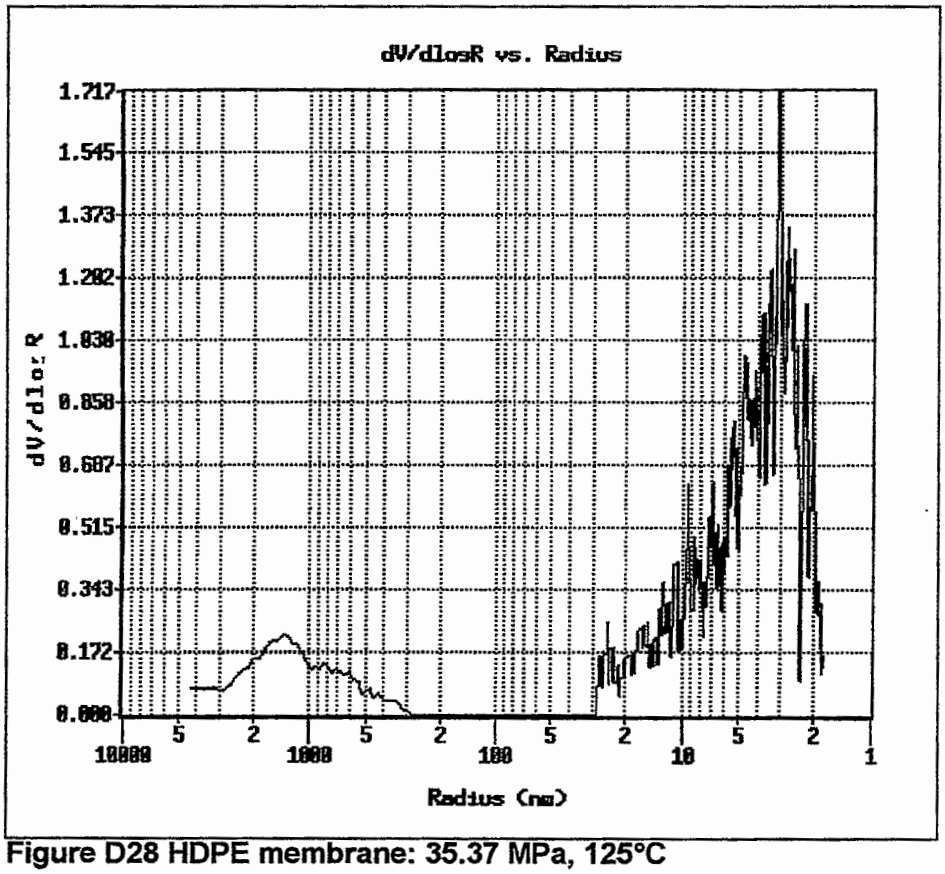

Figure D28 HDPE membrane: 35.37 MPa, 125°C

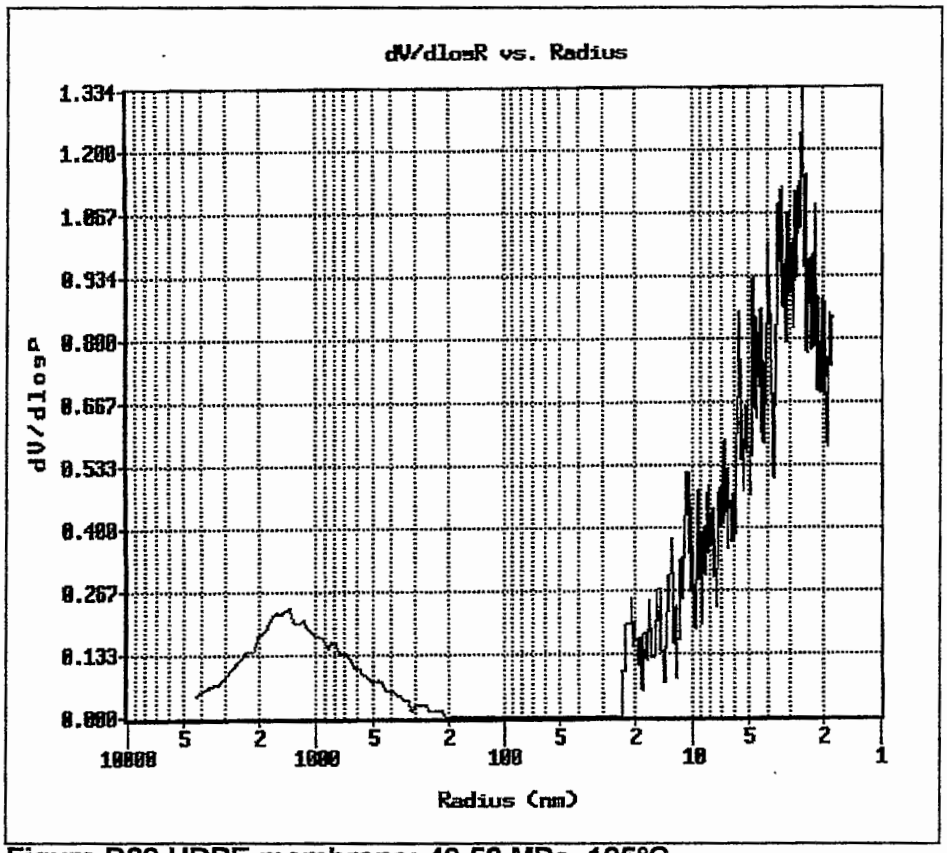

Figure D29 HDPE membrane: 49.52 MPa, 125°C

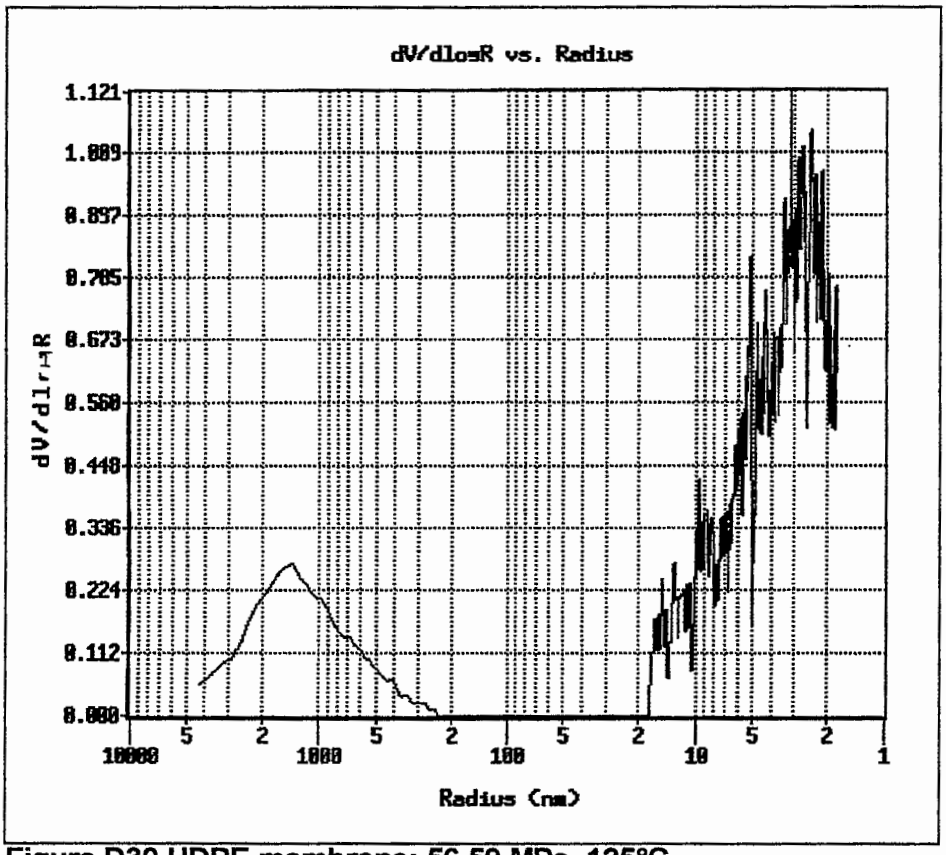

Figure D30 HDPE membrane: 56.59 MPa, 125°C

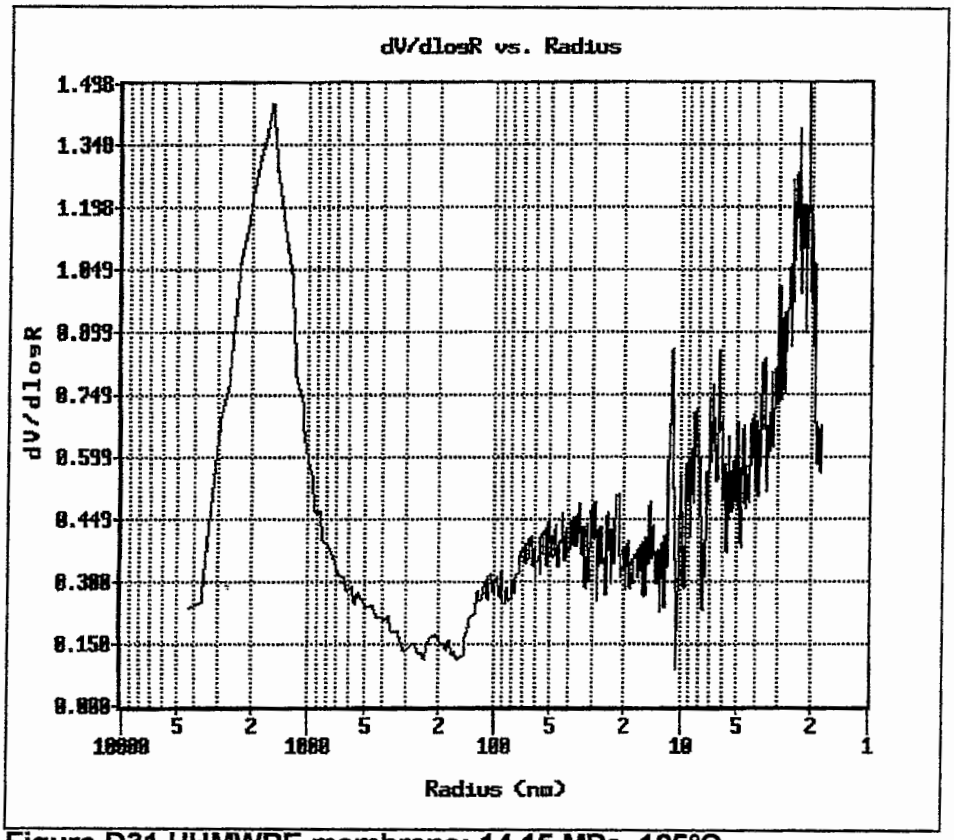

Figure D31 UHMWPE membrane: 14.15 MPa, 125°C

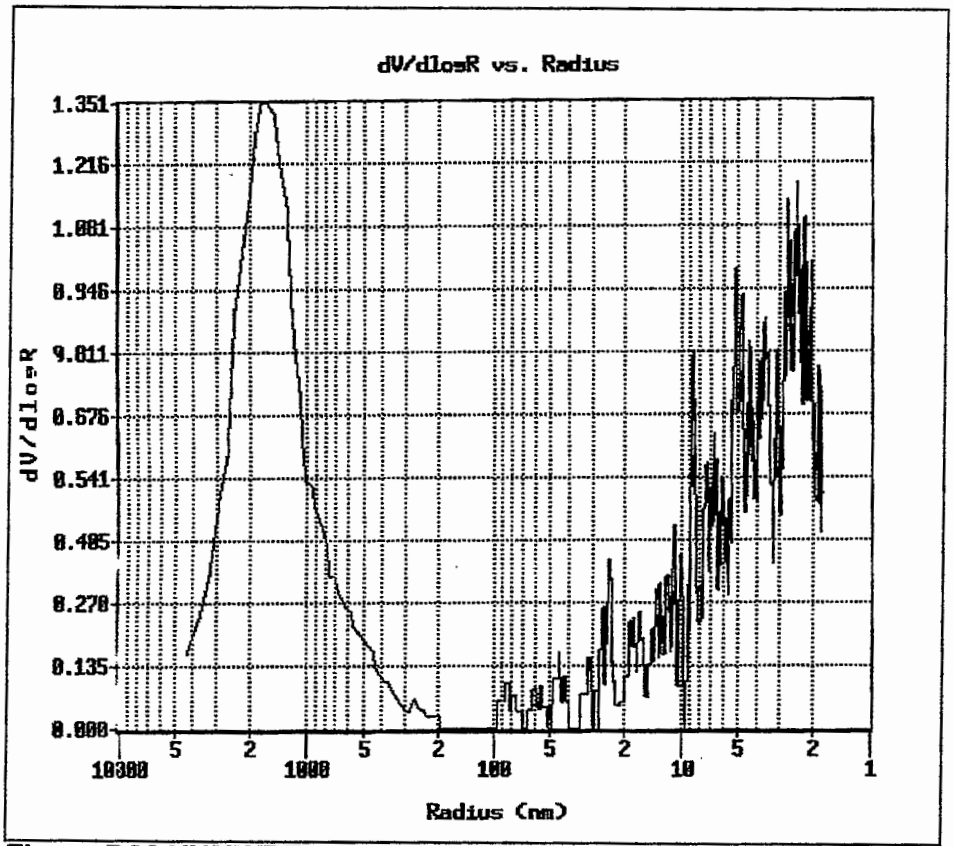

Figure D32 UHMWPE membrane: 21.22 MPa, 125°C

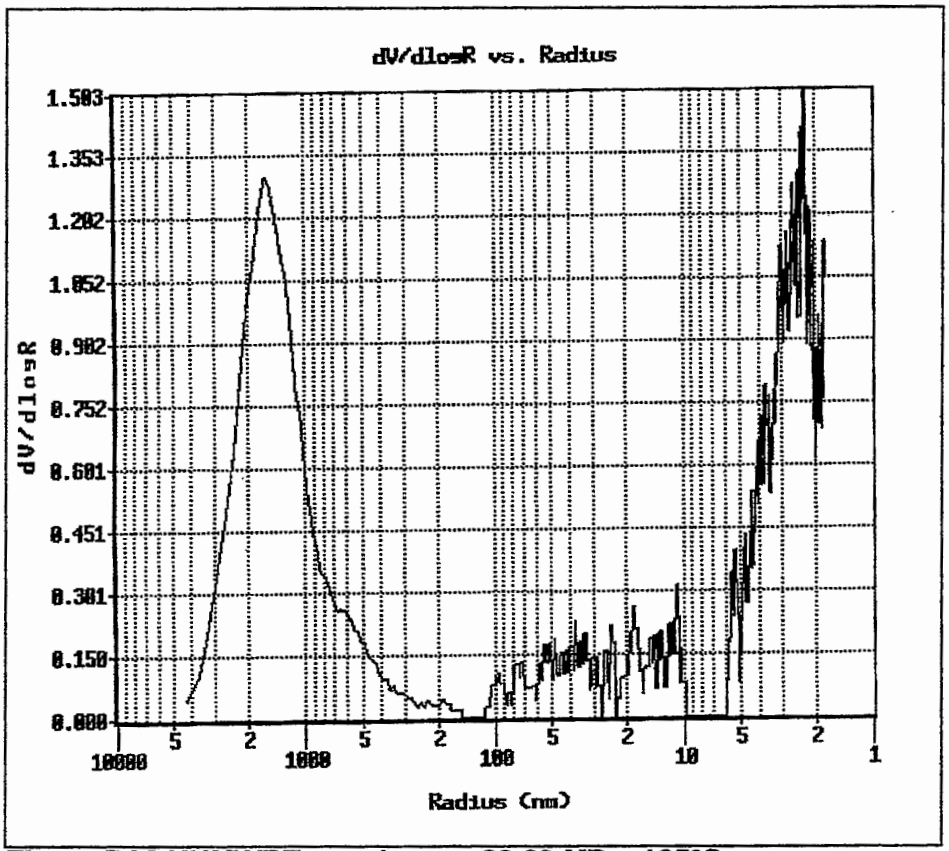

Figure D33 UHMWPE membrane: 28.29 MPa, 125°C

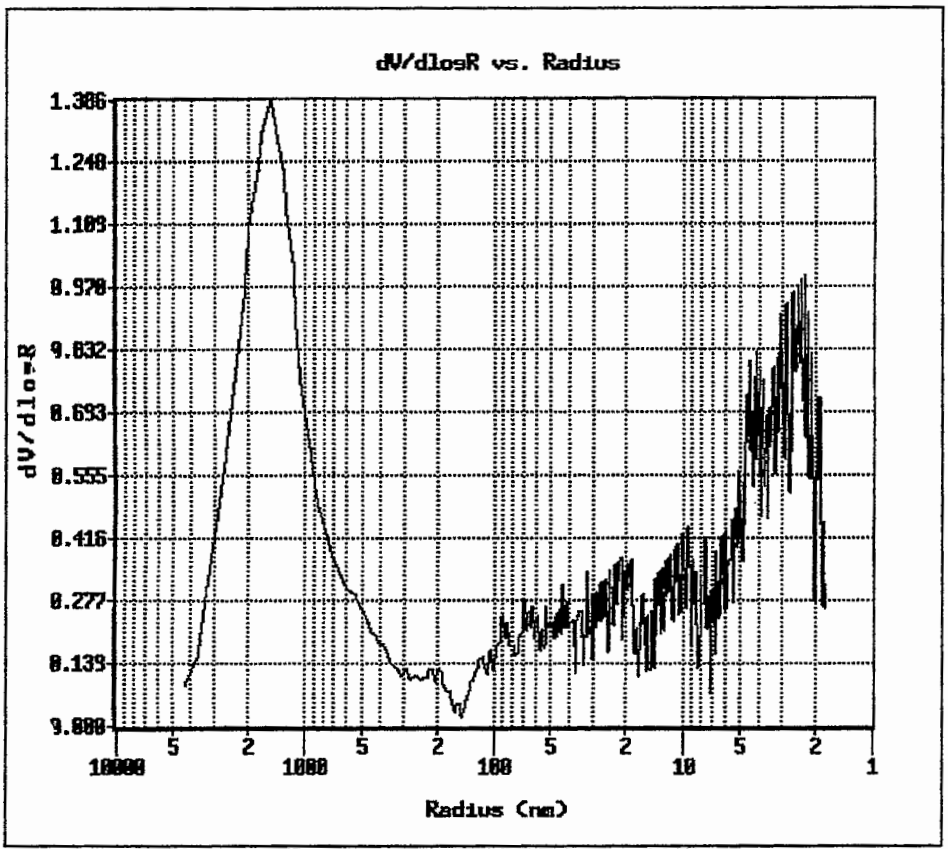

Figure D34 UHMWPE membrane: 35.37 MPa, 125°C

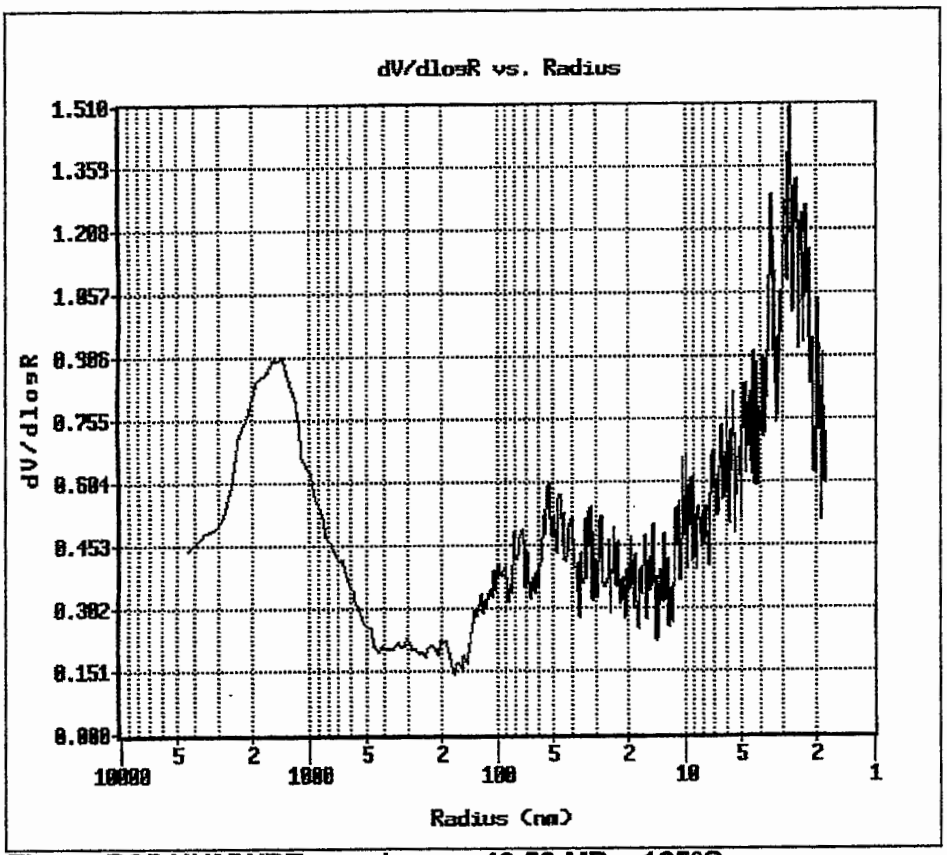

Figure D35 UHMWPE membrane: 49.52 MPa, 125°C

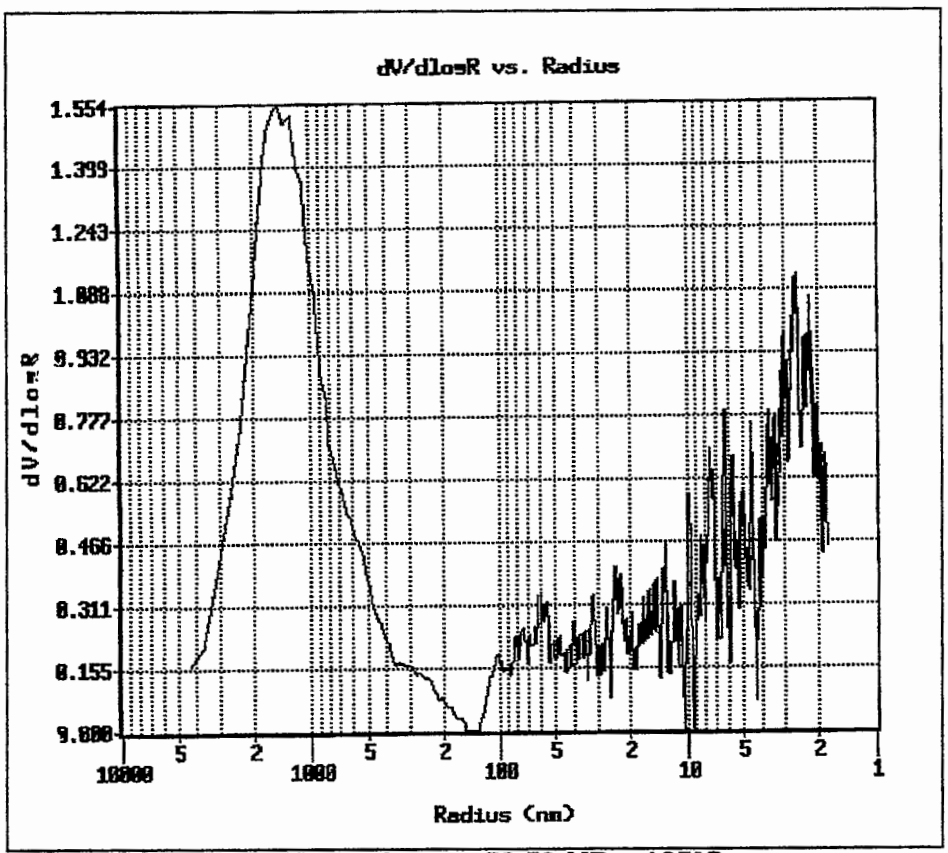

Figure D36 UHMWPE membrane: 56.59 MPa, 125°C

D2 Experimental design

The following curves were obtained from the porosimeter. The membranes used in these experiments were manufactured according to the experimental design.

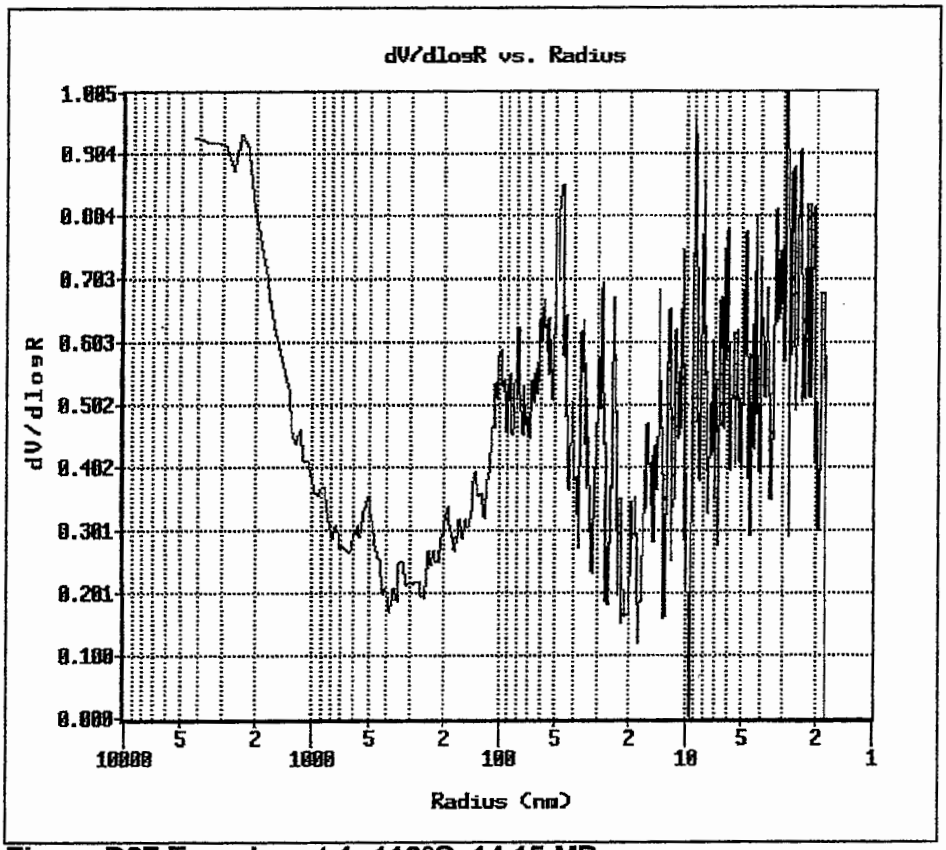

Figure D37 Experiment 1: 110°C, 14.15 MPa

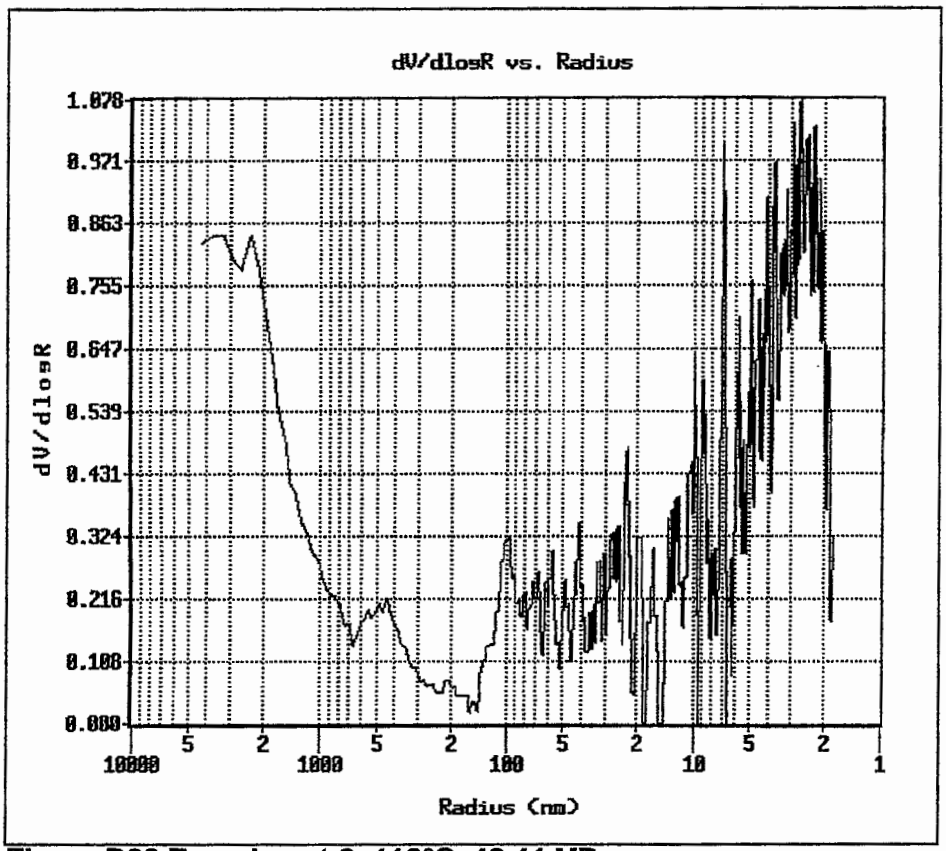

Figure D38 Experiment 2: 110°C, 42.44 MPa

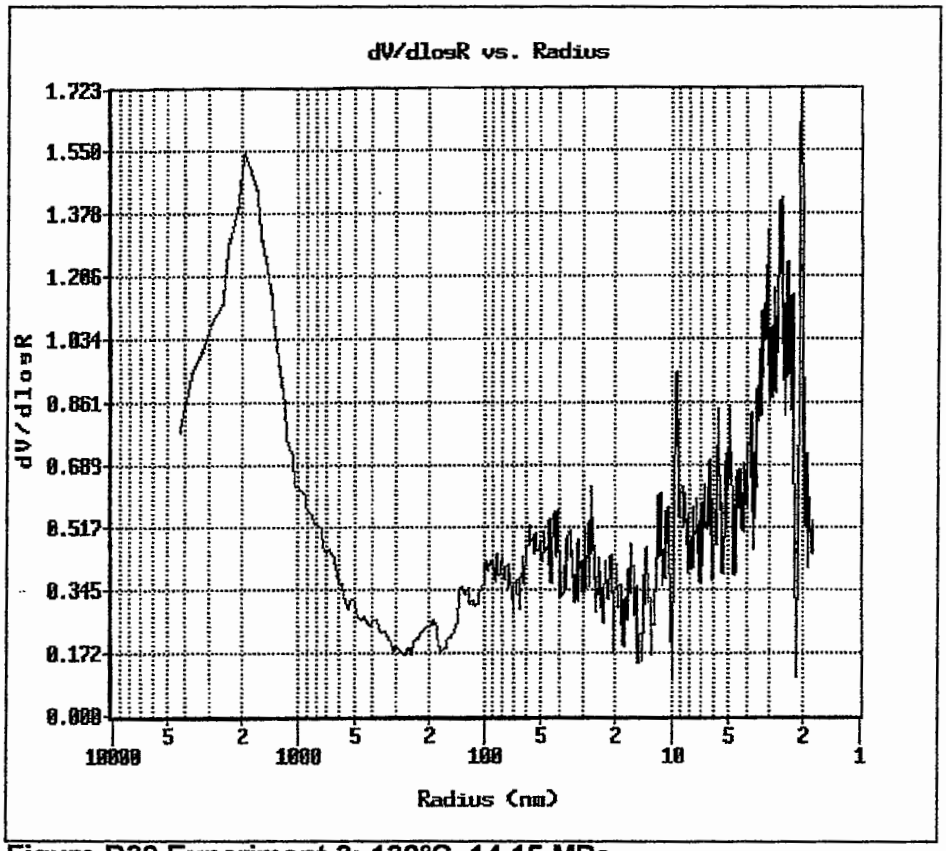

Figure D39 Experiment 3: 130°C, 14.15 MPa

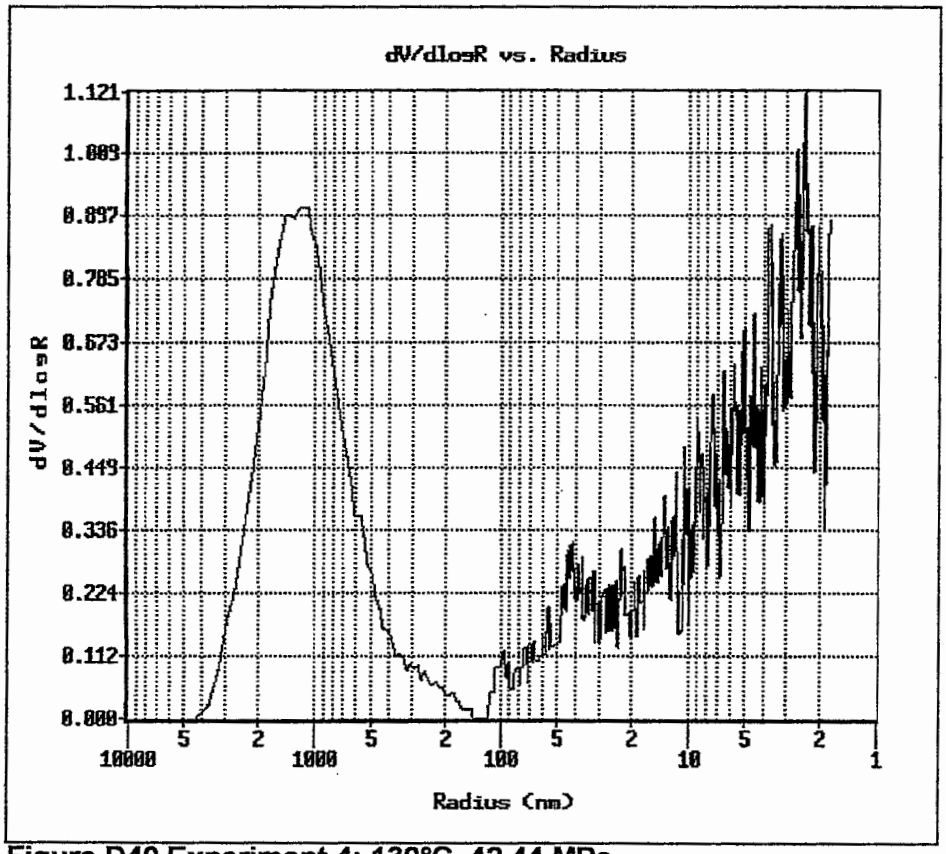

Figure D40 Experiment 4: 130°C, 42.44 MPa

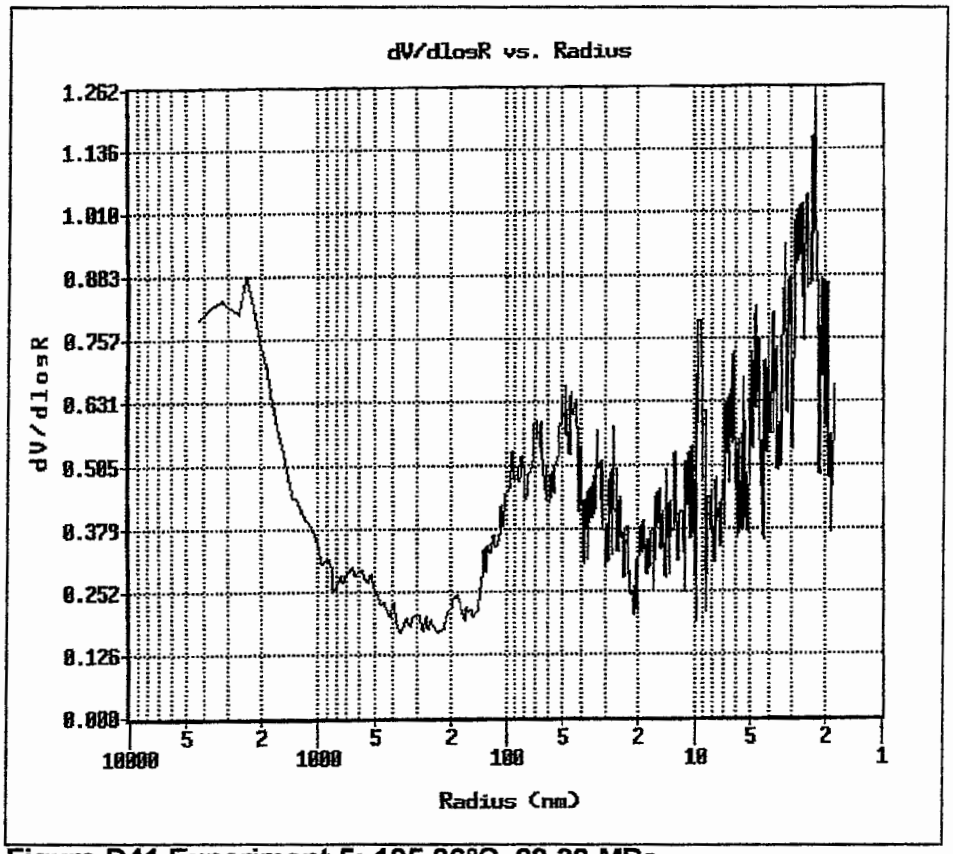

Figure D41 Experiment 5: 105.86°C, 28.30 MPa

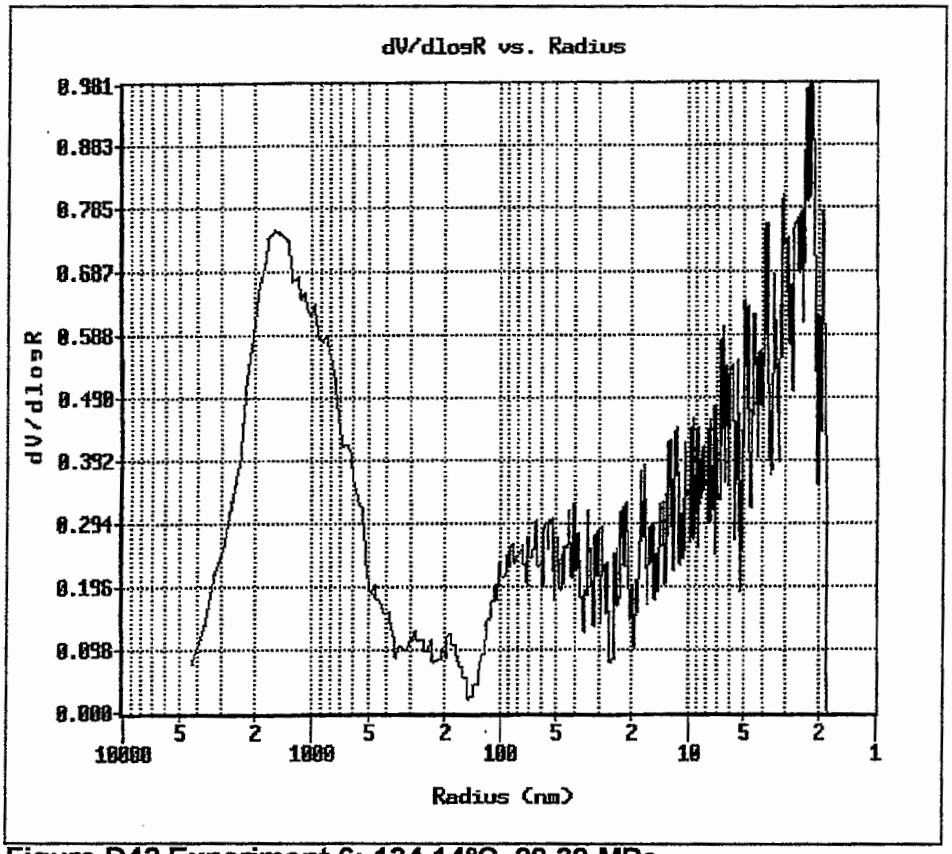

Figure D42 Experiment 6: 134.14°C, 28.30 MPa

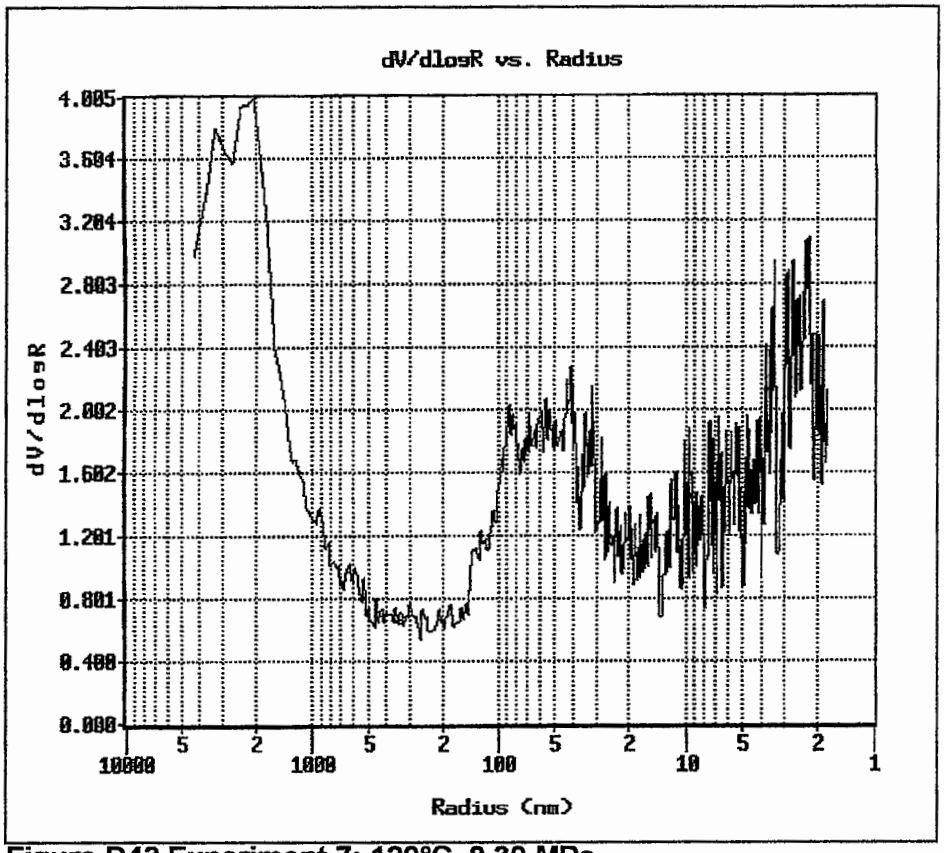

Figure D43 Experiment 7: 120°C, 8.30 MPa

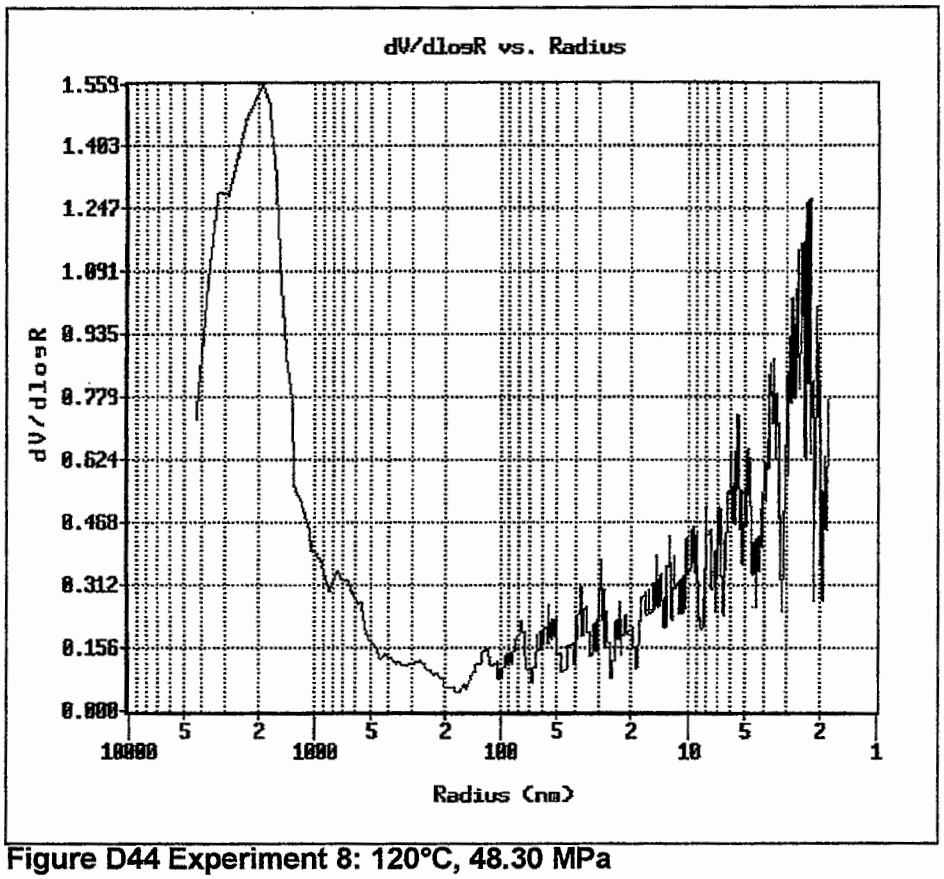

Figure D44 Experiment 8: 120°C, 48.30 MPa

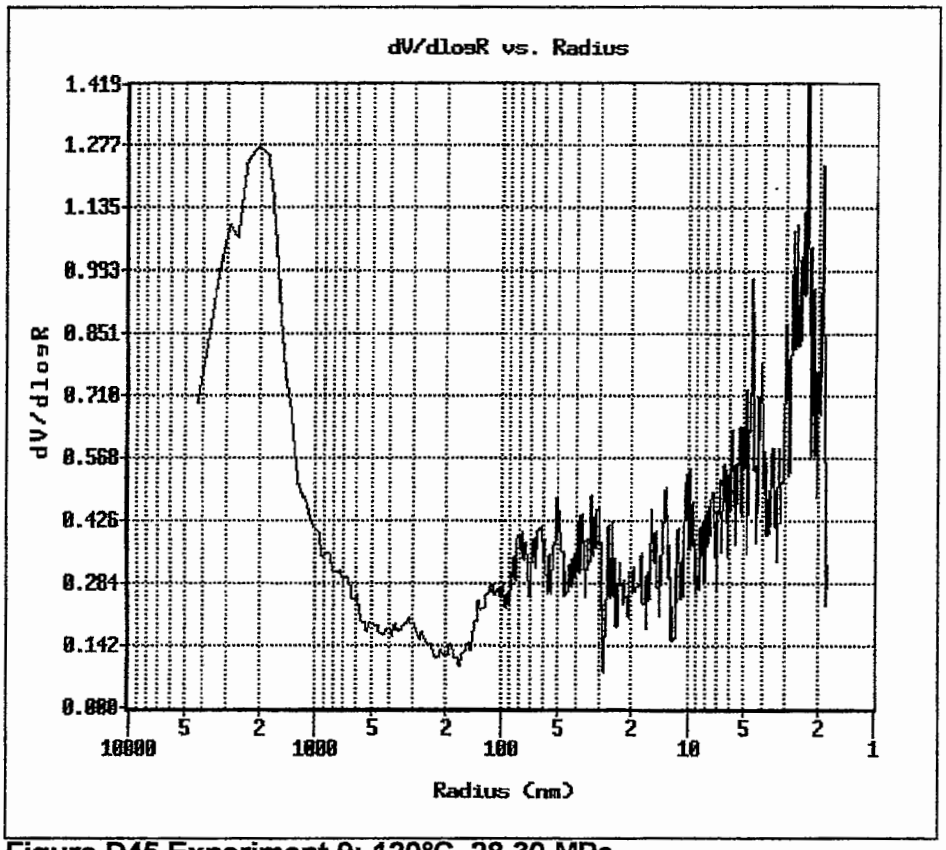

Figure D45 Experiment 9: 120°C, 28.30 MPa

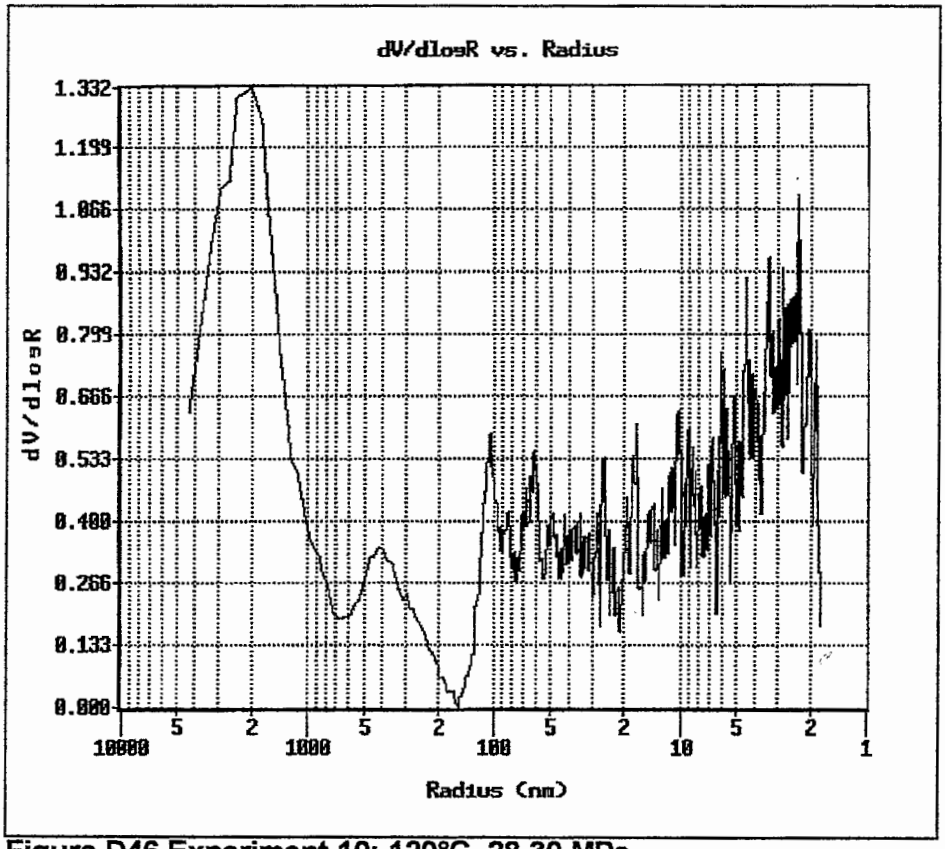

Figure D46 Experiment 10: 120°C, 28.30 MPa

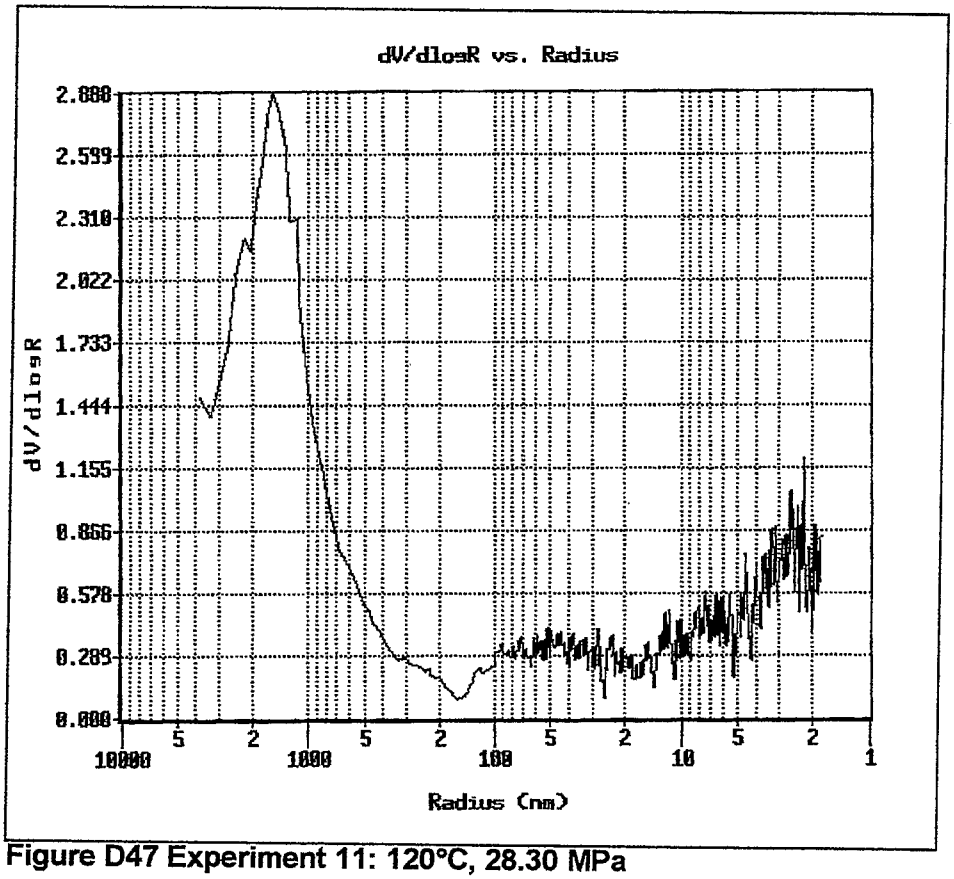

Figure D47 Experiment 11: 120°C, 28.30 MPa

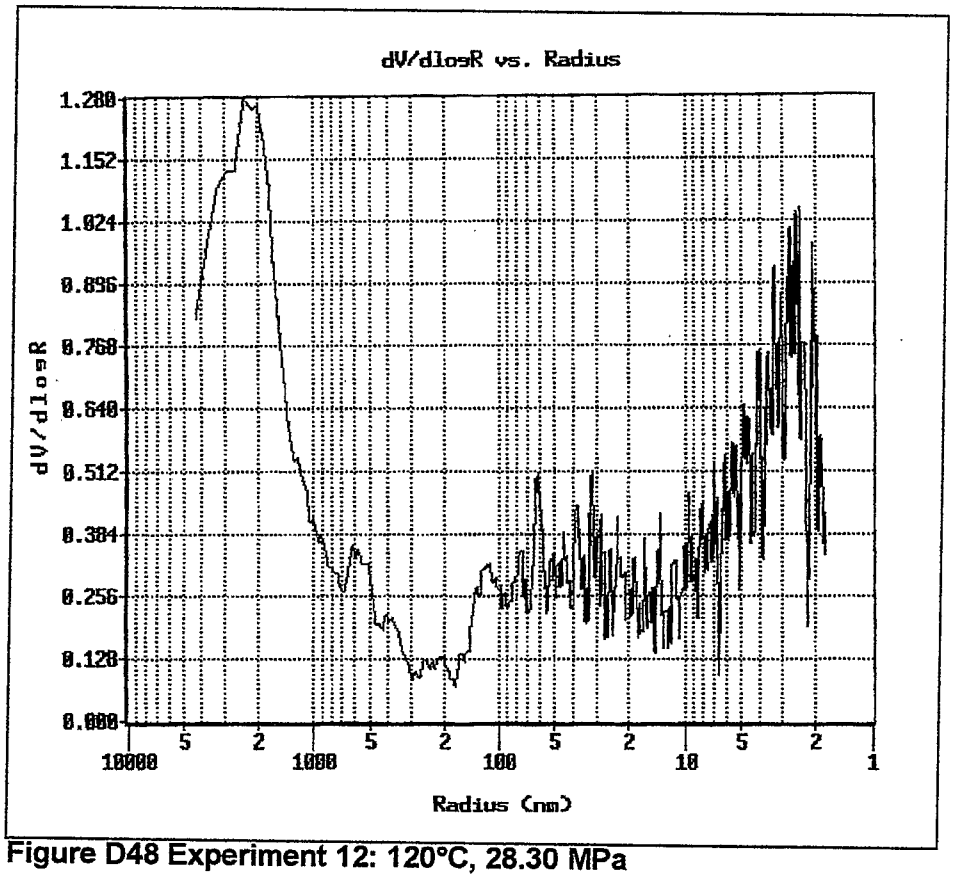

Figure D48 Experiment 12: 120°C, 28.30 MPa

APPENDIX E

Direct Microscopic Measurements

The Philips scanning electron microscope (SEM) of the Potchefstroom University was used for direct microscopic observations on the polymeric membranes. The photographs taken during the investigation confirmed the results obtained from the porosimeter. These photographs are shown on hte next few pages:

Figures E1 to E5: LDPE at 42.44 MPa and different temperatures.
Figures E6 to E9: LDPE at 125°C and different pressures.
Figures E10 to E14: HDPE at 42.44 MPa and different temperatures.
Figures E15 to E19: HDPE at 125°C and different pressures.
Figures E20 to E24: UHMWPE at 42.44 MPa and different temperatures.
Figures E25 to E29: UHMWPE at 125°C and different pressures.

The membranes produced at 110°C and 14.15 MPa could not be viewed under the SEM because the particles were bombarded from the membranes with the 10 kV electron beam.

E1 Low density polyethylene (LDPE)

E1.1 Constant pressure (42.44 MPa), different temperatures

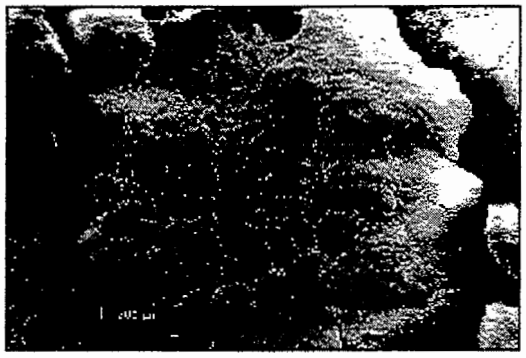

Figure E1 LDPE: 115°C

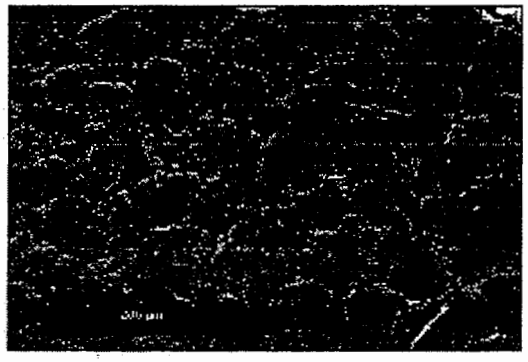

Figure E2 LDPE: 120°C

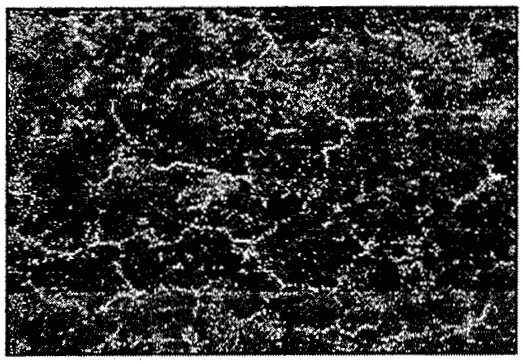

Figure E3 LDPE: 125°C

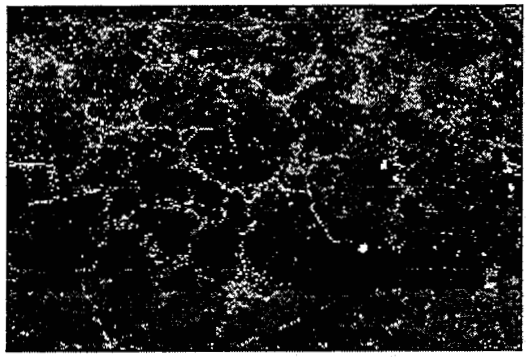

Figure E4 LDPE: 130°C

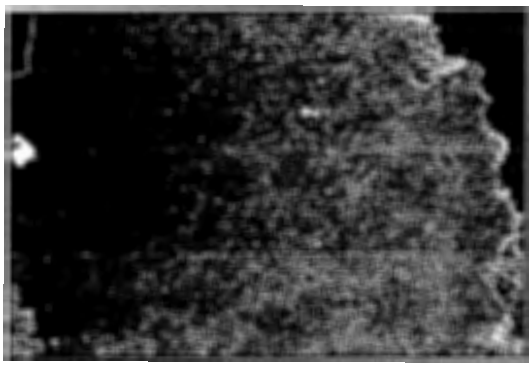

Figure E5 LDPE: 140°C

E1.2 Constant temperature (125°C), different temperatures

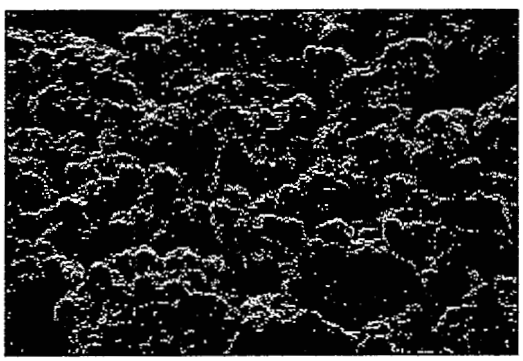

Figure E6 LDPE: 28.29 MPa

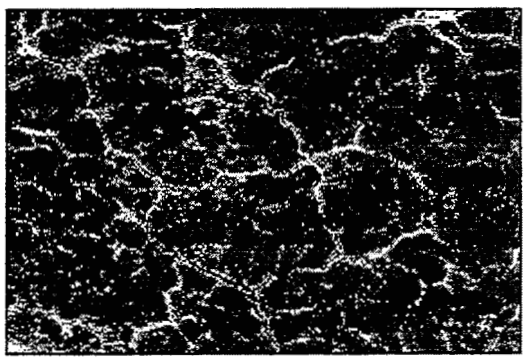

Figure E7 LDPE: 35.37 MPa

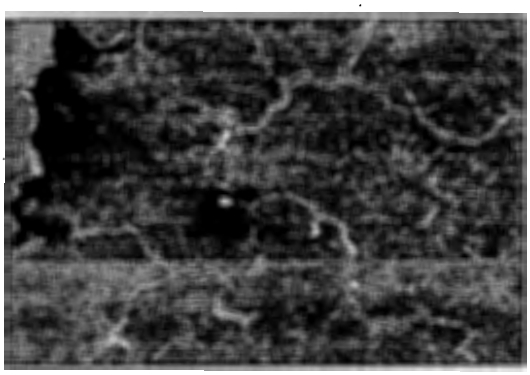

Figure E8 LDPE: 49.51 MPa

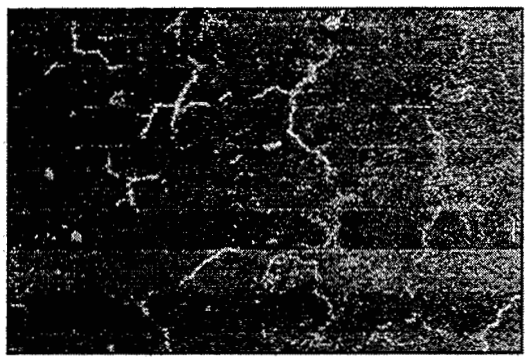

Figure E9 LDPE: 56.59 MPa

E2 High density polyethylene (HDPE)

E2.1 Constant pressure (42.44 MPa), different temperatures

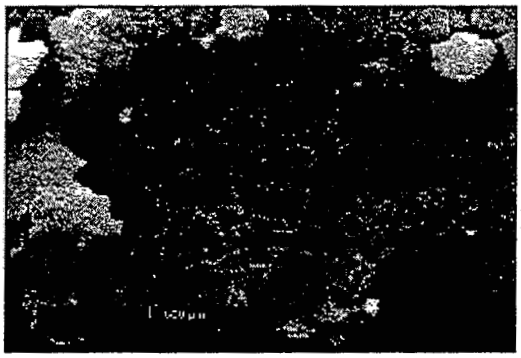

Figure E10 HDPE: 115°C

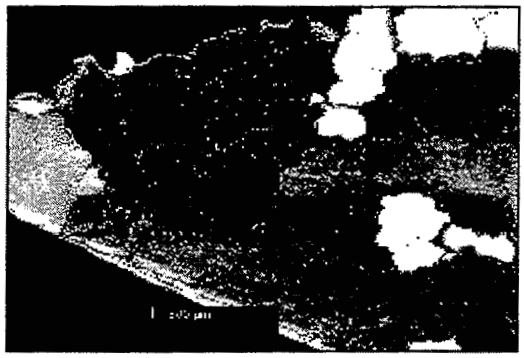

Figure E11 HDPE: 120°C

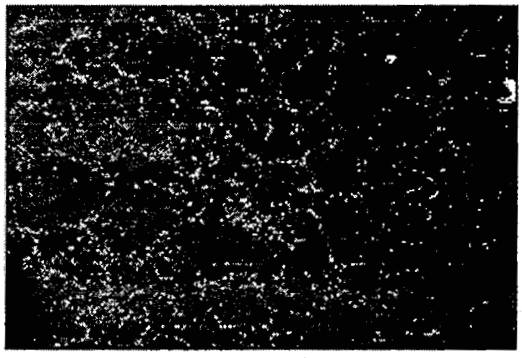

Figure E12 HDPE: 125°C

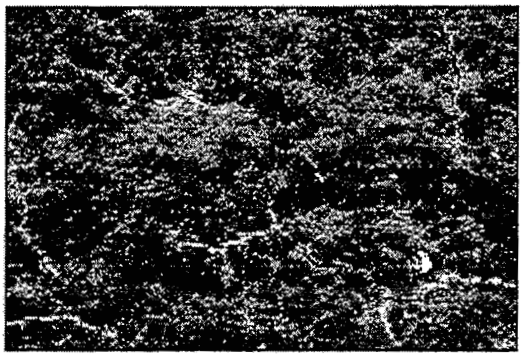

Figure E13 HDPE: 130°C

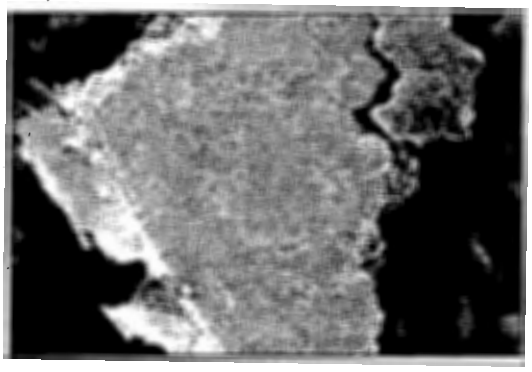

Figure E14 HDPE: 140°C

E2.2 Constant temperature (125°C), different pressures

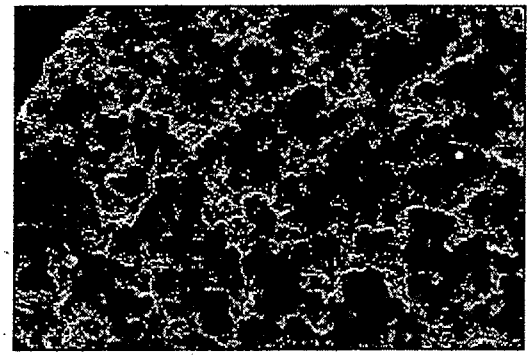

Figure E15 HDPE: 21,22 MPa

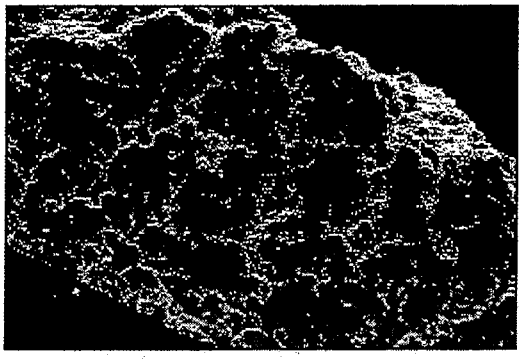

Figure E16 HDPE: 28.29 MPa

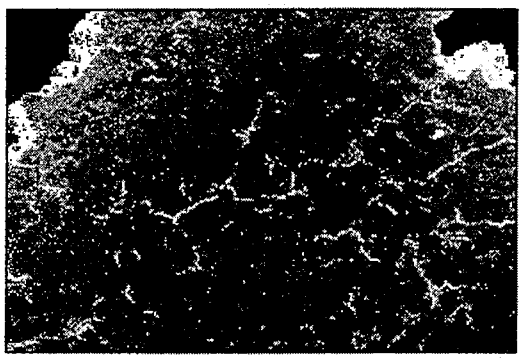

Figure E17 HDPE: 35.37 MPa

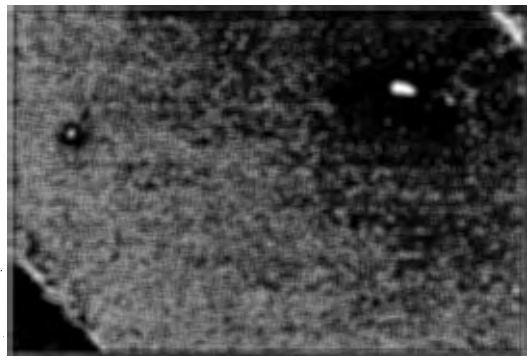

Figure E18 HDPE: 49.51 MPa

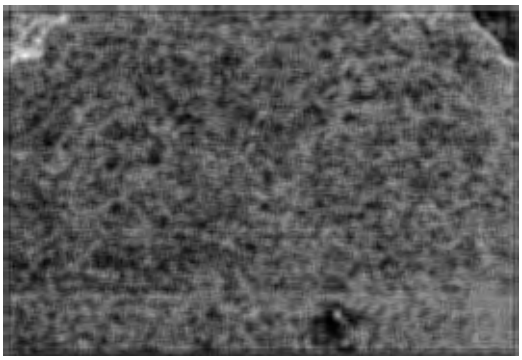

Figure E18 HDPE: 56.59 MPa

E3 Ultra high molecular weight polyethylene (UHMWPE)

E3.1 Constant pressure (42.44 MPa), different temperatures

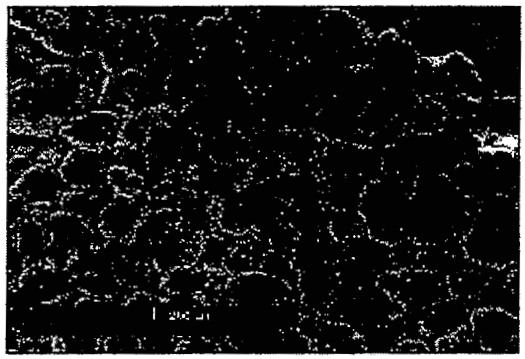

Figure E20 UHMWPE: 115°C

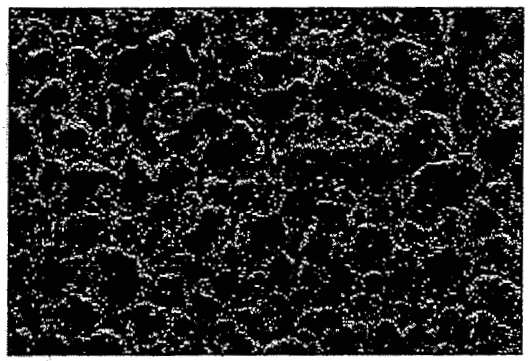

Figure E21 UHMWPE: 120°C

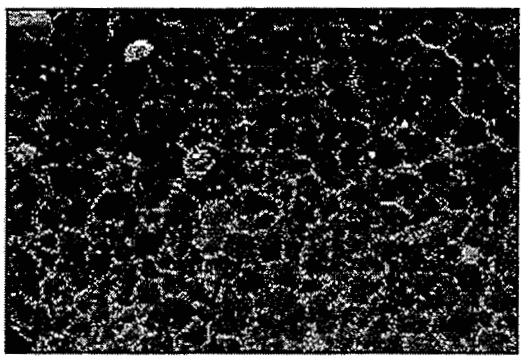

Figure E22 UHMWPE: 125°C

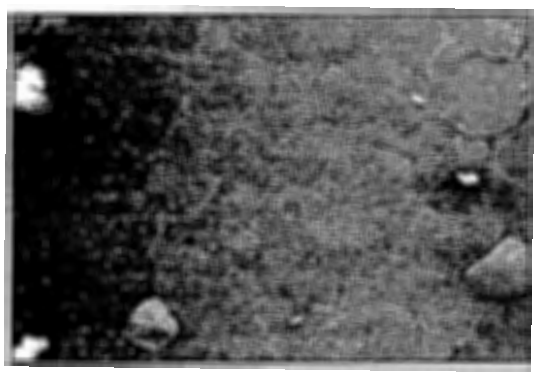

Figure E23 UHMWPE: 130°C

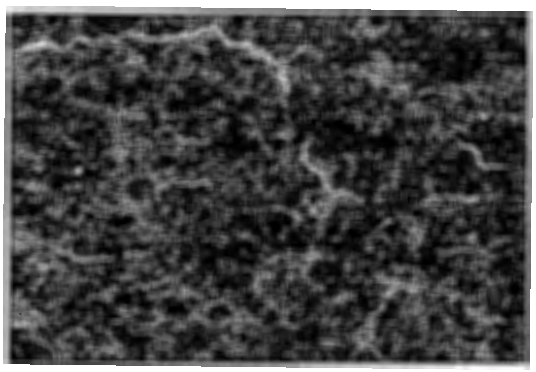

Figure E24 UHMWPE: 140°C

E3.2 Constant temperature (125°C), different pressures

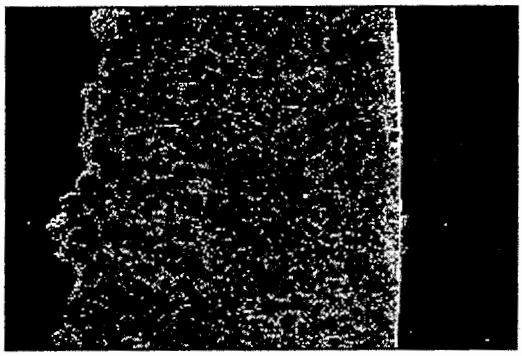

Figure E25 UHMWPE: 21.22 MPa

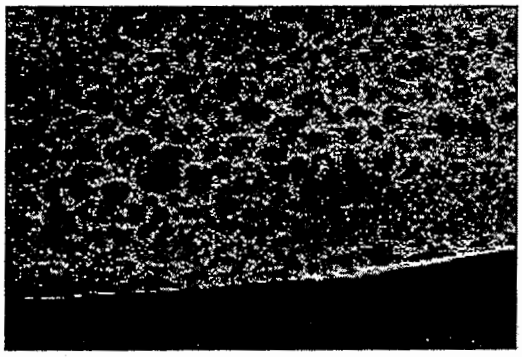

Figure E26 UHMWPE: 28.29 MPa

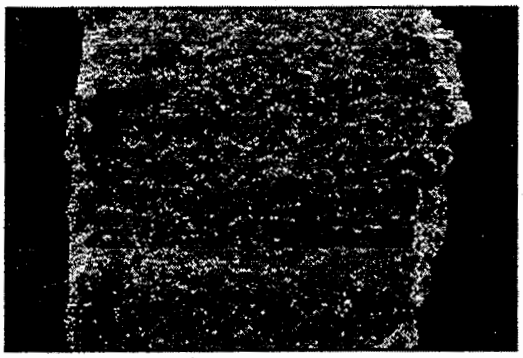

Figure E27 UHMWPE: 35.37 MPa

Figure E28 UHMWPE: 49.51 MPa

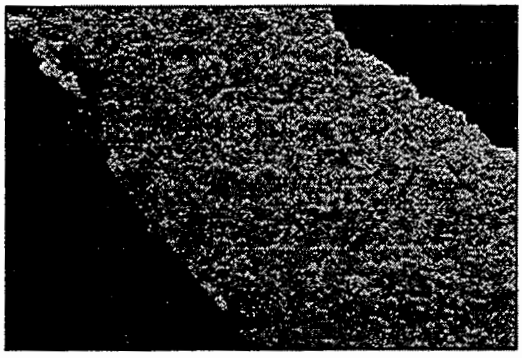

Figure E29 UHMWPE: 56.59 MPa